1-1-2009

Durability of concrete containing ternary blends of high calcium fly ash and slag

Seyon Kandasamy
Ryerson University

DURABILITY OF CONCRETE CONTAINING TERNARY BLENDS OF HIGH CALCIUM FLY ASH AND SLAG

By

Seyon Kandasamy
Bachelor of Engineering, Ryerson University, Toronto, Ontario, 2007

A thesis

presented to Ryerson University

in partial fulfillment of the

requirements for the degree of

Master of Applied Science

in the Program of

Civil Engineering

Toronto, Ontario, Canada, 2009

Author's Declaration

I hereby declare that I am the sole author of this thesis.

I authorize Ryerson University to lend this thesis to other institutions or individuals for the purpose of scholarly research.

Seyon Kandasamy Date

I further authorize Ryerson University to reproduce this thesis by photocopying or by other means, in total or in part, at the request of other institutions or individuals for the purpose of scholarly research.

Seyon Kandasamy Date

Borrowers Page

Ryerson University requires the signatures of all persons using or photocopying this thesis. Please sign below, and give name and date.

Name	Signature	Date

Durability of Concrete Containing Ternary Blends of High Calcium Fly Ash and Slag
Master of Applied Science, 2009

Seyon Kandasamy
Department of Civil Engineering
Ryerson University

Abstract

This thesis investigates the performance of ternary blends containing high calcium fly ash (HCFA) and slag against: sulfate attack, alkali-silica reaction (ASR), salt scaling, and freeze-thaw damage. In addition, compressive strength, permeability and fresh properties were evaluated. In terms of sulfate attack, the performance of HCFA was significantly enhanced when slag was added to the mix, and the same was found for ASR. The high efficacy in resisting ASR of HCFA/slag blends was found to be a result of the blends' ability to bind and retain alkalis. Regarding the salt scaling, the tested ternary concretes failed the Ministry of Transportation Ontario limit, 0.8 kg/m^2; however, enhanced performance was achieved when the samples were cured by wrapping with plastic sheets. Ternary blends achieved high resistance to freezing/thawing and less bleeding compared to those of the control mix without slag or HCFA; however, setting time was dragged by about an hour.

Acknowledgements

I would like to express my sincere gratitude to Dr. Medhat Shehata for his invaluable guidance, supervision and encouragement during the course of this project. I am infinitely indebted to Dr. Shehata who made my career at Ryerson a real success with his enormous and in-depth knowledge, teaching ability, and ever-caring support.

I also wish to thank Mr. Narayan Shrestha for the help with concrete casting and Mr. Richard Sluce for conducting thermal gravimetric analysis. The support from the technical staff of the Concrete Laboratory, Mr. Nidal Jaalouk and Mr. Mohamad Aldardari is greatly acknowledged.

Funding for this project was provided in the form of Ontario Graduate Scholarship (OGS) and by a grant from Natural Science and Research Council of Canada (NSERC). Financial supports from these two sources are greatly acknowledged.

Table of Contents

List of Figures

List of Tables

List of Appendices

List of Notations

AMBT	Accelerated mortar bar test
ASR	Alkali-silica reaction
BSE	Back-scattered electron
C-A-S	Calcium-AluminoSilicate-Hydrate
CH	Calcium hydroxide
C-S-H	Calcium-Silicate-Hydrate
FA	Fly ash
GGBFS	Ground-granulated blastfurnace slag
HAPC	High alkali Portland cement
LAPC	Low alkali Portland cement
M	Molarity; Mol/L
N	Normality
Na_2O_e	Equivalent alkali content
PC	Portland cement
ppm	Particles per million
RCPT	Rapid chloride permeability test
RH	Relative Humidity
SCC	Self consolidating concrete
SCM	Supplementary cementing material
SEM	Scanning electron microscope
w/c	Water to cementing materials ratio
XRD	X-Ray Diffraction

Chapter 1. Introduction

1.1 General

While in service, concrete experiences different durability issues. Among them, sulfate attack, alkali silica reaction (ASR), salt scaling and frost damage are few deterioration mechanisms that have gained significant attention in the past decades. The damage caused by these durability issues lowers the serviceability and sometimes the load carrying capacity of concrete. In addition, they accelerate the deterioration of concrete by allowing aggressive chemicals to ingress.

Sulfate attack is mainly characterised by formation of ettringite while ASR is characterized by formation of expansive gel. Formation of ettringite due to sulfate attack and/or formation of silica gel due to ASR exert pressure and crack the concrete, leading to reduction in the load carrying capacity (Mindess et al.,2003). On the other hand, salt scaling causes the spalling of the concrete surface due to the de-icing salt application coupled with freezing temperature. Salt scaling is known to reduce serviceability of flat works and it may also facilitate the ingress of other aggressive chemicals. Especially, corrosion can be a consequence of salt scaling as the chlorides easily penetrate through the eroded surface to attack the reinforcing steel bars (Mindess et al., 2003; Valenza and Scherer, 2007a,b,c). Finally, freeze-thaw damage is caused by the increase in volume as the water turns ice within concrete. The pressure exerted during the volume increase is sufficient to crack the concrete and to reduce the structural capacity. However, it is widely accepted that if the aggregates are not frost susceptible, then air

entrainment is a successful protection for freeze-thaw damage as the entrained air provide room to relieve the hydraulic pressure (Mindess et al., 2003).

Available literature contains theories explaining the mechanisms for each of the above mentioned durability issues. For example, swelling and crystal growth theories accounts for expansion of ettringite due to sulfate attack (Cohen, 1983); double layer theory explains the ASR gel expansion (Prezzi et al., 1997); and hydraulic and osmotic theories states reasons for frost/salt actions (Valenza and Scherer, 2007c; Mindess et al., 2003).

While few researchers tried to understand the mechanism of various durability issues, others have researched the material parameters of concrete to address those issues. For many decades, fly ash and slag are incorporated into concrete with the intention of enhancing the durability. This has been reported to be the case as fly ash and slag benefits the concrete from the physical and chemical standpoints (Mehta, 1986; Mindess et al., 2003; Monteiro et al., 1997; Tikalsky et al., 1990)

Fly ash is divided by Canadian Standards Association (CSA) into three categories: low calcium fly ash, moderate calcium fly ash, and high calcium fly ash. Low calcium fly ash is found to be very effective in reducing the damage from sulfate attack and alkali-silica reaction. The beneficial action of low calcium content fly ash is mainly due to pore refinement, $Ca(OH)_2$ consumption, pore solution alkalinity reduction and alkali binding ability. High calcium content fly ash, on the other hand, is found to be not effective and the reasons are attributed to its higher alkali and calcium, and lower silica contents (Thomas et al., 1999).

Slag is also widely used in order to control the deterioration issues at the appropriate replacement levels. Slag benefits through several actions including $Ca(OH)_2$ consumption, pore solution alkalinity reduction, and lowering Ca/Si ratio of Calcium-Silicate-Hydrate (C-S-H). These are of special importance in case of alkali silica reaction (Hooton, 2000).

In terms of salt scaling, contradictory results are available in the literature regarding the effects of supplementary cementing materials (SCM) on salt scaling. However, the common view is that incorporating fly ash or slag increases the scaling at least in the laboratory run tests. The possible reasons includes excessive bleeding, improper surface finishing practices, lack of curing, and formation of coarser microstructure due to carbonation (Valenza and Scherer, 2007a,b). With respect to frost damage, the slag or fly ash has shown to perform well if the concrete is adequately air entrained (Bilodeau et al., 1994; Hooton, 2000).

1.2 Objectives

This investigation is carried out to study the resistivity of concrete containing high calcium fly ash and slag against sulfate attack, alkali-silica reaction, salt scaling and frost damage. Earlier research work has shown high calcium fly ash to have low efficiency in resisting ASR and sulfate attack (Shehata, 2001; Thomas et al., 1999; Freeman and Carrasquillo, 1995; Shashiprakash and Thomas, 2001; Tikalsky et al., 1991). The main objective of this study is to enhance the performance of high calcium fly ash by incorporating slag. In addition to evaluating the performance of concrete with different levels of slag/fly ashes, the study looks into the mechanisms by which ternary blends of high calcium fly ash/slag affects the various deterioration mechanisms. Ion migration and calcium hydroxide consumption rates are

investigated to reason out the performance of various binary and ternary blends of high calcium fly ash and slag. For alkali-silica reaction, the alkali binding ability of binary and ternary blends was studied using the flame photometer. For salt scaling test, different curing regimes were used to evaluate the effect of curing conditions, which might affect the degree of hydration, on scaling resistance. In addition to the durability issues, hardened and fresh properties of the ternary and binary blends were also evaluated. This research contributes to the understanding of synergy of high calcium fly ash and slag in ternary blends.

1.3 Thesis Outline

This thesis is divided into 5 chapters. Chapter 1 briefly introduces the issues regarding concrete durability and role of fly ash and slag on controlling the deterioration. Chapter 2 reviews the existing literature on sulfate attack, alkali-silica reaction, salt scaling, and frost damage. The literature review consists of the mechanisms of each of the above mentioned issues followed by the effect of fly ash and slag and the existing laboratory experimental methods.

Chapter 3 consists of the experimental program designed to evaluate the objectives of this study. Chapter 4 presents the results and their analysis. In Chapter 5 conclusions and recommendations are made based on the experimental findings from this study.

Chapter 2. Literature Review

This chapter reviews the existing literature on sulfate attack, ASR, salt scaling, frost damage, and the role of fly ash, slag on the durability issues.

2.1 Supplementary Cementing Materials

The two supplementary cementing materials used in this study are fly ash and slag. The materials properties of fly ash and slag, and their effects on plastic and hardened concrete are reviewed in sections 2.1.1 and 2.1.2.

2.1.1 Fly Ash

Fly ash is derived from combustion of pulverized coal as a by product. Fly ash particles are spherical and ranges in size between 1 – 150 μm. Concrete with fly ash is more workable, requires higher air entrainment dosage to achieve the required air content, and reduces bleeding. Often, concrete with fly ash replacement results in reduced early strength and increased late strength compared to plain concrete (Berry and Malhotra, 1980).

Canadian Standard, CSA A23.5 classifies fly ash into three categories based on its calcium oxide content. Ashes with CaO < 8% is classified as Class F, ashes between CaO 8 and 20% is classified as class CI, and, ashes with CaO > 20% is classified as Class CH. Typical chemical composition of class F ash is SiO_2 > 50%, Al_2O_3 20 – 30%, Fe_2O_3 < 20, CaO < 5% and of Class CH is SiO_2 > 30%, Al_2O_3 15 – 25%, Fe_2O_3 < 10, CaO = 20 – 30% (Mindess et al., 2003).

High calcium fly ash contains lower silica, alumina and ferric oxide contents and higher calcium, sulphur and alkalis. Low calcium content fly ash contains calcium aluminosilicate (C-A-S) glass and virtually no crystalline compounds of calcium. High calcium fly ash contains C-A-S glass and crystalline compounds of calcium (Mehta, 1986). Due to the presence of C-A-S and crystalline compounds of calcium, cementing properties of high calcium fly ash is preferable; in fact, high calcium fly ash produces higher early strength than the low calcium fly ash.

2.1.2 Ground Granulated Blastfurnace Slag (GGBS)

GGBS (slag) is a by-product from iron making process and hence, the chemistry of slag depends on iron making process itself. Typical chemical composition of slag includes CaO = 35 – 45%, SiO_2 = 32 – 38%, Al_2O_3 = 8 – 16%, Fe_2O_3 < 2%, and sulphur = 1 – 2%. Fineness of slag varies; and finer the slag grains, higher the rate of reaction due to higher surface area. Usually, slag is finer than the Portland cement it replaces. The specific gravity of slag is around 2.9. Concrete incorporating slag is easier to handle and finish as slag particles are finer than Portland cement. However, slag concrete often requires higher dosage of air admixtures to obtain similar air content as Portland cement concrete. Further, slag concrete may retard the initial and finial setting times compared to that of Portland cement concrete (Hooton, 2000; Mindess et al., 2003).

The hydration of slag concrete is very slow due to the presence of an amorphous coating around slag grains (Mindess et al., 2003). The rate of hydration of slag gets faster when it is activated with alkali compound. When slag is incorporated with Portland cement, alkalis and calcium hydroxide produced from hydration of Portland cement activates slag (Mindess et al., 2003).

The C-S-H produced from the reaction of slag is lower in Ca/Si ratio and is able to incorporate more alkalis (Na^+ and K^+) and Al_2O_3 (Hooton, 2000).

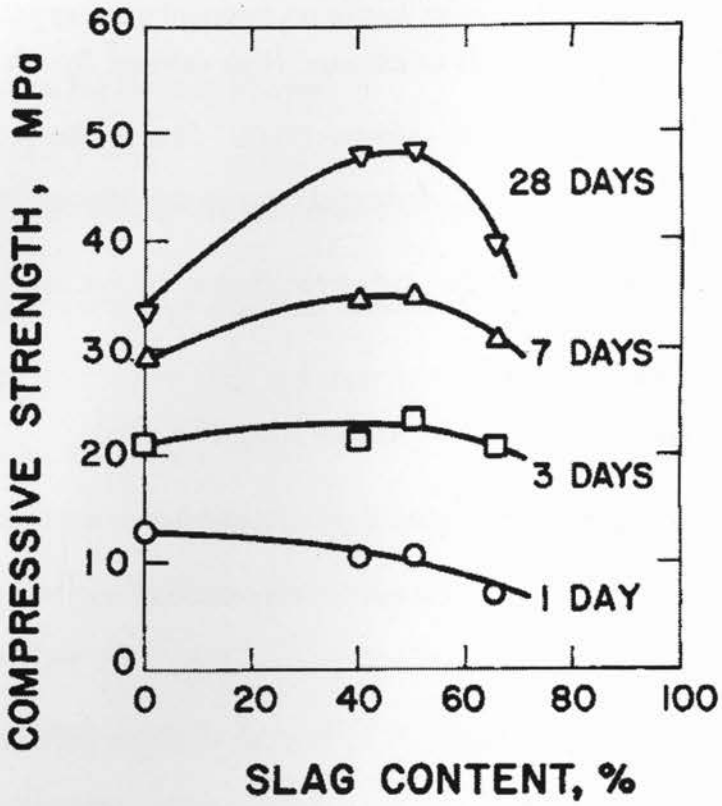

Figure 2.1: Influence of slag replacement level on compressive strength at age 1, 3, 7, and 28 days (Roy and Idorn, 1982)

Compressive strength of concrete with slag will be lower in early days (1 – 3 days) but with time slag stats to contribute to strength gain that will exceed plain Portland cement concrete. Figure 2.1 shows the typical pattern for strength of concrete with various slag contents. Note that by day 3 the concrete incorporating slag gained higher strength than the plain Portland cement concrete.

2.1.3 Ternary Blends

In the past, attempts have been made to incorporate more than one SCM into concrete mixtures to achieve synergetic effect. Combining two SCMs is thought to be beneficial if one could offset the shortfalls of other. For instance, when silica fume and fly ash are combined, the synergy could be expected in terms of strength development, reduction in water demand, increased sulfate resistance, lower permeability, reduced heat release and, reduced cost. For example, silica fume would contribute for low early strength properties of fly ash while fly ash contributes to the long term strength development that silica fume lacks (Thomas et al., 1999). Thomas et al. (1999) observed significant improvement in performance of ternary blends containing silica fume and high calcium fly ash where their study showed ternary blends of silica fume and high calcium fly ash enhanced the early properties of concrete, ASR and sulfate resistance.

Dehuai and Zhaoyuan (1997), Berry (1980), and Douglas and Pouskouleli (1991) reported compressive strength development of ternary blends containing low calcium fly ash and slag. Their results did not show any evidence of synergy in terms of strength development; rather, it seemed that the each SCM manifested their individual cementitious properties.

2.2 Concrete Durability

SCMs have been used to increase the resistance of concrete against durability issues. SCMs are known to increase the resistance through various actions including $Ca(OH)_2$ consumption due to pozzolanic reaction, refining pore structure, diluting the reactive constituents such as C_3A in Portland cement, and incorporating alkalis and aluminum into C-S-H thus making them unavailable for the deteriorative reactions (Ramyar and Inan, 2007; Tikalsky and Corrasquillo,

1992; Wee et al., 2000; Mindess et al., 2003; Hooton, 2000). The following parts of the literature review involves the contribution of fly ash, slag and their combination to enhance concrete durability in terms of sulfate attack, ASR, salt scaling, and freeze-thaw damage. First, the overview and mechanism of each of these deterioration modes are presented followed by the effect of SCMs on each durability issues and the summary of widely used laboratory evaluation methods.

2.3 Sulfate Attack

In hardened concrete, alkali sulfate attack occurs through five different actions (Hime and Mather, 1999; Santhanam et al., 2001, 2003):

1. Ettringite formation
2. Gypsum formation
3. Thaumasite formation
4. Crystallization, and
5. Cycling from anhydrous sodium sulfate to dehydrate sodium sulfate

To illustrate the process of sulfate attack, a mortar cube could be exposed to Na_2SO_4 solution. Once the mortar came into contact with Na_2SO_4, the reaction between sodium sulfate, calcium and aluminates takes place and ettringite and gypsum form. The formed ettringite and, perhaps, gypsum expand, creating tensile force within the mortar. The expansive force induces cracking inside the mortar. Once the mortar is cracked, salt solution can easily penetrate to the core to react with the hydration products. The reaction products accumulate in the cracks and pores. The zones of accumulation extend further into the mortar as more reaction products form (Santhanam et al., 2003).

Typical sources of sulfate in concrete are soil, water and cementing materials in the form of Na_2SO_4, K_2SO_4, $MgSO_4$, $CaSO_4$. For the sulfate ions from the external sources to migrate, high permeability and presence of moisture are essential.

The abovementioned five different forms of sulfate attacks are reviewed below.

2. 3.1 Ettringite Formation

Calcium sulfoaluminate hydrate (ettringite) is a major factor causes deterioration of concrete due to sulfate attack. Ettringite could form in fresh concrete and hardened concrete. Ettringite formed in fresh concrete is called primary ettringite (Equation 1) and is harmless because the concrete is fresh and can accommodate the stress results from the expansion (Hime and Mather, 1999).

$$3CaO{\cdot}Al_2O_3 + 3(CaSO_4{\cdot}2H_2O) + 26H_2O \rightarrow 3CaO{\cdot}Al_2O_3{\cdot}3CaSO_4{\cdot}32H_2O \quad \text{[Equation 1]}$$

Other type of ettringite is formed in the hardend concrete, called secondary ettringite, (Equation 2) causes cracking and spalling as the non-uniform expansion exerts stress within the rigid concrete (Hime and Mather, 1999).

$$6Ca^{+2} + 3SO_4^{-2} + Al_2O_6^{-6} + 32H_2O \rightarrow 3CaO{\cdot}Al_2O_3{\cdot}3CaSO_4{\cdot}32H_2O \quad \text{[Equation 2]}$$

2.3.2 Factors Governing Secondary Ettringite Formation

The two essential factors for the secondary ettringite to form are high permeable concrete and presence of water within the concrete. The permeability has to be sufficient for the sulfate ions to enter into the concrete from external sources and water must be available to carry the entering sulfate ions. In addition, pre-existing micro-cracks, higher cuing temperature (associated with

certain cement types), and alkali content influence the formation of secondary ettringit (Collepardi, 2003; Escadeillas et al., 2007). The role of pre-existing cracks are evident fro high vulnerability of prestressed concrete structures to sulfate attack since higher localize stresses created when the pre-stressed cables were cut cause micro-cracks (Collepardi, 2003 Presence of microcracks allows water to penetrate more easily to leach the alkalis. When alkali are removed faster, the secondary ettringite forms faster (Escadellias et al., 2007). Often th concrete with high early strength cement and cured at elevated temperatures (above 70°C) result in expansion due to secondary ettringite (Figure 2.2). Figure 2.2 was obtained by curing morta bars made up of Type 5 cement at various temperatures and 100% relative humidity (RH) for 2 hours. Followed by the curing period, the specimens were stored in lime solution and periodi length measurements were taken. As in Figure 2.2, the specimens went through higher curin temperature expanded more than the ones with lower curing temperature. One school of though that explains the secondary ettringite formation from higher heat curing is that when concrete i cured at higher temperature, normal ettringite formation does not occur. Hence, highe concentration of sulfates in pore solution is sustained for longer period to result in secondar ettringite formation (Ramlochan et al., 2003). Another school of thought is that at higher hea treatment, sulfates enter into C-S-H which is to be released later to form secondary ettringit (Ramlochan et al., 2003).

Increase in alkali content increases the risk of expansion since higher the alkali content give higher rate of hydration for C_3S, which may increase the formation of secondary ettringit (Escadeillas, 2007; Taylor, 2001). Another concept is that increase in alkali content increases th

pH of pore solution where higher pH of pore solution increases the sulfate content in C-S-H and induces monosulfate formation rather than ettringite (Tayer et al., 2001; Escadeillas et al., 2007).

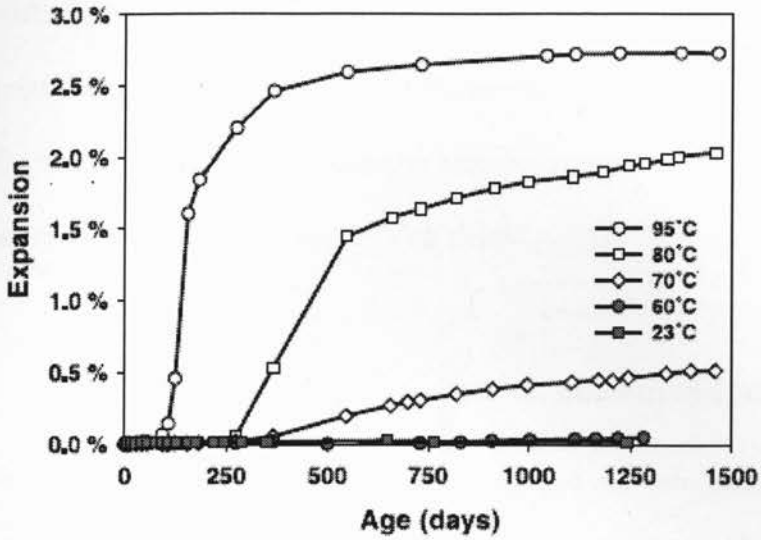

Figure 2.2: Concrete cured at higher curing temperature experiences higher expansion (Ramlochan et al., 2003)

2.3.3 Expansion Mechanisms of Secondary Ettringite

In the literature, two theories have been proposed to explain the expansion mechanism for secondary ettringite; one is crystal growth theory by Cohen and other is swelling theory by Mehta (Cohen, 1983). Cohen in his crystal growth theory stated that ettringite crystallize and the thickness of ettringite crystals increases as more ettringite is formed. Once the thickness of the ettringite exceeds the thickness of surrounding solution, the ettringite exerts pressure on adjacent hydration product wall.

Mehta, on the other hand, suggested that the expansion is caused by swelling of ettringite particles by absorbing water. According to Mehta, ettringite crystals with small specific area

will absorb little water and therefore, will not cause expansion. Mehta observed that concr with finer ettringite particles expand a lot compared to the ones with coarser ettringite. This obvious since finer particles have more surface area to absorb more water (Cohen, 1983).

What is common in both theories are that size of ettringite particles affect the expansion a presence of lime, water and expansive materials results in smaller ettringite crystals, whe absence of lime results in larger ettringite crystals (if lime is not present, the aluminates reac faster and produces larger crystals), which don't expand significantly (Cohen, 1983).

2.3.4 Gypsum Formation

Formation of gypsum may not be a primary cause for immediate deterioration however it coul be severe in the long run. And, no well defined mechanism is established for damage caused b gypsum formation (Tian and Cohen, 2000). Formation of gypsum is given by Equation 3 where calcium, sulfate, and water react to form gypsum.

$$Ca^{2+} + SO_4^{-2} + 2H_2O \rightarrow CaSO_4 \cdot 2H_2O \qquad \text{[Equation 3]}$$

Cement with increased C_3S content is more vulnerable as it would hydrate faster to produce more $Ca(OH)_2$ which would lead to increased gypsum formation. Tian and Cohen (2000) used two types of cement; one with limited C_3S (in Figure 2.3a, labelled "Alite") and other with plenty of C_3S (Figure 2.3b). In addition, samples were made with replacement of these two cements with an SCM (silica fume). The specimens were soaked in 5% Na_2SO_4 and lime water. The obtained results are shown in Figure 2.3. Figure 2.3a shows the expansion of specimens made with limited C_3S content cement with and without SCM and soaked in Na_2SO_4 solution. Figure 2.3a also contains the expansion of specimen made with limited C_3S cement under lime

solution. After 1 year the specimen without the SCM (i.e. SF) expanded dramatically while the one soaked in limewater did not show any expansion. In Figure 2.3b, similar blends were made (but with cement rich in C_3S) and submerged under Na_2SO_4 and limewater. In Figure 2.3b, the blend without any SCM (i.e. C_3S-Na_2SO_4) expanded dramatically after 1 month under Na_2SO_4 solution but the same blend under limewater did not expand.

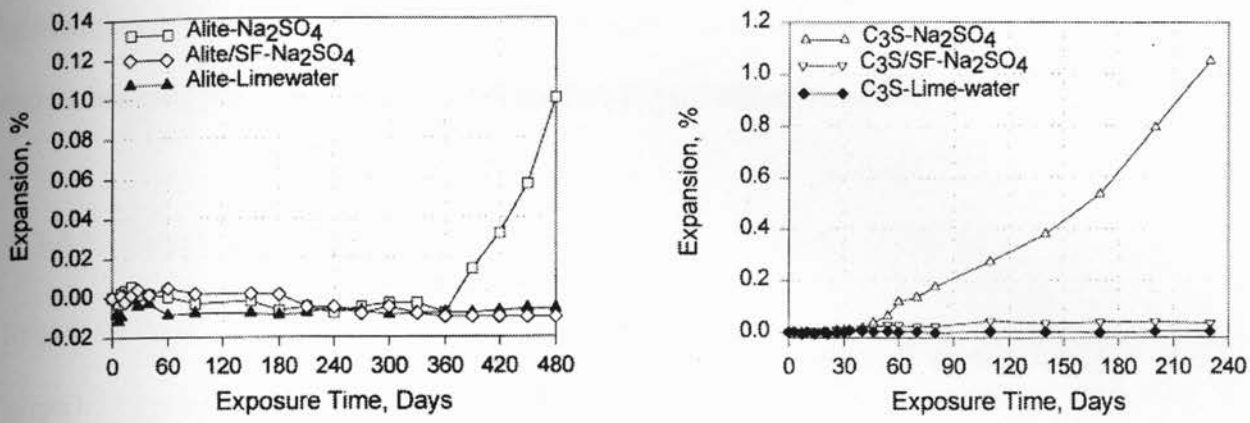

a) b)

Figure 2.3: Effect of C_3S content on gypsum formation (Tian and Cohen, 2000)

a) Contains the expansion of specimens made with limited C_3S cement with and without SCM incorporation under Na_2SO_4 and lime water. B) Shows the expansion of specimens made with cement rich in C3S with and without SCM incorporation under Na_2SO_4 and lime water.
(Legend:
Alite-Na_2SO_4 – specimen made with limited C_3S cement and soaked in Na_2SO_4;
Alite/SF-Na_2SO_4 – specimen made with limited C_3S cement and silica fume and soaked in Na_2SO_4;
Alite-Limewater – specimen made with limited C_3S cement and soaked in limewater;
C_3S-Na_2SO_4 – specimen made with rich C_3S cement and soaked in Na_2SO_4;
C_3S/SF-Na_2SO_4 – specimen made with rich C_3S cement and silica fume and soaked in Na_2SO_4;
C_3S-Limewater – specimen made with rich C_3S cement and soaked in limewater)

As Figure 2.3 shows, limited C_3S cement (alite) specimens soaked in Na_2SO_4 had the same expansion as the specimens soaked in lime water and specimens with SCM replacement until 1 year. On the other hand, C_3S rich specimens soaked in Na_2SO_4 showed distinguishable

expansion compared to the ones soaked in lime water and the ones with SCM replacement. In addition to the expansion measurements, X-Ray diffraction (XRD) analysis conducted on these specimens confirmed the presence of high gypsum peaks on Alite-Na_2SO_4 specimen after 440 days and C_3S-Na_2SO_4 specimen after 220 days while less amount of gypsum were detected on specimens with SCMs. This study confirmed that formation of gypsum results in expansion. This study also confirmed that incorporation of SCM to consume $Ca(OH)_2$ for pozzolanic reaction will reduce the availability of $Ca(OH)_2$ to form gypsum; and sufficient supply of C_3S will induce early expansion as more $Ca(OH)_2$ is formed due to rapid hydration (Tian and Cohen, 2000).

2.3.5. Thaumasite Formation

The ettringite allows broad range of ions to substitute into its chemical structure. Thaumasite forms when such a substitution takes place in the structure of ettringite. Si^{4+} trivalent ions substitute Al^{3+} in ettringite to result in a silica-based compound thaumasite, $2CaO{\cdot}SiO_2{\cdot}2CaSO_4{\cdot}2CaCO_3{\cdot}30H_2O$. In addition to sulfate, a source of $CaCO_3$ and water are also essential for thaumasite. However, unlike ettringite, presence of alumina is not required for thaumasite. The source of $CaCO_3$ is could be internal or CO_2 from atmosphere (Bellmann and Stark, 2007). Cabonation would decompose C-S-H to initiate thaumasite formation (Brown, 2002; Mulenga et al., 2003). Beside $CaCO_3$, it was thought that lower temperatures as a condition for significant thaumasite formation; however, thaumasite was detected in higher temperatures as well (Brown, 2002). The study conducted by Mulenga et al. (2003) shows that sulfate tests performed at lower temperatures end up with more destruction than those at higher temperatures. Mulenga et al. (2003) made mortar bars 0, 20, 30, 40, and 50% replacement with

fly ash. Those bars were soaked in Na_2SO_4 solution and kept at 20°C and 8°C to study the thaumasite formation. For the first 56 days, the bars at both temperatures showed similar level of expansion after which the bars at 8°C expanded dramatically. Further, the bars kept at 20°C sustained themselves even after 120 days where the bars at 8°C became mushy and incohesive before 120 days. XRD investigations showed that specimens kept at 20°C showed mainly ettringite phases and no signs of thaumasite; and the specimens at 8°C showed mainly thaumasite phases. Their study confirmed the strong effect of temperature on formation of thaumasite and the more destruction that thaumasite brings than that of ettringite alone.

2.3.6 Crystallization

Salt crystallization occurs as the water evaporates from the salt solution. The crystallization is given by Equation 4 which occurs in concrete pores (Hime and Mather, 1999).

$$2Na^{+} + SO_4^{-2} \text{ (aqueous)} \rightarrow Na_2SO_4\text{(solid)} \qquad \text{[Equation 4]}$$

If the pores where the crystallization occurs are located near the surface, the crystallization exerts pressure large enough to cause deterioration (Neville, 2004). Capillary action plays a significant role in salt crystallization. The sulfate from the soil could enter into the concrete by capillary action where concrete with finer pores and SCMs would be more vulnerable (Nehdi and Hayek, 2005).

In addition to crystallization, variations in temperature and humidity will cause the salt to change between dehydrated to anhydrous forms as shown in Equation 5 (Nehdi and Hayek, 2005; Neville, 2004; Hime and Mather, 1999).

$$Na_2SO_4 + 10H_2O \Leftrightarrow Na_2SO_4 \cdot H_2O \qquad \text{[Equation 5]}$$

The above reversible reaction (Equation 5) involves volume increase of around 315% which causes destructive pressure (Nehdi and Hayek, 2005).

Nehdi and Hayek (2005) tested the cylinders (made of three different w/c: 0.3, 0.45, and 0.6) partially soaked in salt solution and partially exposed to the atmosphere. Nehdi and Hayek intended to observe the efflorescence* deposit on the portion of concrete exposed to atmosphere. Specimen with 0.45 w/c gave higher efflorescence deposit than the ones with 0.6 and 0.3 w/c. One would expect that lower w/c would give more efflorescence because of higher capillary suction. However, here moderate w/c gave higher efflorescence. The reason explained is that amount of salt transported depends on two factors; capillary suction and permeability. Lower w/c will provide greater capillary suction but lower volume of solution is transported due to lower permeability. Higher w/c will provide higher amount of volume transport but will reduce the capillary rise. Due to the balance between capillary rise and volume of solution transported at moderate w/c, optimum amount of sulfate solution got transpored at 0.45 w/c; thus, more efflorescence formed on the specimens of 0.45 w/c.

2.3.7 Role of Slag and Fly Ash on Sulfate Attack

SCMs are blended with Portland cement to provide some resistant to sulfate attack. Main benefits of SCMs are due to the dilution effect of C_3A from Portland cement (PC), and pozzolanic effect. Replacement of PC with SMCs reduces the availability of free C_3A to produce ettringite. Through pozzolanic action, SCMs consume the portlandite that would otherwise be

* Efflorescence is a white deposit forms on above-ground parts of concrete structures due to sulfate exposure.

used to produce gypsum and ettringite. The secondary C-S-H formed from pozzolanic reaction refines the concrete which becomes less permeable (Ramyar and Inan, 2007; Tikalsky and Corrasquillo, 1992; Wee et al., 2000; Mindess et al., 2003).

With regard to thaumasite formation, ability of SCMs to lower Ca/Si ratio of C-S-H through the consumption of $Ca(OH)_2$ due to pozzolanic and/or latently hydraulic reactions will increase the resistance. C-S-H with Ca/Si of 1.7 has shown to easily convert to thaumasite but when the ratio is reduced to 1.1, C-S-H had more resistance against conversion into thaumasite (Bellmann and Stark, 2007). Addition of slag or fly ash was able to lower the Ca/Si ratio of C-S-H and lead to silica rich C-S-H which is more resistant to the conversation into thaumasite (Bellmann and Stark, 2007).

2.3.7.1 Role of Slag on Sulfate Attack

Al_2O_3 content of slag is emphasized as a predominant factor that influences the performance of slag against sulfate attack (Wee et al., 2002; Gollop and Taylor, 1996a,b; Mangat and Khatib, 1995). Gallop and Taylor (1996b) stated that at a certain replacement level of slag, the resistance increases with decreasing Al_2O_3 of slag. It is also found that slag with lower Al_2O_3 content increase the resistance even at lower dosages while the slag with higher Al_2O_3 contents needs higher replacement to have similar resistance (Gollop and Taylor, 1996b). When the Al_2O_3 content of slag is in the range of 8 – 10%, a 50% replacement level is sufficient for good resistance whereas Al_2O_3 of 13 – 15% requires around 70% replacement level for good resistance (Mangat and Khatib, 1995).

Slag with lower Al_2O_3 increases the resistance mainly through dilution effect. Slag with higher Al_2O_3 shows resistance at the higher replacement rates because the Al_2O_3 of slag is incorporated into C-S-H, hence not freely available for ettringite formation (Gollop and Taylor, 1996b). Amount of aluminum ions that could be accommodated increases with decreased Ca/Si ratio of C-S-H. At lower slag replacement level, Ca/Si ratio of C-S-H of PC-Slag system is very close to that of 100% PC. At higher slag replacement level, Ca/Si of C-S-H of PC-slag system is lower than that of 100% PC. Lower Ca/Si ratio may lead C-S-H to incorporate much of the released Al^{3+} ions into C-S-H (Gollop and Taylor, 1996b).

Gollop and Taylor (1996b) tested three different slags each with 11.2, 13.4, and 16.0% Al_2O_3 content, respectively. All the blends were composed of 69% slag and 31% PC. After the exposure to 0.25 mol/L sodium sulfate solution for 6 months, the performance of these blends was accessed by various means such as visual examinations and scanning electron microscopic (SEM) analysis. Evaluations showed that the mixes with slag of 13.4% and 16.0% Al_2O_3 contents performed worse than the one without any slag replacement. The slag of 11.2% Al_2O_3 performed superior to all the mixes including 100% PC. Further, Gollop and Tayer (1996b) increased the proportion of the 13.4% Al_2O_3 content slag to 92% replacement to evaluate the improvement at relatively higher replacement level. The mix at 92% replacement performed superior not only to one with same slag at 69% replacement but to all of the above mixes. This confirmed few important points about slag in sulfate environment. First, increasing Al_2O_3 of slag decreases the resistance. Second, lower replacement levels of higher Al_2O_3 slag may worsen the case. Third, when replaced at higher level, higher Al_2O_3 slag performs well.

Wee et al. (2000) published results of performance of concrete mixtures incorporating slag at 0, 65, 75, 85% replacement levels under 5% Na_2SO_4 solution. The slag used in their study had an Al_2O_3 content of 14%. The visual inspection of the specimens after an year under sulfate solution showed that incorporating slag enhanced the resistance in the order of 0% replacement (mostly damaged)>65% >75%>85% replacement levels. Wee et al. (2000) concluded that higher slag replacement of portland cement resulted in enhanced resistance to sulfate attack in concrete. Although slag contains higher portion of Al_2O_3 which would promote ettringite formation, increasing the slag content increased the resistivity because some of Al_2O_3 locked as Mullite ($3Al_2O_3 \cdot 2SiO_2$) and not freely available for the reaction (Wee et al., 2000).

2.3.7.2 Role of Fly Ash on Sulfate Attack

Class F fly ashes have shown enhanced sulfate resistance (Shashiprakash and Thomas, 2001; Tikalsky et al. 1990). However Class CH fly ash was found to be not effective when exposed to sulfate solution and no consistency has been observed with Class CH fly ash level of replacement and degree of resistivity. For example Figure 2.4 shows the expansion of mortar bars made with high C_3A Type I PC, and 20% and 40% Class CH fly ash mixes. Use of Class CH fly ash slowed down the expansion for 12 months but did not control the expansion. 20% fly ash mix expanded more than the control while 40% fly ash showed less expansion than the control. However, another publication of the Thomas et al. (1999) showed 40% Class CH fly ash expanded more than 20% Class CH fly ash; and 20% Class CH fly ash mix expanded more than the control mix. Freeman and Carrasquillo (1995) also reported results showing 35% Class CH fly ash mortar bar expanded lot more than 25% Class CH fly ash.

Yet, research involves high calcium fly ash against sulfate attack so far presented conflicting information (Mehta, 1986). High calcium fly ash is characterized with significant amount of C-A-S glass and crystalline compound of calcium (Mehta, 1986). In PC-fly ash systems, compositions of crystalline and amorphous phases play a major role in resistance to sulfate attack (Tikalsky and Carrasquillo, 1992; Mehta, 1986).

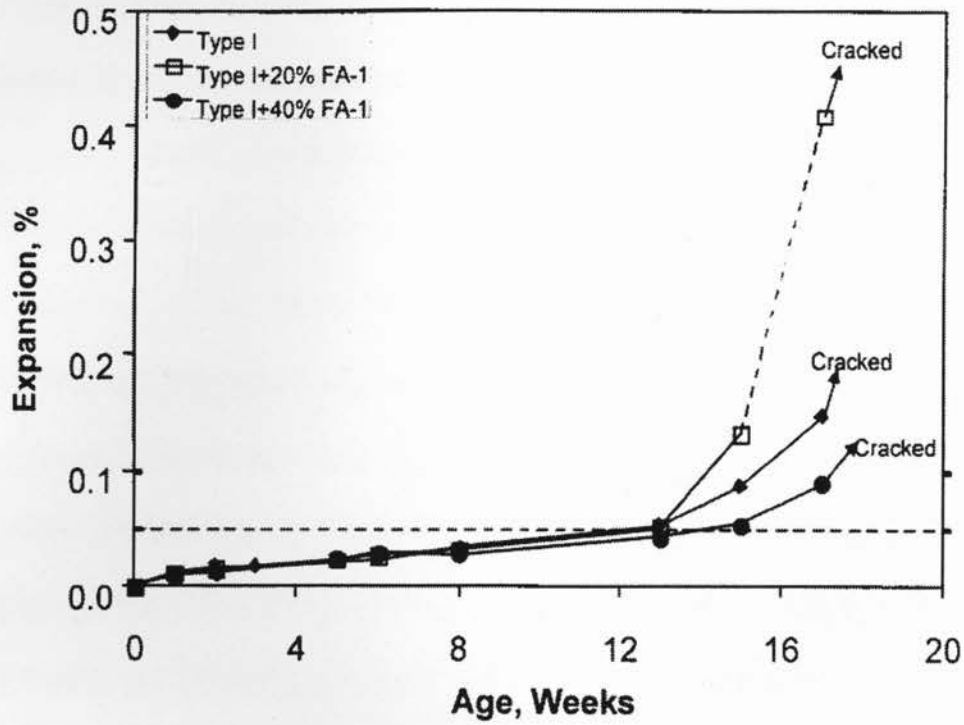

Figure 2.4: Resistance of high C fly ash under sulfate exposure (Shashiprakash and Thomas, 2001)

General belief is that Class F fly ash is associated with increased resistance while Class CH is found to be not effective. Despite this general belief, Mehta's study (1986) showed that not all Class F ashes performed well and not all the Class CH ashes performed poorly. According to Mehta (1986), the mineralogical composition of the alumina-bearing hydration products formed before coming into contact with sulfate ions is the deciding factor. When ettringite presented as

the alumina bearing hydration products before the exposure to the sulfate ions, the PC-fly ash system performed satisfactorily or excellently. Oppositely, presence of monosulfate hydrate and/or C-A-H before the sulfate exposure resulted in poor performance, as ettringite is a stable phase while monosulfate is not stable in sulfate solution. Wheatear ettringite or monofulate/C-A-H will be formed depends on alumina-sulfate ratio. At higher alumina-sulfate ratio, formation of monosulfate/C-A-H will be favoured on the subsequent submersion into the sulfate solution where at lower ratio the ettringite will be favoured (Thomas et al., 1999).

Tikalsky and Carrasquillo (1992) stated calcium oxide content and calcium aluminate composition of the amorphous phase of fly ash determine whether a given fly ash increases or decreases the resistance. Increase in CaO content results in shorter cracking time for fly ash concrete. Fly ashes with increased portion of crystalline phases such as anhydrite, lime, periclase, sodalites, and tricalcium aluminates and fewer portions of inert minerals such as mullite, quartz, ferrite, spirel are more prone to sulfate deterioration. Calcium aluminate-rich glasses are more susceptible to long term sulfate expansion (Tikalsky and Carrasquillo, 1992). Tikalsky et al. (1990) stated that high calcium and low silica fly ashes are less resistance to sulfate attack. Figure 2.5 shows the relationship between calcium/silica content of fly ash and the deterioration that Tikalsky et al. (1990) obtained. As Figure 2.5 shows, fly ashes with higher calcium and less silica content took less time to crack whereas fly ashes with less Ca/Si ratios sustained longer period without cracking.

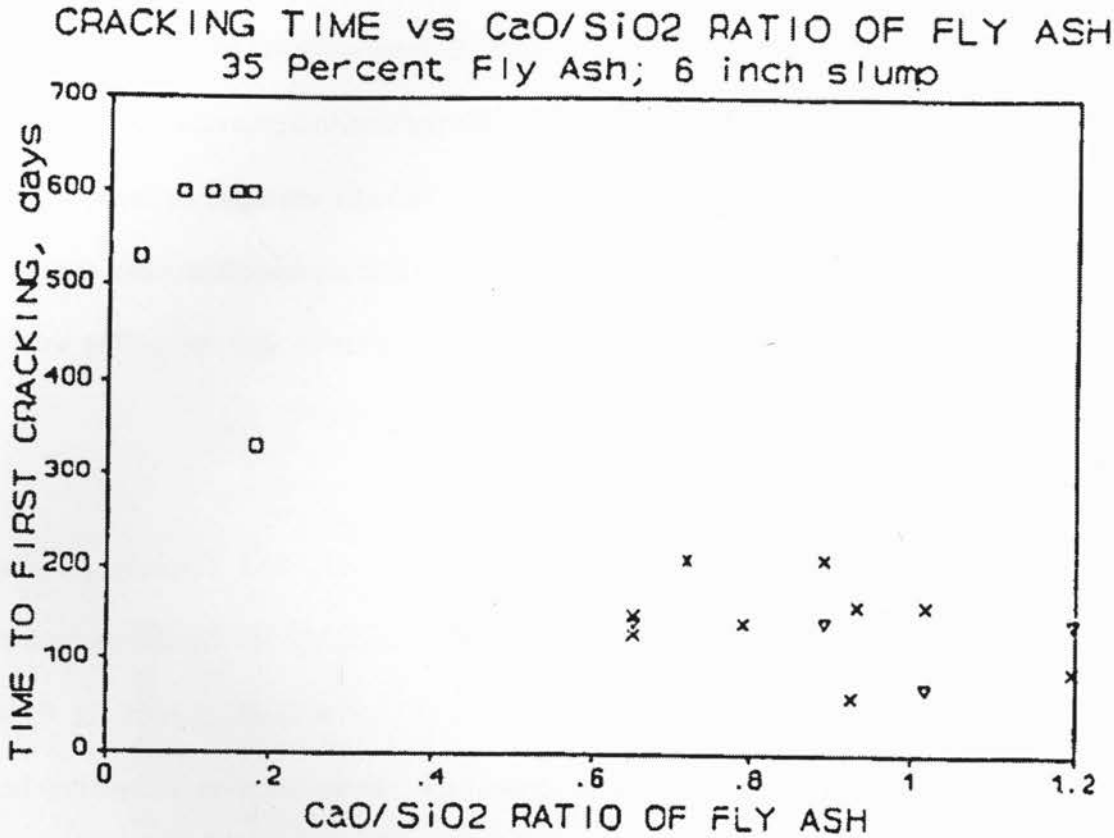

Figure 2.5: Relationship between calcium, silica content of fly ash and deterioration (Tikalsky et al., 1991)

Beside CaO, other aspects of fly ash might also play roles in sulfate resistance. Higher proportion of Fe_2O_3 may promote the formation of iron rich ettringite which is less expansive than the iorn-poor ettringite (Tikalsky and Carrasquillo, 1992). Dunstan (1980) related CaO and Fe_2O_3 determine the performance of any fly ash. A factor called R-value where R= (CaO% – 5)/Fe_2O_3 is derived based on experimental results. In R-value formula a 5% datum is applied to the CaO% based on the assumption that CaO contributed by mullite is less than 5% and is not a cause of sulfate deterioration (Mehta, 1986; Tikalsky & Carrasquillo, 1993). Over the time R-value formula's validity has been questioned as there are reported instances where the R-value failed to predict the performance of fly ash (Mehta, 1986; Thomas et al., 1999). In addition, a

major shortfall of R-value is that it fails to incorporate the alumina content which would, if high, produce C_4ASH_{12} and C-A-H (Mehta, 1986).

Mixing gypsum with Class CH fly ash was attempted by several researchers (Freeman and Carrasquillo, 1995; Shehata et al., 2008) to increase the performance of high calcium fly ash against sulfate attack. The idea is to add additional sulfate ions in the form of gypsum to consume calcium aluminates (Shehata et al., 2008). Adding excessive gypsum will cause unsoundness and internal sulfate attack (Freeman and Carrasquillo, 1995). Shehata et al. (2008) reported that addition of optimum gypsum content have reduced the 6-month expansion of 20% Class CH fly ash mortar bars by 70% compared to the expansion of the same 20% fly ash mix without any gypsum added. Freeman and Carrasquillo (1995) reported that, at the optimum gypsum addition, out of two fly ashes tested one fly ash at 35% replacement with Type II cement resulted in 21% reduction while another fly ash at the same replacement level resulted in 93% reduction in expansion compared to the control mix made up of 100% Type II cement.

2.3.7.3 Effect of Combination of Slag and Fly Ash on Sulfate Attack

Effects of ternary blends of fly ash and slag on sulfate resistance are rarely available in the literature. Research of Nehdi et al. (2004) includes ternary self-consolidating concrete blends of slag and Class F fly ash. Figure 2.6 shows the results from Nehdi et al. (2004) 9-month expansion of mortars bars submerged into 5% Na_2SO_4 solution. The test specimens were prepared using the extracted mortars of self consolidating concrete (SCC) mixes. The PC-fly ash-slag blend at 50-25-25% replacement level performed better than the control and binary blend of 50%PC-50% Fly ash. The exact reason for the better performance of ternary of slag-fly

ash was not expected due to the higher calcium content of slag compared to Class F fly ash. The reason for this behaviour of fly ash-slag mix was not investigated but Nehdi et al. (2004) speculated lower permeability due to faster hydration of slag could be a reason for the beneficial action of slag-fly ash ternary blend.

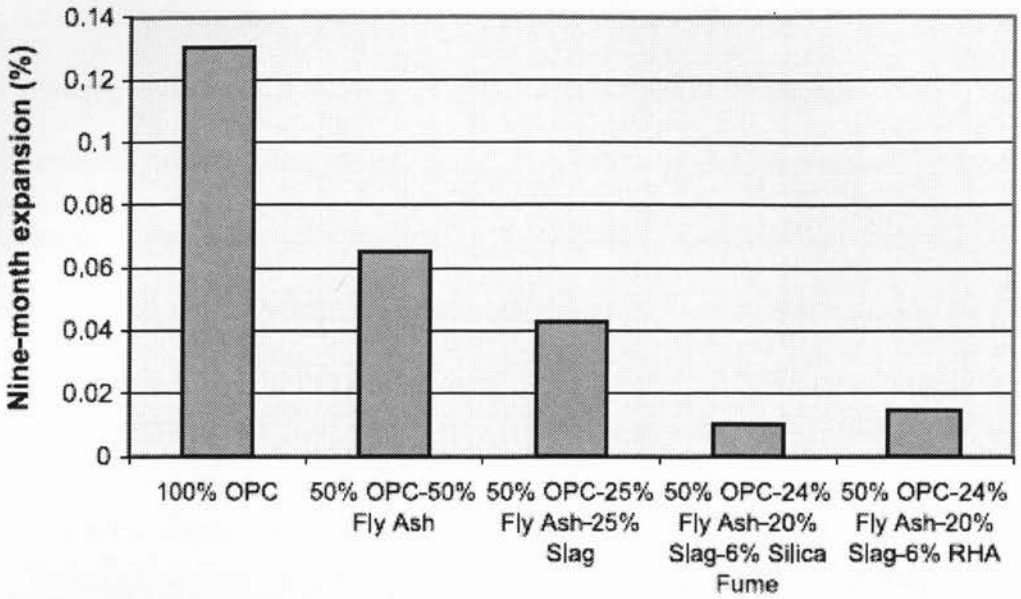

Figure 2.6: Performance of ternary blend of slag-fly ash under sulfate exposure (Nehdi et al., 2004)

2.3.8 Testing and Evaluation for Sulfate Attack (ASTM C1012)

ASTM C 1012 involves monitoring the length change of a mortar bar submerged in sulfate solution for 6 months. W/C is kept at 0.485 for mixes contain 100% PC while w/c for the mixes with SCM is choose to give the similar flow of 100% PC mortar at 0.485 w/c. From the prepared mortar, 25x25x285 mm bars and 50x50 mm cubes are made and cured at 100% RH and 35°C for the 24 hours followed by 23°C in limewater until the cube strength reaches 20 MPa. Once the mortar cube reaches 20 MPa, initial length measurement is taken for each mortar bar and submerged in 5% Na_2SO_4 solution at room temperature. Length measurements were taken after 1, 2, 3, 4, 8, 12, 13, and 15 weeks. After every measurement the bars are transferred into the newly prepared sulfate solution.

One of the main shortfalls of ASTM C1012 is that the sulfate concentration and its pH are not kept constant due continuous submersion of the bars and alkali leaching from the mortar bars, respectively. Further, the test procedure does not represent the field situations as the field concrete is often subjected to wetting and drying cycles and different temperatures around the year. Hence, laboratory results tend to over predict the ability of the mix compared to the field performance. Further, the temperature the test conducted does not take the formation of thaumasite into consideration. As discussed previously, the temperatures between 0 – 5°C favours the formation of thaumasite.

2.4 Alkali-silica Reaction

Alkali-silica reaction (ASR) is a deleterious reaction that takes place in concrete in the presence of sufficient quantities of reactive silica, alkali concentration, and moisture. As a result of ASR, a viscous gel product known as silica-gel forms which, in turn, absorbs water and swells (Saouma and Perotti, 2006).

In the alkali environment (pH ≥ 7), reactive silica grains are negatively charged by ionization of Si-OH group and by the disruption of Si-O-Si bonds as indicated by Equation 6.

$$Si\text{-}O\text{-}Si + OH^- \rightarrow SiOH + SiO^- \quad \text{[Equation 6]}$$

Once reactive silica grains are negatively charged, the positive ions are attracted towards the reactive grains and float around it, forming a layer known as diffusing double layer (Chatterji and Thaulow 2000; Prezzi et al., 1997). The negatively charged reactive grains induce silica ions to diffuse out as a result of which positive ions enter into the reactive grain. Hence, an expansion occurs as Na^+, Ca^{2+}, OH^- and water permeates to the reactive grains. The expansive pressure is the net pressure due to the entering OH^-, Na^+, Ca^{2+}, and water and the diffusing silica ions (Chatterji and Thaulow, 2000). The diffusion of silica is significantly influenced by presence of Ca^{2+} in the neighbourhood of the reactive grain (higher the Ca^{2+} lower the silica diffusion) (Chatterji and Thaulow, 2000). Further it is reported that presence of more bivalent ions compared to the monovalent ions and lower Na_2O_e in the gel system reduce the concrete expansion (Prezzi et al., 1997).

2.4.1 Influence of Aggregate Type on ASR

The rocks that contain reactive silica are cryptocrystalline quartz, and poorly crystalline/metastable silica. Examples include opal, quartz glass, colcanic glass, crypto-crystalline quartz, strained quartz, cristobalite, and tridymite (Fournier and Bérubé, 2000). There is no generalized correlation between particle size of the reactive aggregates and the level of expansion. Researchers have produced conflicting results regarding the effect of particle size on expansion. According to Diamond and Thaulaw (1974) and Fournier and Bérubé (2000), decrease in particle size increases the expansion; where Multon et al. (2008) showed an increased expansion with the increased particle size.

2.4.2 Influence of Alkali Content on ASR

Potential alkali sources are Portland cement, high alkali fly ash, aggregates incorporating alkali-bearing minerals such as zeolites, chemical admixtures, and mixing water. Increase in alkalinity in concrete increases the degree of reaction (Carrasquillo and Snow, 1987; Swamy and Al-Asali, 1988). Swamy and Al-Asali (1988) tested concrete prisms made up of cement alkalinities 2.5, 3.0, 3.5, 4.0, and 5.2 kg/m^3. As shown in Figure 2.7, expansion increased with increase in cement alkalinity. Further noting, increase from 4 to 5.2 kg/m^3 alkalinity resulted in significant increase compared to the increase from 3 to 4 kg/m^3 alkalinity cement. Similarly, decrease from 3 to 2.5 kg/m^3 resulted in significant reduction in expansion than that of 3.5 and 3.0 kg/m^3 alkalinity. It seemed, at least in this particular case, that the alkalinity levels 3 to 4 kg/m^3 is critical beyond which a significant change in expansion behaviour occurs (Swamy and Al-Asali, 1988).

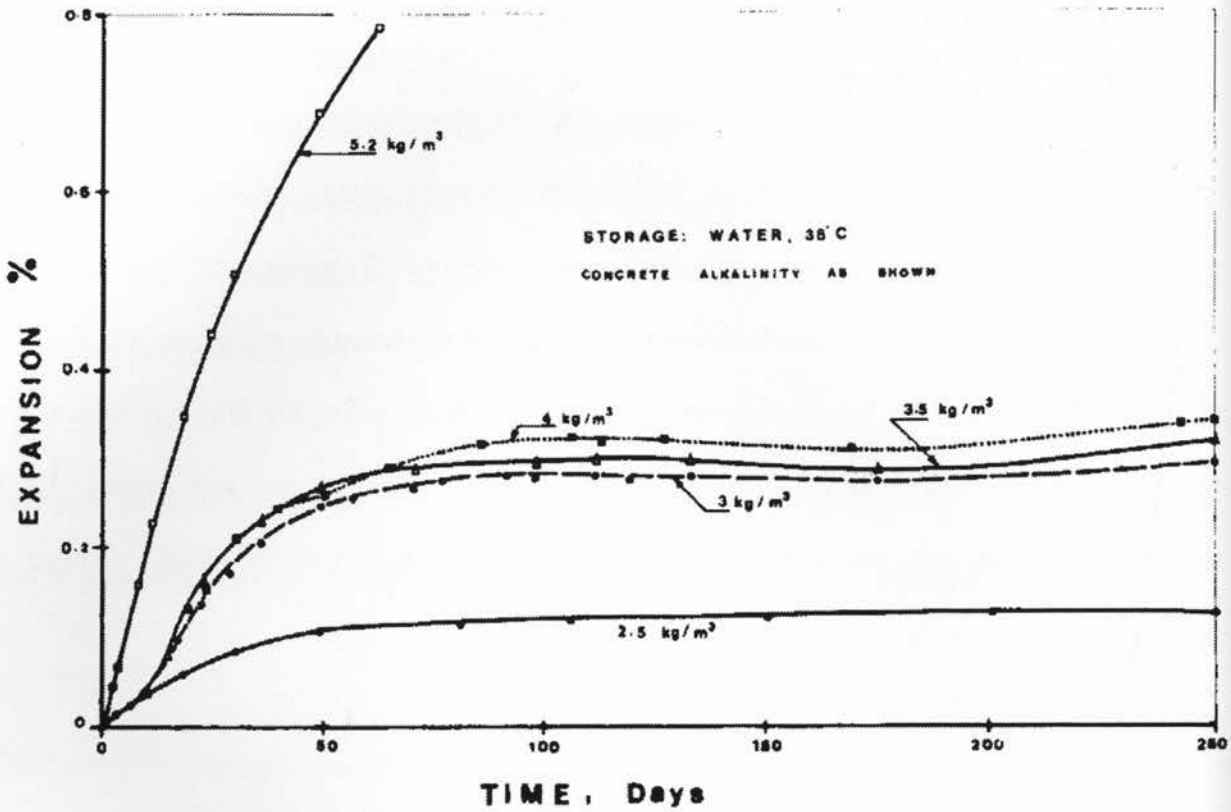

Figure 2.7: Influence of cement alkalinity on ASR expansion (Swamy and Al-Asali, 1988)

2.4.3 Supplementary Cementing Materials on ASR

In most cases, SCMs such as slag or fly ash help controlling ASR. Past research proved the beneficial action of slag, Class F fly ash, and silica fume against ASR (Thomas et al., 1999; Shehata and Thomas, 2000; Monteiro et al., 1997). Beneficial effect comes due to dilution of alkalis (when SCMs contain less reactive materials, ex. less alkali content, than Portland cement), pore size refinement (since SCMs lower permeability), pH reduction (through consumption of $Ca(OH)_2$), and alkalis binding abilities of SCMs (Monterio et al., 1997).

Duchesne and Bérubé (1994a,b) tested various SCMs to evaluate the role of pore solution alkali reduction and portlandite depletion in controlling ASR. They found that there is no "global" relationship exists between the degree of reaction and the depletion of portlandite and pore solution alkali reduction (Figure 2.8). However, specimens with less than 0.65 N (NaOH+KOH) pore solution alkali concentration expanded less than the CSA limit 0.04%. Hence, Duchesne and Bérubé (1994a,b) concluded that unless portlandite is almost completely depleted, pore solution alkali depletion is the dominant beneficial effect that SCMs bring, rather than portlandite depletion.

Ability of an SCM to reduce Ca/Si ratio of C-S-H influences ASR. Surface charge of C-S-H depends on Ca/Si ratio where higher the ratio leads to positive charge and lower ratio leads to negative charge. When surface charge of C-S-H is positive, cations are not incorporated into C-S-H but when the charge is negative, cations are incorporated into C-S-H. Thus, SCMs cause the alkali cations (eg. Na^+) to bind into C-S-H, making them unavailable for ASR (Monteiro et al., 1997).

2.4.3.1 Role of Fly Ash on ASR

Effectiveness of fly ash in mitigating ASR depends on three factors; fineness, mineralogy, and chemistry of fly ash (Shehata and Thomas, 2000, 2002; Malvar and Lenke, 2006). Often fly ash efficacy is related to its chemical constitutions mainly calcium, alkali and silica. This section reviews the literature on efficacy of fly ash based on the chemical constituents.

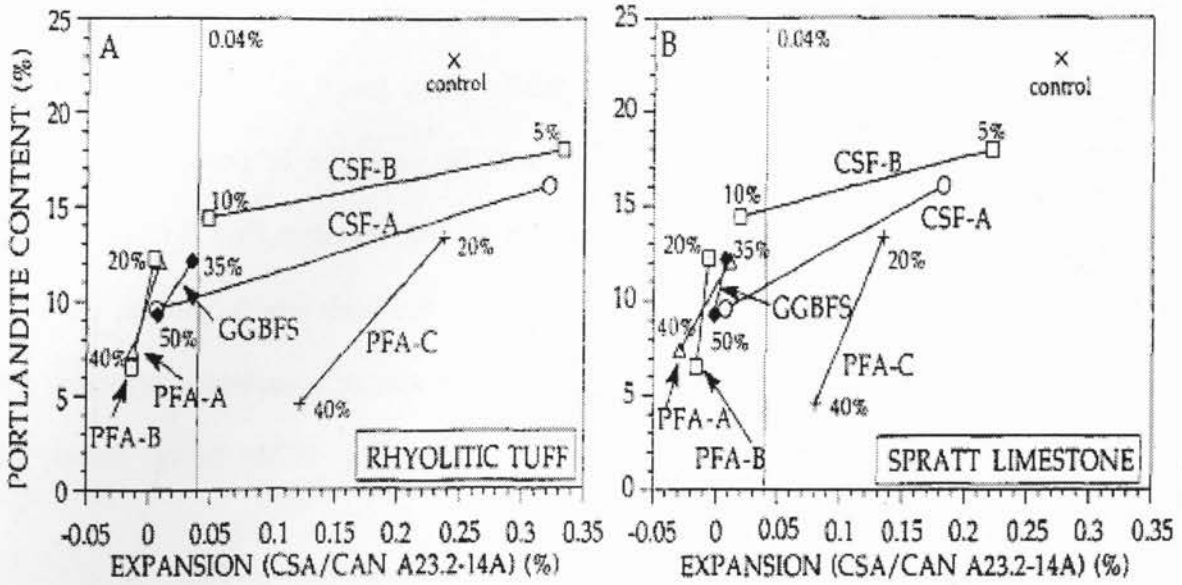

(Duchesne and Bérubé, 1993a)

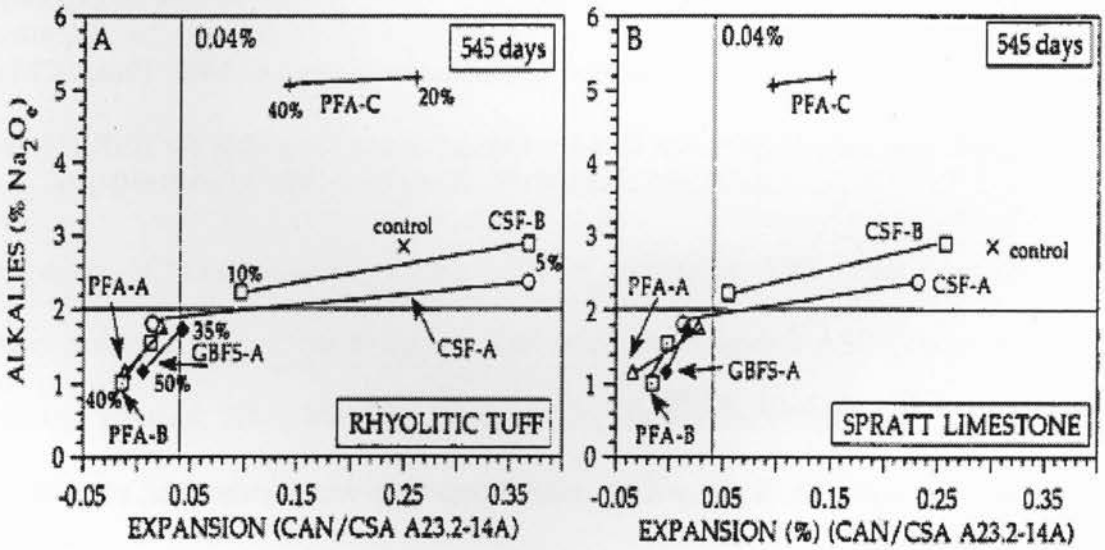

(Duchesne and Bérubé, 1993b)

Figure 2.8: Effect of $Ca(OH)_2$ consumption and pore solution alkalinity reduction on ASR expansion

Research shows that fly ash containing more than 10% CaO is not suitable for controlling ASR. 25% replacement of Class F fly ash provided good mitigation while Class CH fly ash required higher replacement level to obtain similar level of expansion reduction (Malvar et al., 2002; Shehata and Thomas, 2000).

CaO, SiO_2 and alkali content are the primary constituents influence the efficacy of a fly ash (Shehata and Thomas, 2000; Malvar and Lenke, 2006). Shehata and Thomas (2006) showed good correlation between the parameter Na_2O_e x CaO/SiO_2 of cementing blend and the amount of available alkali for ASR (Figure 2.9). The parameter Na_2O_e x CaO/SiO_2 was obtained from the chemical analysis of the cementitious materials and calculated based on the proportion of each cementitous material in a mix. The contributed alkalis were determined from the amount of alkalis leached from the hydrates of the paste into the surrounding alkali solution (Shehata and Thomas, 2006).

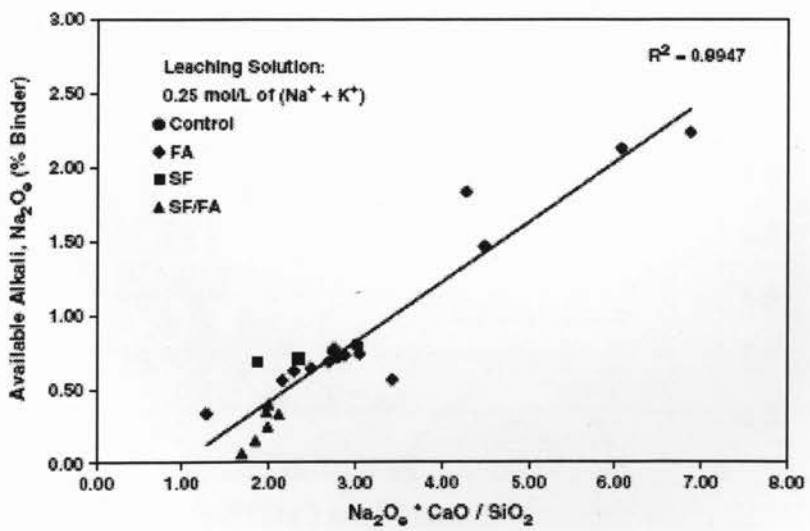

Figure 2.9: Relationship between the parameter of alkalies, calcium and silica oxides, and available alkali for ASR (Shehata and Thomas, 2006)

2.4.3.1.1 CaO and SiO_2 content of Fly ash

Figure 2.10 shows expansion of mortar bars as a function of SiO_2 and CaO of the fly ash, respectively. The analysis was done by Malvar and Lenke (2006) using several published data. As Figure 2.10 show, expansion is inversely proportional to SiO_2 content and linearly proportional to CaO content of the fly ash.

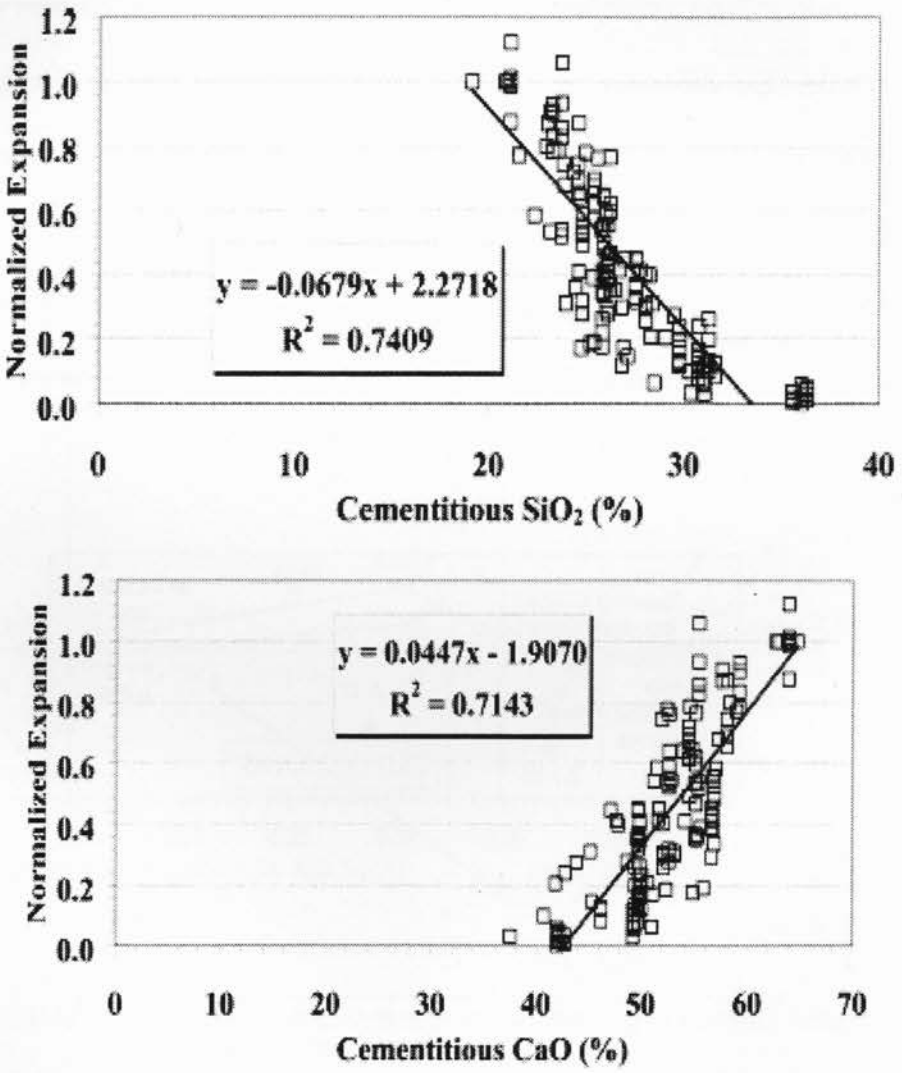

Figure 2.10: Influence of SiO_2 and CaO content of fly ash on ASR expansion (Malvar and Lenke, 2006)

Contarary to Shehata and Thomas (2006) and Malvar and Lenke (2006) who found a relationship between quantity of CaO in fly ash and the degree of reaction, Carrasquillo and Snow (1987) did not find a clear relationship between CaO content of fly ash and expansion as shown in Figures 2.11a and b where Figure 2.11a shows replacement of high alkali Portland cement (HAPC) and Figure 2.11b shows replacement of low alkali Portland cement (LAPC) with 28% fly ash. Duchesne and Bérubé (1994a) also reported that among the two fly ashes tested, the prism with the higher calcium (12.0% CaO; 75% SiO_2+Al_2O_3) content expended less than the one with the lower calcium fly ash (1.9% CaO; 64% SiO_2 + Al_2O_3). Duchesne and Bérubé (1994a) expressed the opinion that SiO_2 + Al_2O_3 contents of the fly ash plays the leading role rather than calcium content; and pointed out that in most cases low calcium fly ashes have more SiO_2+ Al_2O_3 than high calcium fly ashes, and the low calcium fly ash used in their study had less SiO_2 + Al_2O_3 than that of high calcium fly ash of their study.

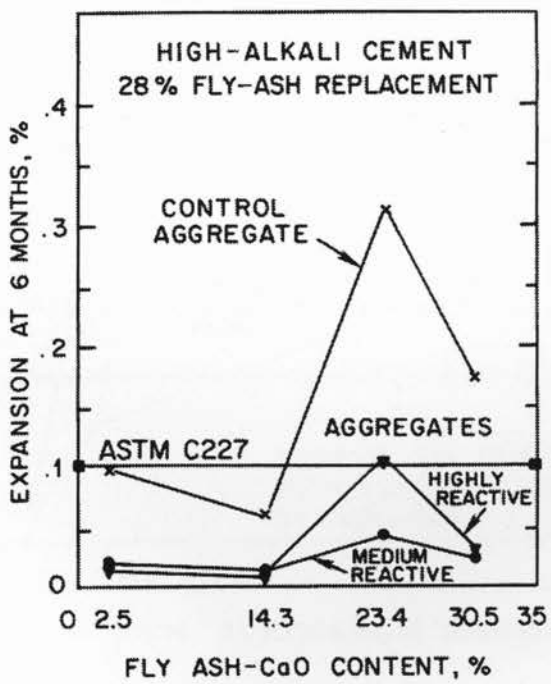

Figure 2.11 a)

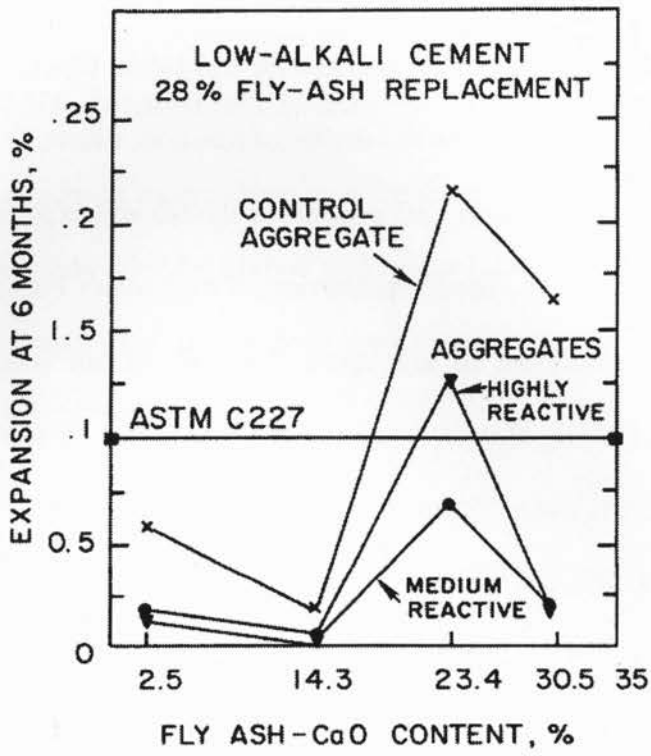

Figure 2.11 b)

Figure 2.11: Role of CaO of fly ash on ASR expansion (Carrasquillo and Snow, 1987)

Class F fly ashes have been very effective reducing the pore solution alkalinity compared to Class CH fly ashes. It was found that if a particular fly ash at certain replacement level was able to lower the pore solution alkalinity to 0.6 mol/L or less, then the expansion of concrete prism will be within the provided CSA/ASTM limit (0.04% expansion in two years) (Shehata and Thomas, 2000).

2.4.3.1.2 Alkali Content of Fly Ash

Carrasquillo and Snow (1987) showed that degree of ASR increases with the alkali content of fly ash. Carrasquillo and Snow (1987) used four different fly ashes along with HAPC in mortar bars.

Mortar bars were made with different aggregates (Highly reactive and control aggregates), and different fly ash replacement levels (17% and 34%). The expansion at 6 months is plotted against the alkali content of the fly ashes. Results, as in Figure 2.12, showed that increase in alkali content of fly ash increased the expansion. This could be due to availability of alkalis from fly ash for the contribution of pore solution alkalinity (Carrasquillo and Snow, 1987). Carrasquillo and Snow (1987) further showed that for fly ashes with less than 1.5% of alkali content the expansion of mortar bars decreases as the replacement level increases. However, for the fly ashes with greater than 1.5% alkali content, the expansion is higher than the control mixes if the mortar bars is not replaced with sufficient fly ash.

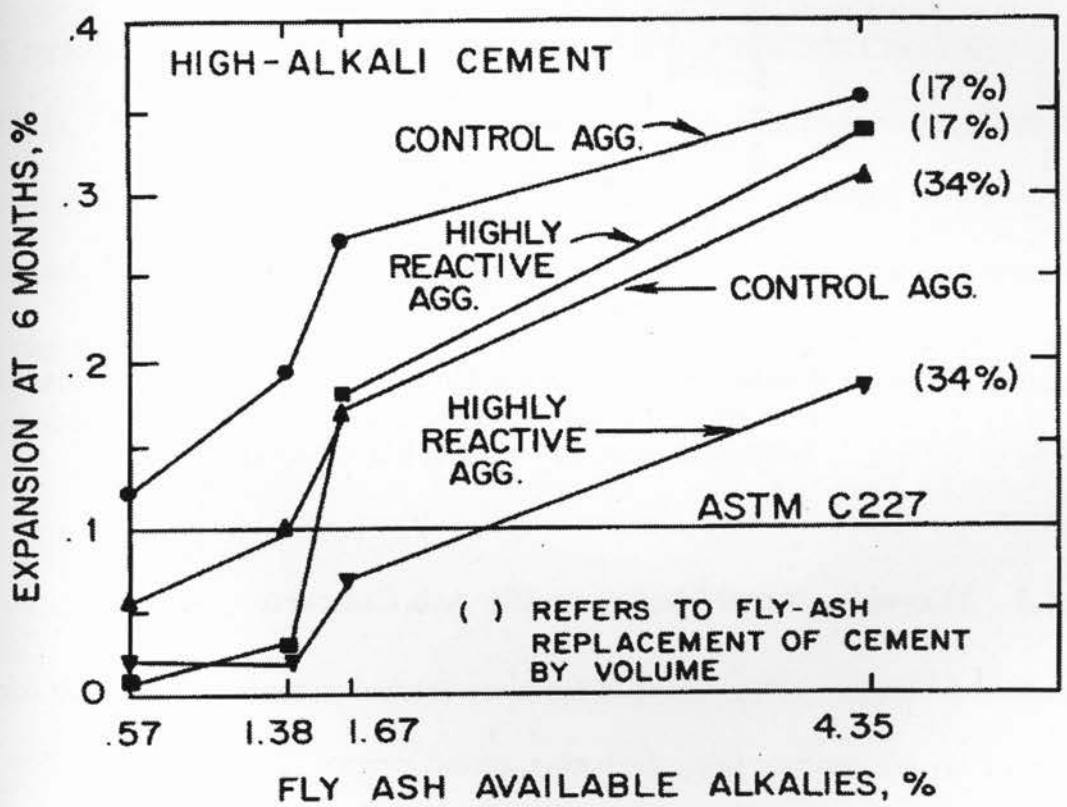

Figure 2.12: Role of alkali content of fly ash on ASR expansion (Carrasquillo and Snow, 1987)

Shehata and Thomas (2006) investigated the level of alkali leaching from pastes of various supplementary cementing materials into the surrounding alkali solution. They took two fly ashes of the similar calcium content (17.51% and 18.37%) but different alkali content (1.68% and 5.35%). Apparently, as in Figure 2.13, the fly ash with higher alkali content had leached more alkalis, indicating that the fly ash has more alkalis than its hydrates can bind (Shehata and Thomas, 2006). This high alkali contributed by fly ash was also associated with higher expansion of the corresponding concrete prisms (Shehata and Thomas, 2006).

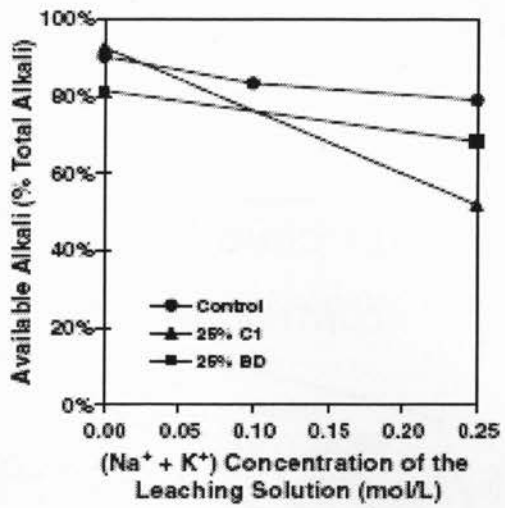

Figure 2.13: Available alkalis of two fly ashes, C1 and BD (Shehata and Thomas, 2006)
(Calcium Oxide: C1 = 17.51%; BD = 18.37%)
(Alkali content: C1 = 1.68%; BD = 5.35%)

2.4.3.1.3 Microstructural Studies on Fly Ash Concrete

Bleszynski and Thomas (1998) published the microstructual analysis performed on control and 40% Class F fly ash concrete using the back-scattered electron (BSE) technique. The analysis conducted on control concrete showed distinct calcium, sodium, and potassium bands at the reaction sites. The Ca/Si ratio is found to vary from the interface to the centre of the reactive

particle where the ratio is higher at the interface and lowered towards the centre. In the case of 40% fly ash concrete, no distinct high calcium band was observed (Bleszynski and Thomas, 1998). Bleszynski and Thomas (1998) stated that in Portland cement concrete presence of high calcium band of gel acted as a membrane which supplied alkalis to the reactive aggregate grains but prevented the gel to diffuse out, creating expansive pressure. Absence of high calcium band around the reactive grain in 40% fly ash concrete indicated that consumption of $Ca(OH)_2$ by fly ash is a reason for less expansion of fly ash concrete (Bleszynski and Thomas, 1998).

2.4.3.2 Role of Slag on ASR

Slag is beneficial at relatively higher replacement level (Figure 2.14); for instance, around 40% GGBFS replacement is needed to achieve the comparable benefit of 25% Class F fly ash (Malvar et al., 2002). The mechanism by which slag reduces the ASR expansion at higher replacements is not well understood yet (Thomas and Innis, 1998). However, researchers have found out that the concretes with slag have reduced and maintained the pore solution alkalinity lower than the control concrete (Duchesne and Bérubé, 1994b). Further, the analysis on ASR gel composition gives few indications the role of slag on controlling ASR.

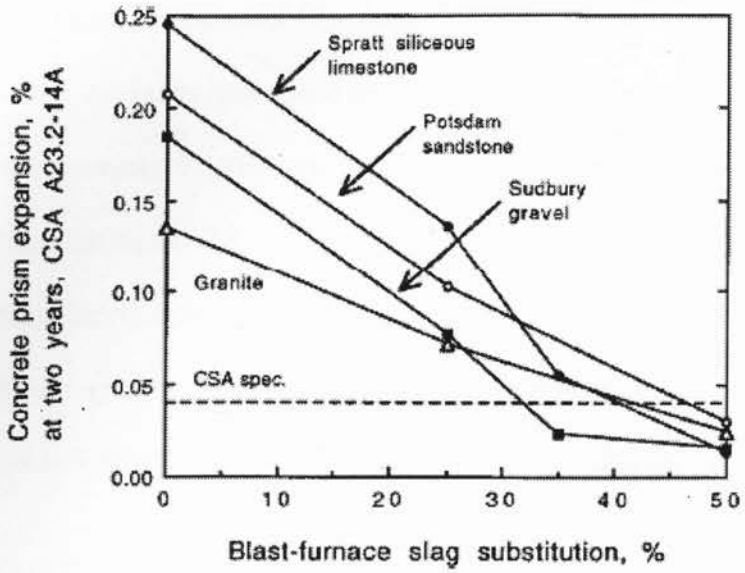

Figure 2.14: Effect of slag on ASR expansion (Rogers et al., 2000)

2.4.3.2.1 Studies on Gel Composition of Slag Concrete

Analysis performed by Arano and Kawamura (2000) showed that the gel of 20% slag mixture had less alkali content than the control mix; and the OH^- ions in the pore solution was reduced but only to a little extend compared to the control.

Monteiro et al. (1997) compared the effect of supplementary cementing materials on ASR expansion and obtained the gel composition for the corresponding mixes. They found 45% slag replacement did not have significant reduction but 55% slag replacement significantly reduce the expansion. This gap between 45 and 55% replacement level cannot only be explained based on the alkalinity of the SCM (i.e. slag) alone (Monteiro et al 1997). Gel composition showed that 55% slag had higher CaO content, less Na_2O_e than 45% slag mix; the ratios of CaO/Na_2O_e for 55% slag mix is higher than that of 45 % slag. These findings supported the double layer theory

that presence of more monovalent ions than divalent ions promotes the expansion (Monteiro et al., 1997; Chatterji, 2000).

2.4.3.2.2 Pore Solution Alkalinity of Slag Concrete

Rasheeduzzafar and Hussain (1991) reported that besides being as alkali dilutant, at higher replacement levels, slag is very active in removing alkalis from pore solution. Rasheeduzzafar and Hussain (1991) found that this beneficial effect is clear especially with lower alkali cement and as the alkalinity of the cement increases alkali removal ability of slag decreases. Duchesne and Bérubé (1994b) also produced results showing that alkalinity of the pore solution of slag concrete is less than that of control as in Figure 2.15.

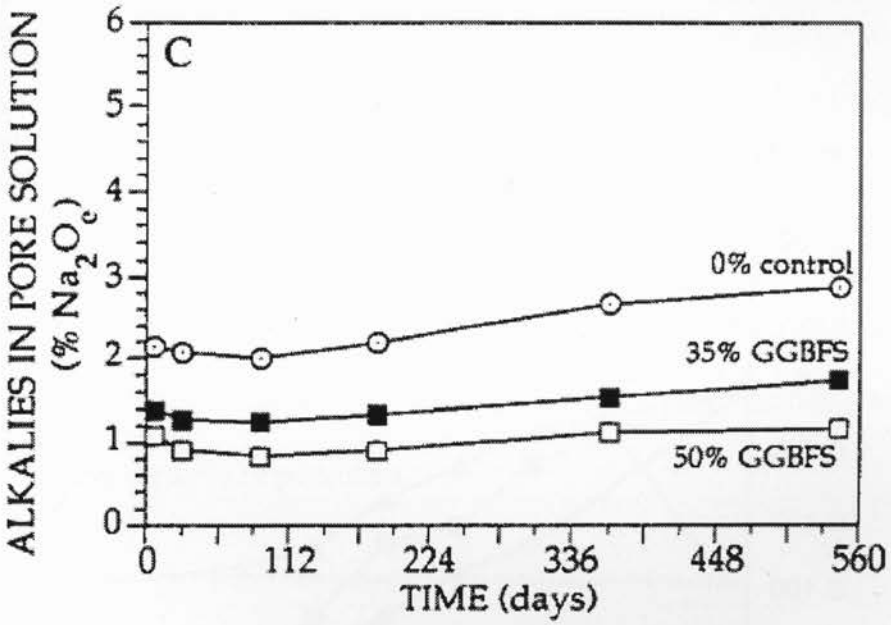

Figure 2.15: Effect of slag replacement on pore solution alkalinity (Duchesne and Bérubé, 1994b)

2.4.3.3 Effect of Combination of Slag and Class CH Fly Ash on ASR

If slag and Class CH fly ash are used individually, then their approximate individual replacements of slag and Class CH fly ash requires above 40% (Rogers et al., 2000; Shehata and Thomas, 2000). Shon et al. (2000) showed that when slag and Class CH fly ash are combined with Portland cement, as ternary blends, synergistic effect takes place resulting in enhanced resistance to ASR. Figure 2.16 shows that expansion of mortar bars soaked in 1M NaOH solution at 80°C (AMBT). Figure 2.16 indicates that ternary blend mortar bars expanded less than the binary blends of slag and fly ash at all replacement levels. Further it is evident that in order to fall below the potentially reactive criteria (0.1% at 14 day as indicated in Figure 2.16), around 30% Class CH fly ash and 40% slag is needed in binary blends. However, it is noticeable in Figure 2.16 that 15% fly ash + 25% slag ternary blend met the 0.1% limit easily.

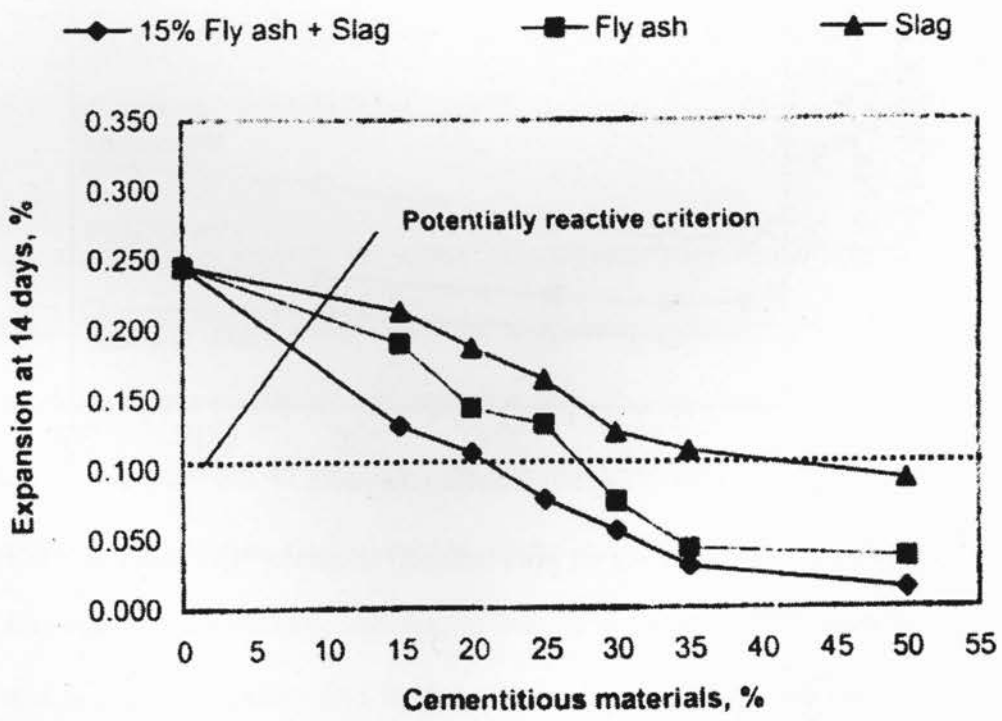

Figure 2.16: Teranay blends against ASR (Shon et al., 2000)

2.4.4 Laboratory Evaluation for ASR

2.4.4.1 Accelerated Mortar Bar Test

Accelerated mortar bar test (AMBT) is adopted as a standard test by ASTM C 1260, AASHTO T 303 and CSA A23.2-25A. In CSA A23.2-25A, mortar bars are casted using the specified aggregate gradation, cementing materials and a w/c 0.5 (w/c varies between aggregate types). Produced specimens are cured at in the standard curing room for 24 hours. After demolding, the mortar bars are submerged in water and heated at 80°C for another 24 hours after which the initial reading is taken. After the initial reading, the bars are submerged in 1N NaOH solution at 80°C. The test has been criticised as being conservative in the sense that in reality the concrete may not be exposed to high concentration external alkali source and the reaction may not last longer (Malvar et at., 2002). And, it is also likely that alkali content of the cement will have little, if any, influence on the expansion since the plenty of alkalis are provided from the solution (Malvar et al., 2002). However, this test is a quick screening tool to detect potential reactive aggregates and to detect slowly reacting aggregates (Malvar et al., 2002). In concrete, the SCMs control the ASR by alkali binding where as in AMBT SCMs limit the expansion by reducing the permeability. Further, AMBT supplies external alkalis which makes difficult to evaluate the ability of alkali binding capacity of pozzolans.

2.4.4.2 Concrete Prism Test

Concrete mixtures are casted using the reactive aggregates, cementitious materials and w/c ranging from 0.42 to 0.45 into the moulds of 25 x 25 x 285 mm. The alkali content is brought to 1.25% Na_2O_{eq} of the Portland cement mass. After 24 hours of initial curing in the standard

curing room, the specimens are demoulded, initial reading taken and placed in 100% RH and 38°C environment. Length change is monitored periodically at least for 1 year if no SCMs are used and 2 years if SCMs are used. Unlike AMBT, in the prism test, no alkalis are fed externally; hence, any alkali contribution has to come from the concrete itself. Though prism test better represent the real situation, it is less conservative and may fail to detect slowly reacting aggregates; and the test conditions permit the alkalis to leach out of the concrete (Malvar et al., 2002; Thomas et al., 2007).

2.4.4.3 Alkali Leaching Test

Shehata and Thomas (2006) described a method to evaluate the ability of a paste to bind alkalis. The experiment stats with preparation of paste sample(s) w/c of 0.5 and curing over water (23°C) for 28 days. After the curing period, the paste is to be broken into pieces and screened between 1.25 and 0.18 mm sieves. Then the broken fragments get transferred into bottles with various concentrations of pre-determined alkali solution (0mol/L, 0.1M, 0.25M and 0.4M). For each alkali concentration, one control bottle kept without any paste fragments. The bottles are tightened and left for a period of 3 months to achieve chemical equilibrium. Then, the change in concentration of the surrounding alkali solution is measured using flame photometer with respect to the control bottle. Increase in concentration is attributable to leaching of alkali from the paste. More alkali leaching would indicate the availability of more alkalis for ASR (Shehata and Thomas, 2006).

2.5 Salt Scaling

Salt scaling is a deterioration mechanism arises due to the use of deicer salt on concrete surfaces. The damage is in the form of removal of cement paste chips and, sometimes, aggregates. Unlike freeze-thaw, salt scaling does not have an impact of mechanical properties of concrete such as strength or stiffness (Valenza and Scherer, 2007a). However, scaled concrete may create a path for water and/or other chemical to enter to further reduce the durability. Researchers found that regardless of type of salt used a pessimum salt concentration exists around 3% (Çopuroğlu and Schlangen, 2008; Valenza and Scherer, 2007c). However, most of the mechanisms used to explain the salt scaling is from freeze-thaw deterioration that fail to explain the existence of pessimum salt concentration (Valenza and Scherer, 2007c).

One speculation is that different thermal strain forms as the ice melts. Presence of salt reduces the melting point of ice. Once the melting point of ice is reduced, it would obtain the heat necessary to melt from the concrete surface. Heat will be lost from the surface but the core remains at the same temperature, resulting in differential temperature throughout the concrete body. Differential temperature causes stresses to develop at the surface (Valenza and Scherer, 2007b).

Second thought is that once the concrete surface is pooled with salt solution, pore solution will start to equilibrate with the salt solution. The increase of salt concentration in the pore solution will increase the degree of saturation at the surface. Increased level of saturation will results in frost action at the surface. Depth of concrete that equilibrate with the pool of solution on the surface increases with time (Valenza and Scherer, 2007b).

A third thought is that when the ice form from the salt solution, ice does not incorporate any salt ions; hence, the concentration of the remaining solution increases when the salt solution frozen. A pressure, called osmotic pressure, is created as a result of movement of liquid from low concentration region to higher concentration region. In the case of salt scaling osmotic pressure is created as water moves from the regions where ice formed to the regions of remaining brine solution (Valenza and Scherer, 2007b).

2.5.1 Effect of Air Content on Scaling

Air entrainment reduces the scaling in two ways; by reducing bleeding and by helping to relive the hydraulic pressure (Valenza and Scherer, 2007a,b; Pigeon et al., 1996). When bleeding is reduced the resulting surface will be stronger which would provide more resistance. Surfaces finished with accumulated bleeding water tend to be weaker, porous, and may contain pockets that would transport salt solution below the surface (Mindess et al., 2003). Figure 2.17 shows that there is a huge improvement when the concrete is air entrained.

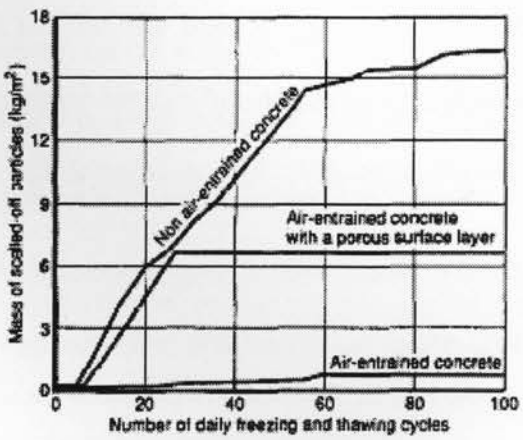

Figure 2.17: Effect of air entrainment in salt scaling resistance (Pigeon et al., 1996)

2.5.2 Effect of Salt Concentration

None of the above given explanation for the occurrence of salt scaling account for the pessimum amount. Valenza and Scherer (2007c) proposed a mechanism saying that since ice layer contracts faster than the concrete, contraction of ice layer creates tensile stresses. Based on the viscoelastic analysis of the stresses on ice, Valenza and Scherer (2007c) stated that pure ice does not crack in the freezing temperature range of salt scaling tests. When the concentration is pessimum, the ice contains brine pockets and flaws that would promote the cracking of ice. Once the ice is broken, tensile stress develop in concrete along the perimeter of the broken ice pieces. When the concentration of the solution is high, the ice layer is not strong enough to exert stress as it contains too much brine pockets (Valenza and Scherer, 2007c).

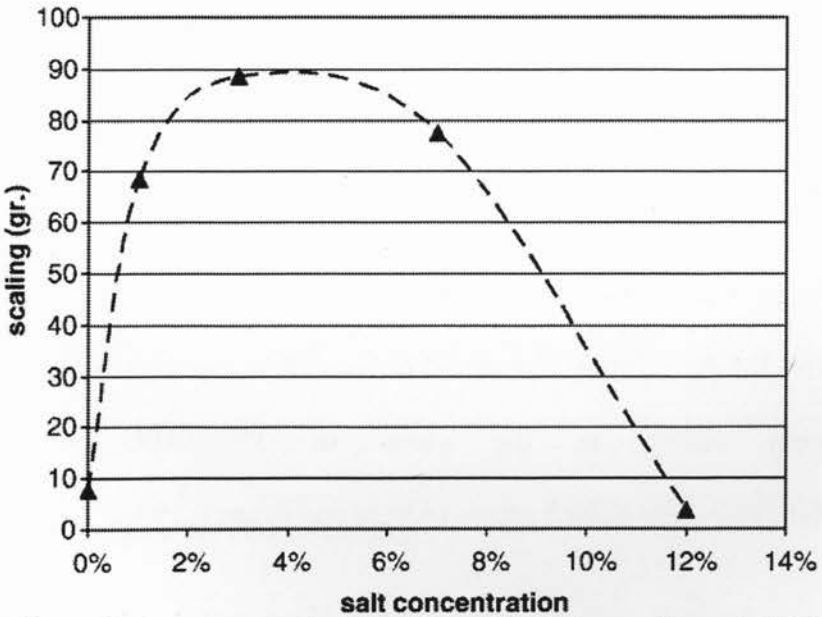

Figure 2.18: Effect of salt concentration on salt scaling (Çopuroğlu and Schlangen, 2008)

2.5.3 Effect of Water-Cement Ratio and Strength

Scaling resistance increases as the w/c ratio decreases. Lower w/c will result in less bleeding and higher strength. Less bleeding will produce stronger surface to resist salt scaling. It is also worth to note that lower w/c will result in lower permeability and lower permeability may be susceptible for larger hydraulic pressure (Panesar and Chidiac, 2007; Valenza and Scherer, 2007a).

2.5.4 Effect of Curing Conditions

Afrani and Rogers (1994) performed salt scaling test under various curing conditions; moist room at 23°C, covered with wet burlap and polyethylene in ambient outdoor conditions, curing compound in ambient laboratory air, and curing compound in ambient outdoor air. The tested concrete includes Control HAPC, Control LAPC, 50%slag, 25% Slag, and 51%fly ash+25%slag. Afrani and Rogers (1994) did not remove the curing compound prior to the test. The wet burlap in outdoor conditions performed better than laboratory moist room curing or laboratory curing compound curing with an exception of one case; 50%GGBFS + 50% HAPC. Curing compound has performed better than moist room curing in mixes of 100% LAPC, but worsened the mix 50%GGBFS +50%HAPC. Curing compound did not show any significant difference compared to moist room curing in the cases of 75%HAPC + 25%GGBFS and 24%HAPC+51%PSFC+25%GGBFS mixes (Afrani and Rogers, 1994).

Bilodeau et al. (1991) tested control (100%PC) , 20% Class F fly ash and 30% Class F fly ash concretes with different curing periods; 3, 7 and 14 days using curing membrane. After the curing periods of 3, 7 and 14 days, the specimens were brushed to remove the membrane from

the surface. The specimens were dried for various periods before starting the cycles. The specimens cured with membrane showed significant improvement in scaling resistance. Further, extended moist room curing did not have any significant improvement in scaling resistance. In fact, few mixes have shown adverse effects due to longer curing in the moist room. For example, 20% fly ash mix cured in the moist room for 3 days and dried 4 weeks scaled less than the same mix cured in the moist room for 7 days and dried for 4 weeks. Similar observation was made on 30% fly ash mix for 3 days curing and 14 days curing (Bilodeau et al., 1991).

2.5.5 Effect of Cementing Materials on Salt Scaling Resistance

Contradictory results exist regarding the supplementary cementitious materials resistance to salt scaling. Some research has shown that incorporating SCMs into the mix worsen the situation where other research has shown that SCM mixes performed well (Bouzoubaa et al., 2008).

In the laboratory produced scaling slabs, porous layer on the concrete containing SCMs is thicker than concrete without SCMs. Such a noticeable porous layer is not observed in the field. Presence of a thicker porous layer in lab slabs with SCMs may give an indication that SCMs perform poorly with respect to salt scaling (Bouzoubaa et al., 2008).

2.5.5.1 Role of Fly Ash on Salt Scaling

Concrete incorporating fly ashes have shown more scaling than the control specimens (Bouzoubaa et al., 2008). Common reasons attributed to the poor performance of fly ash are that fly ash acts as inert materials at the early stage, reducing the hydration rate and increasing the

effective w/c. Also, fly ash increases the more porous interfacial transition zones at the early stages that will promote the scaling (Marchand et al., 1997; Thomas, 1997).

Figure 2.19 presents the results from Bouzoubaa et al. (2008) showing fly ash concrete scaled a lot more than the control concrete. In addition, Figure 2.19 shows the discrepancy between the testing procedure, namely ASTM and Bureau de normalization de Quebec (BNQ). The discrepancy between the two test standards indicates that specimen preparation and finishing techniques influence the results to a greater extend. Such a discrepancy is attributed to the differences in testing procedure between two standards. Unlike ASTM, BNQ does not require to brush the bleed water. Determining the end of bleeding is subjective and if brushing is done too early or too late, the air void system at the surface may be destroyed. Finishing the concrete right after screeding is considered as a better option rather than waiting for bleeding to stop when no significant bleeding is expected. Also, BNQ standard requires the slabs to be submerged in the salt solution for 7days prior to the beginning of the cycles. This step will make the pore solution in equilibrium with the solution on the top of the slabs, thus reducing the osmotic pressure. Reduction in osmotic pressure could also be a reason for improved performance in BNQ test standard (Bouzoubaa et al., 1998).

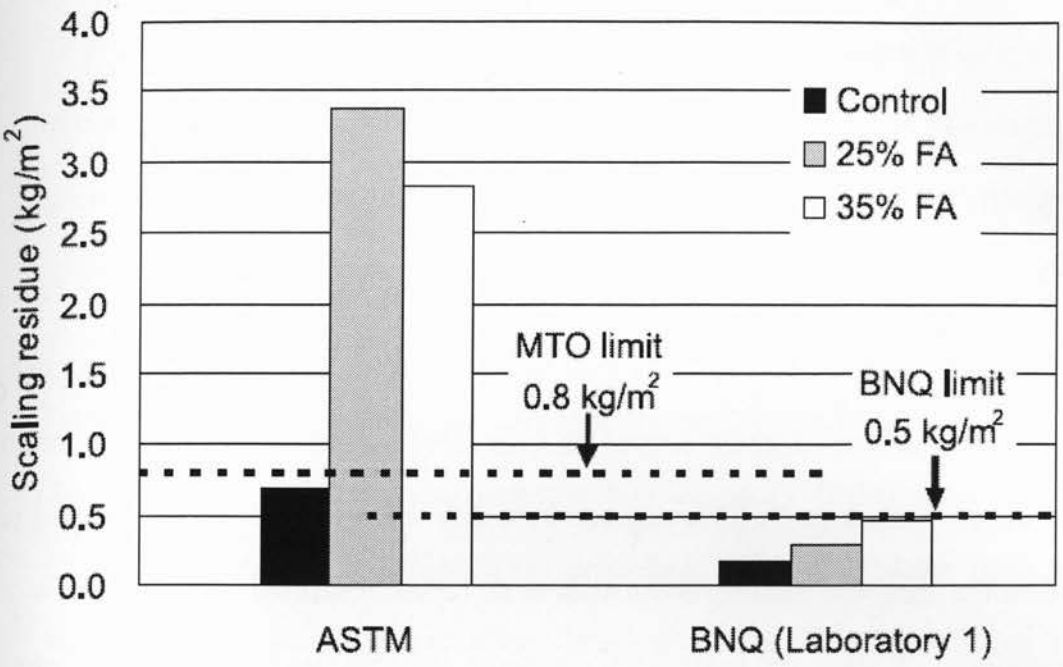

Figure 2.19: Effect of laboratory test procedure in salt scaling residue (Bouzoubaa et al., 2008)

Bilodeau et al., 1994 investigated the susceptibility of air-entrained concrete incorporating fly ashes from 8 different sources according to ASTM standard. All the concrete with fly ash performed poorly with the ASTM scaling rating of 5 after 50 cycles. The poor performance was partly attributed to the finishing practices and to the lower compressive strength at the beginning of the cycles (Bilodeau et al., 1994).

Talbot et al. (2000) conducted ASTM C 672 on concretes with Class F fly ash and Class CH fly ash at replacements of 40% and 20%. Concrete with 20% and 40% Class F resulted in 2.01 and 2.90 kg/m^2, respectively. Concrete with 20% Class CH fly ash resulted in 2.77 kg/m^2. The control 100% PC concrete ended up with 1.09 kg/m^2. This indicates that the concrete with fly ash (both low calcium and high calcium fly ashes) perform poorly. However, Class CH fly ash have

shown to perform slightly better than Class F fly ash, as generally Class CH fly ash is able to retain more air due to its lower organic content (Thomas, 1997).

2.5.5.2 Role of Slag on Salt Scaling

Lack of consistency exists on the performance of slag against salt scaling. For example, Bouzoubaa et al. (2008) showed incorporating 25% slag in laboratory produced slabs (as per ASTM) to perform better than the control whereas 35% slag scaled more than the control. When the test was performed on the 25% slag and 35% slag cores, both 25% and 35% slag performed better than the control. Further, Bouzoubaa et al. (2008) tested the 35% slag mix according to BNQ standards. When tested using BNQ standards, the 35% slag mix performed better than the control. The possible reasons for such a deviated behaviour between the two test standards are discussed in 2.5.5.1.

Panesar and Chidiac (2007) performed statistical studies using the published experimental results. The study correlated the slag content with the scaling residue. The general trend reported is that increasing the slag content increases the scaling. The scaling of formed surface is less than that of on finished side due to bleeding and destruction of the air void system.

There are a few possible reasons postulated in the literature for the poor performance of slag concrete. They are,

1. Excessive bleeding. Delayed setting time of slag will result in longer bleeding period. Unless steps are taken to carefully monitor and to judge the end of bleeding period, the concrete may be finished prematurely before bleeding stopped. Finishing before bleeding stops will leave a weaker layer at the surface (Afrani and Rogers, 1994).

2. Inadequate length of curing. The heat of hydration for slag concrete is normally less than that of a plain PC concrete. Relatively low internal curing temperature may result in coarser and less matured microstructure for slag concrete. Extended curing period for slag concrete may allow denser hydration products to form that may in turn enhance the scaling resistance (Afrani and Rogers, 1994).
3. Carbonation. $Ca(OH)_2 + CO_2 \rightarrow CaCO_3 + H_2O$. Firstly, carbonation in slag concrete forms products called aragonite and vaterite that are more soluble than calcite. Secondly, carbonation in slag concrete may decalcify C-S-H as availability of $Ca(OH)_2$ will be reduced through the pozzolanic reaction of slag. Both of these actions will result in coarser micro structure in slag concrete making it more vulnerable for salt scaling (Valenza and Scherer, 2007a,b; Stark and Ludwig, 1997). Figure 2.20 a) shows that as the carbonation on slag concrete increases, the scaling deepens. Figure 2.20 b) shows that capillary porosity increases for carbonated slag concrete compared to the non-carbonated slag concrete; and, insignificant difference in capillary porosity of carbonated and non-carbonated plain concrete mix (Stark and Ludwig, 1997).

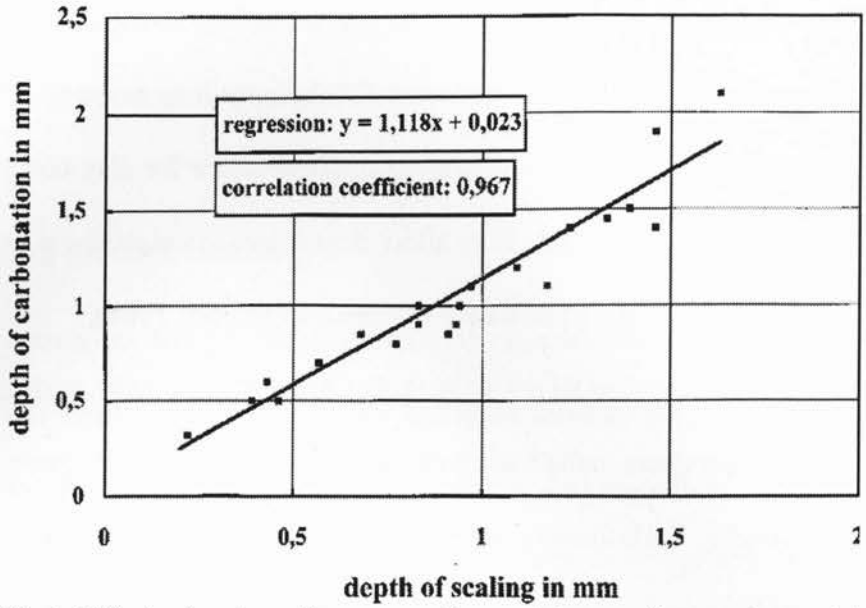

Figure 2.20 a): Effect of carbonation on scaling resistance of concrete containing slag (Stark and Ludwig, 1997)

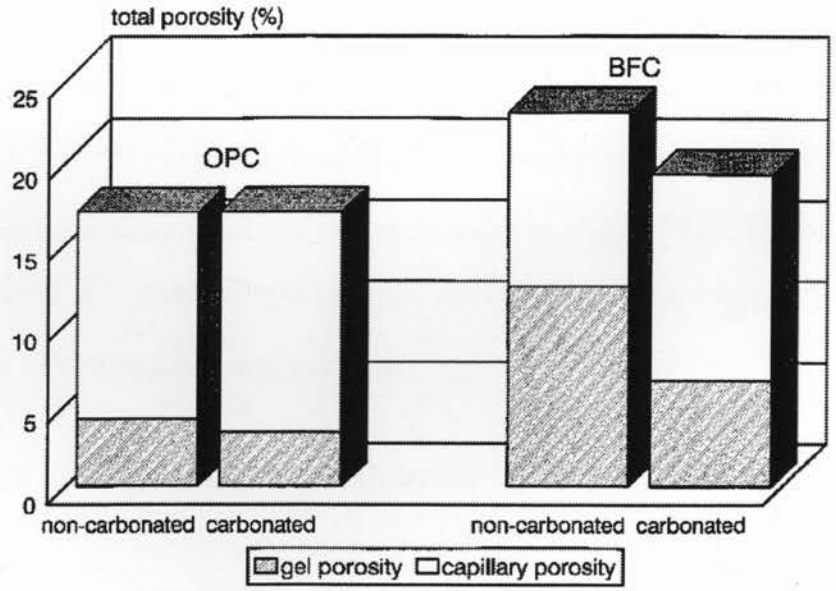

Figure 2.20 b): Effect of carporation on capillary porosity of concrete with and without slag (Stark and Ludwig, 1997)

2.5.5.3 Effect of Combination of Slag and Fly Ash on Salt Scaling

Hooton and Boyd (2007) studied concrete with 10% Class CH fly ash (CaO = 35.6%0 and 25% slag (with Blaine fineness 432 m^2/kg). Their results show that when tested according to MTO LS-412, the ternary blend did not perform better and performed poorly compared to 35% slag, 25% slag, 15% fly ash, and 100% OPC (Table 2.1 shows the results performed at three laboratories, MTO, Lafarge and U of T).

Table 2.1: Scaling results of Boyd and Hooton (2007)

		Average cumulative mass loss (kg/m^2)		
Mixture	Composition	MTO	Lafarge	Univ. of Toronto
L1	50% slag	1.60	2.02	1.44
L2	35% slag	0.50	1.24	—
L3	25% slag	0.60	0.52	—
L4	25% slag+10% fly ash	1.40	1.55	1.40
L5	15% fly ash	0.36	1.24	—
L6	100% OPC	0.14	0.13	—

2.5.6 Laboratory Evaluation for Salt Scaling

In ASTM C 672: Standard test method for scaling resistance of concrete surfaces exposed to de-icing chemicals, concrete specimens of 300x300x75 mm are made by consolidating 70 times with the steel rod followed by strike off of the excessive concrete with a wood trowel. Final finishing is not carried out until the bleeding stops. Once the bleeding stooped, the wood trowel is used to finish the surface with maximum of three strokes. The concrete slabs are then moist

cured at 23°C and 100% RH for 14 days followed by another 14 days of drying period at 23°C and 50% RH. After the drying period 4% $CaCl_2$ solution is pooled on top of the concrete slab to a depth of 6 mm and exposed to the freezing and thawing cycles. Each freeze/thaw cycle is 24 hours long whose freezing portion consists of 16 – 18 hours at -17.8±2.8°C and thawing portion consists of 6 – 8 hours at 23±3°C. When the depth decreases due to evaporation, water has to be added to bring the depth 6mm. The scaled masses are collected every 5 cycles for 50 cycles by washing the slab with water, and the collected masses are dried to a constant mass at 105°C before weighed. In addition to the collection of scaled concrete, visual rating is done based on a scale 0 to 5 where 0 is given for no scaling, 1 is given to slight scaling, and 5 is given to severe scaling.

MTO LS-412 is similar to ASTM C672 with few differences. MTO standard requires using NaCl instead of $CaCl_2$. The standard does not specify to wait for bleeding to stop before finishing. However, places emphasise on finishing by requiring to use wood trowel with the maximum of 2 stokes; back and forth once. The solution depth has to be maintained at 6 mm and if the depth decreases the NaCl solution has to be added to bring the depth to 6 mm where in ASTM standard water is added to maintain the depth at 6mm.

MTO LS-412 specifies to use 3% NaCl solution to wash the scaled off particles during the collection process every 5 cycles where in ASTM C672, water is used to wash off the particles. LS-412 specifies the limit of 0.8 kg/m^2 after 50 cycles as the satisfactory performance for a concrete.

2.6 Freeze-thaw Damage

Non-air entrained concrete is not immune to freeze-thaw cycles (Mindess et al., 2003). Different theories have been cited to explain the mechanism(s) of freeze-thaw damage. Among them, hydraulic pressure theory and osmotic theory are popular. The former is attributed to the pressure due to the volume change when the ice forms. The later is attributed to the pressure created by the movement of water from lower solute concentration to higher solute concentration. As the ice forms, there is a 9% increase in volume. This increase in volume compresses the unfrozen water in the pores. Unless, there is enough room to accommodate the unfrozen water that is being compressed, hydraulic pressure will be created (Mindess et al., 2003). Osmotic theory states that when the ice in pores freezes, the solute concentration of remaining unfrozen water increases near the freezing sites. Due to osmosis between the unfrozen water around the freezing sites and the water in the unfrozen sites, water will move causing osmotic pressure (Mindess et al., 2003).

Entraining air bubbles within the concrete increases the immune to freeze-thaw damage. Entrained air bubbles function as pressure chambers where squeezed water will enter and form ice. Once ice is formed inside the air bubble, more water will be drawn towards the bubbles due to osmotic pressure. In turn, the amount of water available in cement paste is reduced. Hence, air entrained concrete is more resistance to freeze and thaw damage (Mindess et al., 2003).

2.6.1 Role of Fly Ash on Freeze-thaw damage

Bilodeau et al. (1994) tested eight different Type F fly ashes under freeze and thaw cycles using ASTM C 666. After, 300 cycles all the mixes performed well where the lowest durability factor was 96. The researchers extended the test period to 1000 cycles after the excellent performance of the specimens at 300 cycles. Even after 1000 cycles, none of the tested specimens performed unacceptably. However, after 1000 cycles, all the tested specimens showed significant surface scaling of 2.24 to 10.93%. In terms of length change, the specimens expanded a little after 300 cycles with the maximum value reported 0.02%. Bilodeau et al. (1994) indicated that even after 1000 freeze-thaw cycles, the core of fly ash concrete remained in very good condition but surface scaling was observed. Malhotra (1990) have also reported results showing that air entrained concrete incorporating around 55% Class F fly ash performed well with durability factor of 99 after 300 cycles.

2.6.2 Role of Slag on Freeze-thaw Damage

Slag does not possess any detrimental effect from freezing and thawing cycles when aggregates are non-frost susceptible, air entrainment is adequate, and adequate strength gain is achieved prior to exposing to freeze and thaw cycles (Hooton, 2000).

2.6.3 Laboratory Evaluation for Freeze-thaw Damage

ASTM C 666 is widely used in North America to evaluate freeze-thaw resistance of concrete specimens. In this method, concrete specimens are subjected to 300 freeze and thaw cycles. Each cycle consist of lowering temperature from 4.4°C to – 17.8°C and raising it back from –

17.8°C to +4.4°C in 2 to 5 hours. Durability measurements are taken at least after every 35 cycles. Durability is accessed in terms of reduction in dynamic modulus, weight change and length change. A 40% reduction in dynamic modulus of elasticity or 0.1% expansion is specified as the limits of satisfactory performance. Further, this test allows the concrete to be submerged fully in water or not submerged during the freezing portion of the cycles but requires the thawing portion to be carried out in water.

Chapter 3. Materials and Experimental Program

3.1 Materials

The properties of the materials used in this study to produce cement paste, mortar and concrete mixes are provided in this section. The sources of PC, fly ash and slag could not be kept the same for the entire study due to the shortage of these materials.

3.1.1 Portland Cement (PC)

Two General Use (GU) or Type 10 Portland cements were used in this study, PC1 and PC2. PC 1 was used to prepare the test specimens for sulfate attack, alkali-silica reaction while PC2 was used for salt scaling, freeze-thaw, Rapid Chloride Permeability Test (RCPT) and compressive strength specimens. The chemical compositions of those two cements are given in Table 3.1.

3.1.2 Fly Ash

Three fly ashes were used; FA1, FA2, and FA3. FA1 and FA2 were used in sulfate attack and ASR testing and FA3 was used for salt scaling, freeze-thaw, RCPT, and compressive strength testing. All three fly ashes fall under CSA Classification of Class CH. Table 3.1 lists the chemical composition of these fly ashes.

3.1.3 Slag

Two different slag were used; Slag 1 and Slag 2. Slag 1 was used in sulfate attack and ASR. Slag 2 was used for salt scaling, freeze-thaw, RCPT, and strength tests. The chemical composition of slag is given in Table 3.1.

Table 3.1: Chemical composition of cementitious materials

	Chemical Composition (%)						
	PC1	**PC2**	**FA1**	**FA2**	**FA3**	**Slag1**	**Slag2**
SiO_2	19.58	18.71	33.72	33.26	33.89	34.4	38.15
Al_2O_3	5.35	4.61	18.47	18.24	18.09	7.4	7.59
Fe_2O_3	2.29	2.78	7.04	6.45	6.17	0.94	0.61
CaO	62.84	60.72	27.16	28.73	25.75	43.2	38.07
MgO	2.43	3.12	5.08	5.32	5.92	9.3	10.66
SO_3	4.1	-	2.84	2.59	-	0.83	-
K_2O	1.13	1.10	0.33	0.33	0.45	0.58	0.48
Na_2O	0.21	0.22	1.72	1.94	1.83	0.57	0.35
TiO_2	0.31	0.3	1.41	1.45	1.48	0.44	0.40
P_2O_5	0.11	0.22	0.91	0.88	1.3	175ppm	0.01
S.G.	3.15	3.15	2.65	2.65	2.65	2.94	2.94

3.1.4 Reactive Aggregate

Spratt aggregates used as reactive aggregate. These aggregates are from Spratt quarry in Stittsville near Ottawa. Spratt aggregates are siliceous limestone and are found to be ASR susceptible where cracks are apparent on concrete made up of Spratt. The physical properties of Spratt are listed in Table 3.2.

3.1.5 Caledon Coarse

Caledon coarse aggregates are from a quarry in Caledon, Ontario was used in concrete mixes of salt scaling slabs, freeze-thaw prisms, RCPT and strength cylinders.

3.1.6 Sunderland Fines

Sunderland fine aggregates are non-reactive in terms of ASR and hence, used in concrete mixtures along with Spratt ASR reactive aggregates. This aggregate is obtained from St. Mary Cement, 55 Industrial Street, Toronto, Ontario.

3.1.7 Caledon fines

Natural sand obtained from a quarry in Caledon, Ontario was used in concrete mixes of salt scaling slabs, freeze-thaw prisms, RCPT and strength cylinders. These fines are from a quarry in Caledon, Ontario.

3.1.8 Ottawa Sand

Standard Ottawa sand is silica sand that meets the requirements of ASTM C778. This sand is used to make the sulfate mortar bars as per the requirements of the test, ASTM 1012.

3.1.9 Admixtures

An air entraining admixture and a water reducer are used to provide the air entrainment and the workability.

Table 3.2: Physical properties of aggregates

	Reactive Aggregate	**Caledon Course**	**Sunderland Fines**	**Caledon Fines**
Absorption	0.44	1.53	0.63	0.46
Bulk Relative Density	2.68	2.61	2.64	2.67
Dry Rodded Density, kg/m^3	-	1582	-	-
Fineness Modulus	-	-	3.17	2.67
Grading (% Passing)				
25 mm	100	100	-	-
19 mm	99.5	96.0	-	-
13 mm	63.5	67.7	-	-
9.5 mm	25	46.4	100	100
4.75 mm	0	8.2	92.6	96.2
2.36 mm	-	-	76.1	84.2
1.18 mm	-	-	56.6	69.6
0.60 mm	-	-	37.0	49.6
0.30 mm	-	-	16.5	26.0
0.15 mm	-	-	3.6	8.5
0.075 mm	-	-	1.2	2.0

3.2 Experimental Program

Several experiments were conducted on various concrete, mortar and cement-paste blends to evaluate the performance of ternary, binary, and control blends. Experimental work was designed to study four widely encountered durability issues; sulfate attack, alkali-silica reaction, salt scaling, and freeze-thaw damage. In addition to these four durability issues, the basic properties of concrete were evaluated to see whether the ternary blends meet the fundamentals of concrete – fresh and hardened properties. Purpose of evaluating the fresh and hardened

properties is to ensure that the evaluated concretes, in addition to satisfying the durability criteria, satisfy the fundamentals.

3.2.1 Sulfate Attack

Evaluation for sulfate attack was carried out using ASTM C 1012. ASTM C 1012 involves monitoring the expansion of mortar bars soaked in sulfate solution. Mortars bars and standard mortar cubes (50x50 mm) were prepared. The specimens were cured at 35°C and 100% RH for 24 hours after which they were demolded. Then, the specimens were stored in saturated limewater until the mortar cubes reach 20 MPa. When the mortar cube strength reach 20 MPa, the initial length readings of the mortar bars were taken and submerged in 5% Na_2SO_4 solution.

In addition, the same blends were tested for ion migration using RCPT at the age when the cube strength reach 20 MPa and at 56th day. The RCPT test results were used to study the role of permeability in reducing sulfate attack in the investigated blends. Table 3.3 presents the details of each blend tested for sulfate resistance.

Table 3.3: Blends prepared to evaluate sulfate susceptibility

Mix ID	PC1 (%)	FA1 (%)	FA2 (%)	Slag1 (%)
20 FA	80	20	-	-
40 FA	60	40		
20 Slag	80	-	-	20
30 Slag	70	-	-	30
40 Slag	60	-	-	40
15/15	70	-	15	15
20/20	60	-	20	20
30/30	40	-	30	30
20/30	50	20	-	30
20/40	40	20	-	40
40/20	40	40	-	20

To further study the role of calcium hydroxide consumption, the paste blends were prepared at the cementitious materials combinations shown in Table 3.3. The calcium hydroxide content of the paste samples were determined by the thermal gravimetric analysis (TGA) after 28-days of curing.

3.2.2 Alkali-silica Reaction

To evaluate the alkali-silica reaction, concrete prisms were made with reactive aggregates (Spratt) and Sunderland sand. Stainless steel studs were attached at both ends of the prism to facilitate the length change measurements. The length change of the prisms was monitored for 2 years. In addition, accelerated mortar test was carried out on the same blends used to make prisms. Mortars bars were prepared using the crushed Spratt aggregates and monitored for length change under the exposure of 1N NaOH solution at 80°C. The length readings were taken periodically for 28 days. Table 3.4 presents the cementitious materials combinations of the blends prepared for prisms and mortar bars.

Table 3.4: Blends for ASR Prism and Accelerated Mortar Bar Tests

MIX ID	PC1	FA2	Slag1
20/30	50	20	30
15/15	70	15	15
20/20	60	20	20
40/20	40	40	20
20/40	40	20	40
20 FA	80	20	0
30 FA	70	30	0
50 FA	50	50	0
40 Slag	60	0	40
50 Slag	50	0	50

Further, to evaluate the alkali binding capacity of the ternary blends, cement paste blends were prepared. Table 3.5 summarizes the blends combinations. Paste fragments were stored in solutions of 0 mol/L and 0.25 mol/L alkali concentrations for a period of 1 month after which the change in the concentration in the surrounding solution was measured using flame photometry. Increase in concentration in surrounding solutions is attributable to alkali contributed by paste hydrate and decrease in concentration is attributable to incorporating alkalis from surrounding solution into the hydrates of the paste fragments. Higher increase in concentration of the surrounding solution is an indicator of higher availability of alkali for ASR.

Table 3.5: Blends for leaching test on paste fragments

MIX ID	PC1	FA 2	Slag 1
Control	100	-	-
15/15	70	15	15
20/20	60	20	20
30/30	40	30	30
20% FA	80	20	-
40% Slag	60	-	40

3.2.3 Salt Scaling

Salt scaling resistance was evaluated by exposing concrete slabs (300x300x75 mm) with salt solution pooled on the surface to freezing and thawing cycles. Concrete mixtures were made at w/c of 0.45, constant cementing material factor of 350 kg/m^3. Air entraining admixtures and water reducers were adjusted to obtain around 5% air content and 100 mm slump, respectively. The damage is evaluated by collecting the scaled off mass from the surface of the concrete. Ternary blends, binary blends and control mixtures were tested. The test standard (MTO LS-

412) states the slabs to be cured 14 days in moist room and 14 days at 23°C and 45 – 55% relative humidity. In this study, all the slabs were cured as specified in MTO LS-412 and in addition, slabs from two concrete mixtures were tightly wrapped with polyethylene and cured outside of curing room. The details of the two curing regimes conducted in this study are given in Table 3.6. Table 3.7 contains the cementing materials proportions used to make the concrete mixtures for scaling slabs. Table 3.7 also contains how each mix is cured before being exposed to the salt solution.

The intention of curing outside the curing room is to prevent the moisture dripping on the slabs. Moisture dripping will leach the alkalis and calcium hydroxide which would otherwise be used for pozzolanic and latently hydraulic reactions of SCMs. The slabs were tightly wrapped as to prevent the moisture loss so that the slabs will be cured with the internal moisture. The aim is to sacrifice the moist room curing in order to prevent the leaching of alkalis from the surface. If internal curing is adequate and alkalis are prevented from leaching, then it is expected that the resistance of the slabs when exposed salt will be enhanced. On the other hand, if the internal curing is not adequate, then the surface microstructure will be coarser.

Initially, it was decided to use a curing compound instead of wrapping with polyethylene. However, existing literature shows the controversy that improvement due to curing compound arises because of the removal of the thin layers from the surface as the curing compound is brushed off before exposing to the salt (Valenza and Scherer, 2007a). Exposing the slabs with the curing compound membrane did not seem to be an option as the scaled off mass would include the curing compound membrane along with concrete/paste chips. Hence, it was decided

to use thick polyethylene sheets and duct tape to tightly wrap the slabs. It should be emphasized here that the slabs were tightly wrapped in order to minimize the condensation which would lead to alkali leaching.

Effect of curing regimes on alkali retention ability method is evaluated by measuring the concentration of (Ka+ + Na+) ions released by concrete chips into the surrounding distilled water over the period of one month. Two concrete cylinders were made from the same concrete mix (40% Slag) but one specimen was curing as per Curing Regime A and the other one cured as per Curing Regime B. After the curing and drying period, chips were removed by brushing the top surface and screened to finer particles. Particles then soaked into distilled water and allowed to leach alkalis for one month. After one month, the host solution concentration was measured and reported in ppm.

Table 3.6: Curing Regime for salt scaling slabs

Curing Method	**First 24 hours**	**Next 13 days**	**Following 14 days**
Curing A Description: Moist room curing	Moist Room, slabs were covered with polyethylene sheets to prevent water dripping. Polyethylene sheets were lifted above the slab surface so polyethylene sheets were not touching the slab surfaces	Kept in the moist room, not covered, water dripping allowed	Kept in the laboratory air
Curing B Description: Polyethylene wrapping	"Same as above"	Slabs were tightly wrapped with a thick polyethylene sheet. Then, any left openings were closed with duck tape to prevent moisture loss.	The slabs were unwrapped and left in the laboratory air.

Table 3.7: Tested mixes for salt scaling

Mix ID	PC2	FA3	Slag2	Curing A	Curing B
Control	100	-	-	X	
15/15	70	15	15	X	
20/20	60	20	20	X	X
30% Slag	60	-	30	X	
40% Slag	60	-	40	X	X

3.2.4 Freezing and Thawing

Freezing and thawing damage is accessed by exposing prisms of various ternary, binary and control blends to freezing and thawing cycles. The test standard followed is ASTM 666, Procedure A. Same concrete from the salt scaling slabs was used to make the prism specimens. At the end of every 35 cycles, the damage is accessed by measuring the change in dynamic modulus of elasticity and the weight loss of the prisms. The test continued until 300 F/T cycles.

3.2.5 Compressive Strength and RCPT

Concrete cylinders (height 200 mm; diameter 100 mm) were made for compressive and RCPT from the same concrete used for salt scaling and freeze-thaw tests. Compressive strength was tested at 1, 7, 28, 56 days by crushing 3 cylinders. RCPT was carried out at 7, 28, 56, and 91 days using at least 3 specimens (obtained from the same cylinder) for each age.

3.2.6 Fresh Properties

Ternary, binary and control concrete mixtures were tested for slump, air content, bleeding and setting time. All the mixes were added with constant cement factor, air admixture and water reducer, in addition to w/c.

3.3 Experimental Details

3.3.1 Sulfate Attack Mortar Bars: ASTM C 1012

ASTM C 1012 was followed to measure the expansion of mortar bars under 5% Na_2SO_4 upto 2 years. Mortar is prepared as per ASTM C 305. Stainless steel studs were attached on both ends to facilitate the measurements. The expansion of the bars was taken at 1, 2, 3, 4, 8, 12, 13, 15, 26, 39, 52, 78, and 104 weeks. The length measurements were taken with reference to a standard invar bar and expressed as percentage of the original length. Percent expansion is determined using Equation 8.

$$\% \text{ Expansion} = \left(\frac{\text{Reading at X week} - \text{Initial reading}}{\text{Effective gage length}}\right) x100\% \qquad \text{[Equation 8]}$$

Where effective gage length is taken as 250 mm

3.3.2 RCPT on Mortar Specimens

ASTM C1202 – Rapid Chloride Permeability Test was conducted. This test is intended for testing concrete specimens. However it is used here for mortar mixes. Mortar mixes were made as per ASTM C 305 and cast into the standard cylinders in three layers, each layers compacted 25 times with the steel rod. Just prior to the test, the cylinders were cut using diamond saw to obtain three 50 mm-height test specimens and ASTM C 1202 was followed to obtain the RCPT values. Averages of the three specimens are reported.

3.3.3 Thermal Gravimetric Analysis

Paste samples were prepared at the same cementitious materials combinations shown in Table 3.3 using a high-speed, high-shear food blender. The w/c was kept 0.5 for all the samples. The prepared paste blends were poured into plastic moulds of 2 in. (50 mm) diameter and 4 in. (100 mm) height and cured at 100% relative humidity and 95°F (35 °C) for the first 24 hours. Then, the samples were de-moulded and soaked into limewater at 73.4 °F (23°C) for another 27 days. After that, the samples were taken out of limewater and broken into pieces and soaked into alcohol for 1 week. Then, the samples were stored in the oven at 80°C until the day of analysis. On the day of running TGA, the fragments were taken out of the oven and screened through the 1.18 mm sieve. Analysis was carried using the instrument AutoTGA 2950HR V6.1A on the paste power passed through 1.18 mm sieves.

3.3.4 ASR Prisms

Concrete prism test was carried out as per CSA A23.2-28A. Spratt aggregates used as the reactive aggregates and the cement with alkali content of 0.95% was used to make the prisms. As the standard states, alkali content is increased to 1.25% $(Na_2O)_{eq}$ of Portland cement. Prisms were stored in plastic pails within which the relative humidity was kept 100%. To keep the RH 100%, water is added to 25 mm from bottom of the pail and the internal wall of pails was covered with absorbent cloth. Each pail contained three prisms in upright position where contact between the prisms and water was avoided with the aid of plastic spacers and perforated rack. All the pails were kept in the heat room where the temperature was 38±2°C. Before each measurements, pails were removed from the heat room and kept in the laboratory air for 16 – 20

hours to cool down to the room temperature. Measurements were taken in weeks 1, 2, 4, 8, 13, 18, 26, 39, 52, 78, and 104. Percent expansion is calculated using the Equation 9.

$$\% \text{ Expansion} = \left(\frac{\text{Reading at X week} - \text{Initial reading}}{\text{Effective gage length}}\right) x100\% \quad \text{[Equation 9]}$$

Where, Effective gage length = invar bar length + initial reading – 2(half of the stud length)

3.3.5 Accelerated Mortar Bar

Accelerated Mortar Bar test was carried out on the same blends used in concrete prisms according to CSA A23.2-25A. The reactive aggregates were crushed in the laboratory to obtain the required gradation as in the CSA standard. The aggregates were filled into the cylindrical mould (152 mm diameter and 116 mm height) used for protector test. A 51-mm spacer disk was placed on top of the aggregates and the force was applied on the spacer disk under the compression machine. The crushed aggregates were sieved, washed, and dried before using to make the specimens. W/C of 0.50 was used for all the mixes as this is the CSA requirement for mortar bars made with crushed aggregates. Mortars were prepared as per ASTM C 305. Prepared mortar bars were cured in the moist curing room for 24 hours after which they demoded and heated to 80°C in water. The specimens were kept at 80°C in water in order to offset the thermal expansion from the expansion due to ASR itself. Hence, initial readings were taken after the samples were subject to 80°C in water. After, the initial readings, the bars were transferred into the pre-heated 1 N NaOH solution. Measurements were taken periodically until 28th day from the initial measurement.

3.3.6 Leaching Test on Past Samples

Leaching test was conducted on paste and concrete fragments. Paste specimens were made in plastic moulds and cured over water for 28 days. After 28 days, the specimens were demolded and crushed between 19 mm to 4.75 mm and stored in an oven at 100°C until the beginning of the test. On the day of the test, the fragments were taken out of the oven and further crushed to 2.5 to 1.25 mm sizes. 1.5 g of the paste fragments was introduced to into the 15 g solutions of pre-determined alkalinity and stored in 20 mL plastic bottles. Pre-determined alkali solutions are made at 0 M and 0.25 M concentrations. Distilled water was used for 0 M and 0.25 M solution was made by combining NaOH and KOH. In 0.25 M alkali solution, Na^+ and K^+ are combined at same ratio these two ions are found in Portland cement (PC1) (i.e. 0.843 K^+ : 0.157 Na^+). The quantities used to make 0.25 M solution are given in Table 3.8. A reference bottle full of alkali solution with no paste fragments was also prepared. The bottles were tightened to prevent the evaporation and left in the laboratory for 1 month. After 1 month, Na^+ and K^+ ions were counted (in ppm) from each bottles using the Advanced Technical Services GmbH 200S model flame photometer. Change in alkalinity was computed with respect to the reference bottles.

Table 3.8: Quantities for 0.25mol/L alkali solution

Quantities of KOH and NaOH for 1 L of 0.25 mol/L alkali solution
KOH = 39g/mol x 0.25mol/L x 0.843 = 8.219 g/L
NaOH = 23g/mol x 0.25 x 0.157 = 0.903g/L

3.3.7 Salt Scaling Resistance

MTO LS-412 test standard for salt scaling was used run the test. Slabs were cast into 300x300x75 mm wooden moulds. The concrete mix proportions are given in Table 3.9. After consolidating the excess concrete was screened off. Finishing was not done right after screeding but done after bleeding ceased with 2 strokes by wood trowel. Then, the gentle brushing was applied on the surface to remove any laitance and to leave a slightly textured surface. MTO LS-412 states the slabs to be cured 14 days in moist room and 14 days at 23°C and 45 – 55% relative humidity. In this study, all the slabs were cured as specified in MTO LS-412 and in addition, slabs from 2 concrete mixtures (20/20 and 40 slag) were cured using different method. This curing method the slabs were cured in the moist room for about 20 hours for the slab to develop enough strength to be demolded. After demolding, the slabs were wrapped with thick polyethylene for another 13 days. Then, the wrap was removed and the specimens were let to dry in the lab air for 14 weeks. The scaling residue was collected every 5 cycles and cumulative mass loss is reported.

3.3.8 Effect of Salt Scaling Curing Regimes on Alkali Retention Ability

In order to evaluate the effect of Curing Regime A and B on alkali retention ability on concrete surface, concrete two specimens from the same mix were made and each was cured according to Curing Regimes A and B, respectively. It was made sure that the specimen stored in the moist room stood up with the finish surface facing the water dripping throughout the 14-day curing period. After 14 days curing and another 14 days of drying period, powdered fragments were removed from the finished surfaces with the aid of a steel wire brush. The removed powder was then introduced into the bottles with distilled water with the solid to liquid ratio of 1 to 10. After

one month, the Na^+ and K^+ concentration of the host solution was measured for the two samples using the ATS 200S flame photometer.

3.3.9 Freeze and thaw

Freeze and thaw test was done (as per ASTM C666) on the same mixtures as in salt scaling test. Concrete prisms of 75x75x285 mm were made as the experimental specimens. After 14 days of limewater curing, the initial measurements were taken at 0°C. The damage was accessed using weight loss and pulse velocity (ASTM C 597). Pulse velocity was used to predict the dynamic modulus of elasticity from which the durability factor was calculated after 300 cycles. The relationship between dynamic modulus of elasticity and pulse velocity provided in ASTM C 597 is used obtain the dynamic modulus of elasticity (Equation 10). However, it should be noted that ASTM 666 does not mention about deriving dynamic modulus of elasticity using a relationship with pulse velocity; rather, ASTM C666 states to use the fundamental resonant frequencies (ASTM C215) to obtain the dynamic modulus of elasticity. Due to the unavailability of the equipment complies with ASTM C215, it was decided to use ASTM C 597 to obtain the dynamic modulus of elasticity.

$$V = \sqrt{\frac{E_d(1 - v_d)}{\rho(1 + v_d)(1 - 2v_d)}} \quad \textbf{[Equation 10]}$$

Where; E_d is dynamic modulus of elasticity, v_d dynamic Poisson's ratio, ρ is density.

For v_d, a common value of 0.15 is selected (Mindess et al., 2003).

3.3.10 Compressive Strength and RCPT of Concrete Samples

Cylinders were made from concrete of properties of proportions shown in Table 3.9. Cylinders were cured in the moist room until the day of testing. RCPT specimens were obtained by cutting 50 cm (2 in) specimens using a wet saw. Compressive strength and RCPT were carried out as per ASTM C 39 and ASTM C 1202, respectively.

3.3.11 Fresh Properties

Concrete mixtures were designed (Table 3.9) to study the fresh properties of ternary, binary and control mixtures. These concrete mixtures differs from that used in salt scaling specimens as air admixture and water reducer dosages were kept constant in the mixes. Air content and slump were tested immediately after the mixing process was over. Air content was determined using CSA A23.2-4C, pressure method and slump was tested using CSA A23.2-5C. Bleeding of the concrete specimens was determined according to Method A of ASTM C232. The remaining concrete was sieved through 4.75 mm sieve to obtain the mortar for the setting time as per ASTM C 403.

Table 3.9: Mix proportion of concrete used for salt scaling, freeze-thaw, compressive strength and RCPT

Mix ID	PC2 (kg/m^3)	Slag 2 (kg/m^3)	Fly Ash3 (kg/m^3)	Water (kg/m^3)	Coarse (kg/m^3)	Sand (kg/m^3)	Water Reducer (ml/m^3)	Air Admixture (ml/m^3)	Measured Slump, (mm)	Measured Air Content (Pressure method), %
Control (100% PC2)	350	0	0	157.5	1001.4	795	2250	108.5	160	7.20
15/15 (FA3/Slag2)	245	52.5	52.5	157.5	1001.4	783	750	122.5	140	6.20
20/20 (FA3/Slag2)	210	70	70	157.5	1001.4	779	750	122.5	110	5.0
30% Slag2	245	105	0	157.5	1001.4	789	1143	122.5	160	5.80
40% Slag2	210	140	0	157.5	1001.4	786	750	134.5	130	5.80

Chapter 4. Results and Analysis

The results from this study are presented in this chapter. The results presented here spans from sulfate attack, ASR, salt scaling, frost damage to fundamental properties of concrete.

4.1. Sulfate Attack

Table 4.1: Expansion of mortar bars under 5% Na_2SO_4 solution

Mix ID	4 month	6 month	9 month	1 year	1 ½ year	2 year
Control (100% PC1)	0.115	0.306	1.568	Broke		
20% FA1	0.286	Broke				
40% FA1	Broke					
20% Slag1	0.051	0.069	0.113	0.209	0.367	0.883
30% Slag1	0.033	0.043	0.053	0.079	0.216	0.647
40% Slag1	0.031	0.037	0.040	0.054	0.072	0.140
20% FA1+20% Slag1	0.097	0.271	Broke			
20 FA2+20 Slag1	0.059	0.160	0.281	Broke		
20 FA1+30 Slag1	0.059	0.181	0.247	0.531	Broke	
40 FA1+20 Slag1	0.051	0.059	0.066	0.077	0.110	0.195
20 FA1+40 Slag1	0.041	0.047	0.057	0.078	0.182	0.355
15 FA2+15 Slag1	0.071	0.159	0.398	Broke		
30 FA2+30 Slag1	0.049	0.061	0.077	*		

* not due yet

The expansion of mortar bars submerged in 5% Na_2SO_4 solution after 4 month, 6 month, 9 month, 1 year, 1.5 year, and 2 years time period are presented in Table 4.1. Earlier expansions (i.e. week 1 to 4 months) of sulfate attack mortar bars are presented in Appendix A. The results are analysed for the performance of binary and ternary blends and effect of SCM on the expansion.

4.1.1 Performance of Binary Blends against Sulfate Attack

Binary blends tested include blends with Class CH fly ash and blends with slag. Figures 4.1 and 4.2 present the expansion of fly ash and slag blends, respectively. The 40% fly ash mix broke before 4 months while 20% fly ash specimens lasted slightly longer than 4 months. Replacing PC with Class CH fly ash did not improve the sulfate resistance; instead it has worsened the case. This behaviour is reported elsewhere and commonly attributed to high calcium content, high alkali content, lower silica content, and tendency to form monosulfate prior to exposing to the sulfate solution (Shashiprakash and Thomas, 2001; Freeman and Carrasquillo, 1995).

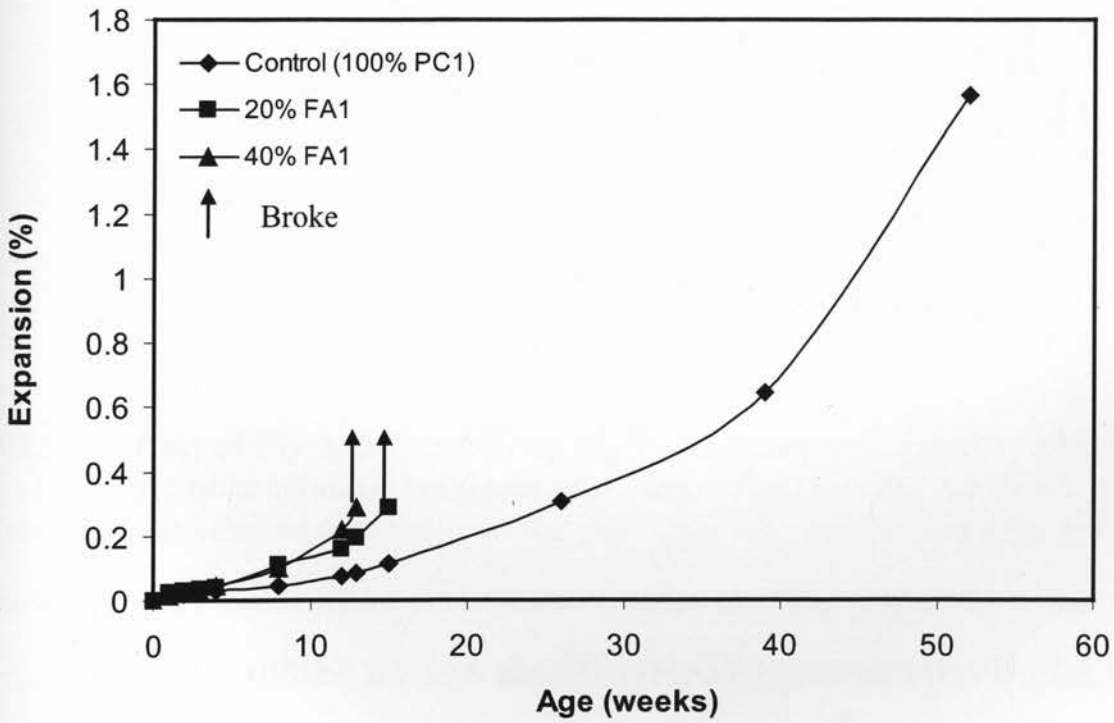

Figure 4.1: Expansion of Class CH fly ash binary mortar bars in 5% Na_2SO_4 solution

On the other hand, binary blends of slag performed well. 20% slag replacement reduced the expansion dramatically compared to the control mix. The 30% and 40% slag replacements further reduced the expansion below ASTM 6-month and 1-year limits, 0.05% and 0.1%. The superior performance of slag blends is attributable to the lower Al_2O_3 (7.4%) content of slag and dilution of C_3A in the cementing materials. In addition, increasing slag content also increases the ability to incorporate Al^{3+} ions into C-S-H (Gollop and Taylor, 1996b).

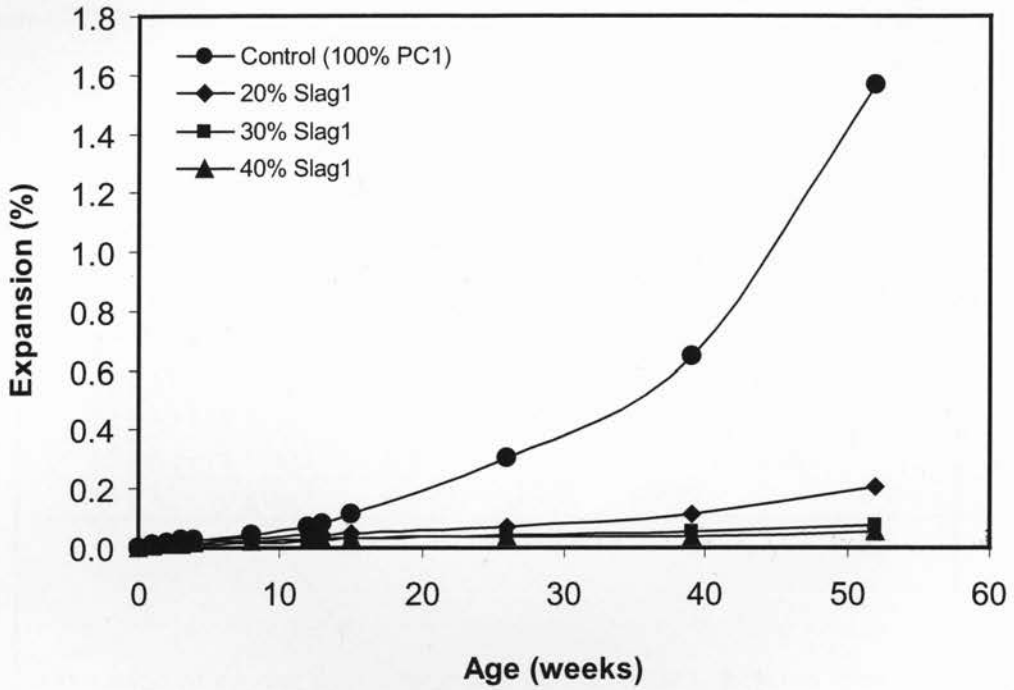

Figure 4.2: Effect of slag contents on the mortar bar expansion under 5% Na_2SO_4

4.1.2 Performance of Ternary Blends Against Sulfate Attack

Figure 4.3 contains the expansion at 1-year of the ternary blends tested in this program. Referring to Figure 4.3, increasing the ternary contents has enhanced the resistance. Besides that, the level of reduction in expansion for 15/15, 20/20, and 20%FA+30% Slag

is not sufficient to meet the ASTM limit at 1 year (0.1% expansion). However, the 40%FA+20% slag and 20%FA+40%slag mixes have performed well. Yet, 20%FA+40%Slag is the only blend that meets the ASTM limits at 6 month and 1 year.

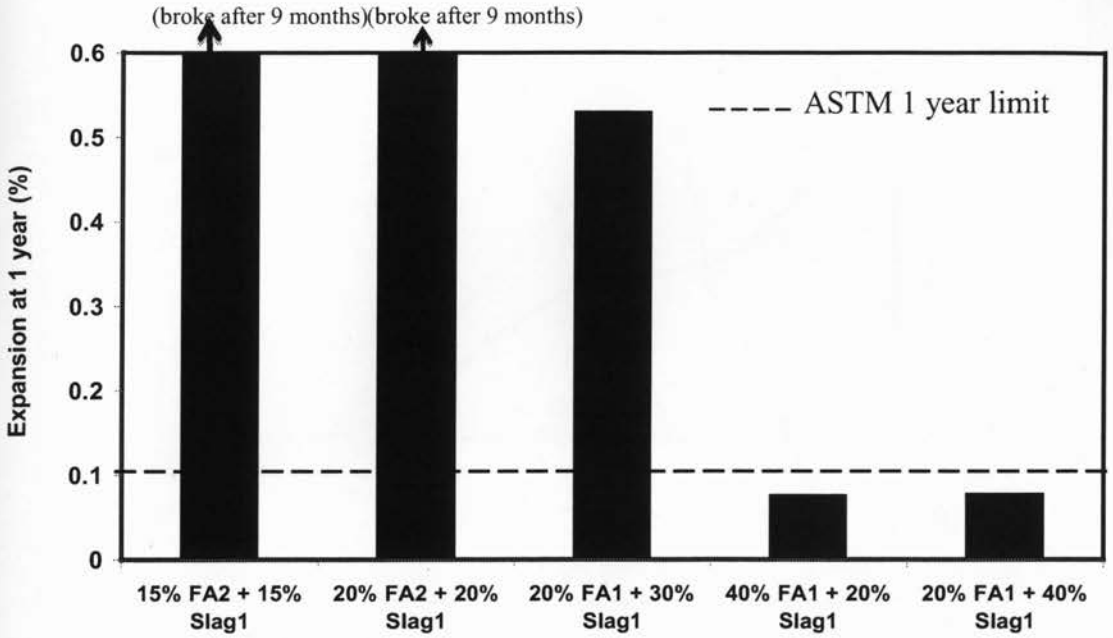

Figure 4.3: Expansion of ternary blends in Na_2SO_4 solution

4.1.3 Effect of Fly Ash Content on the Performance of Ternary Blends

Ternary blends showed promising results that Class CH fly ash could be safely incorporated in concrete mixes when blended together with slag. Figure 4.4 shows the expansion of ternary blends of 20% slag plus various fly ash contents. Figure 4.4 illustrates that increasing the fly ash content in ternary blends decreased the expansion dramatically. For example, 20% FA1 mix expanded more than the control and broke at 15 weeks where 20/20 mix expanded slightly lower than the control, lasted longer than

15 weeks and broke after 6 months. 30%FA1+20%Slag reduced the expansion further than 20/20. And, 40%FA+20%Slag resulted in superior performance even though it had 40% high calcium fly ash.

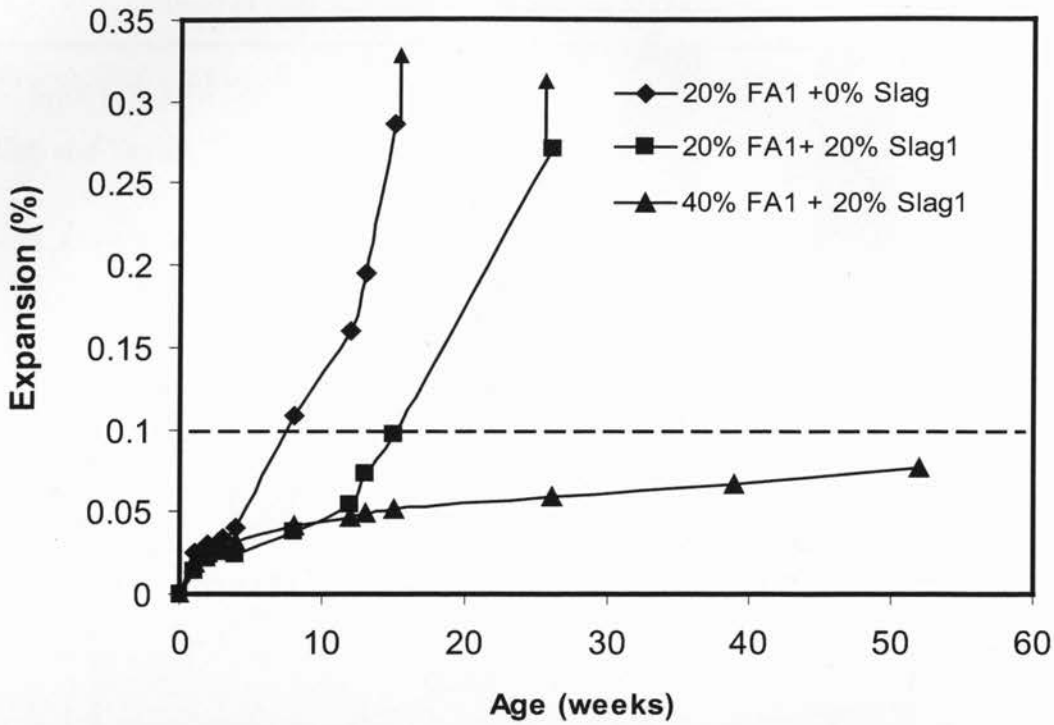

Figure 4.4: Effect of Class CH fly ash and slag in a ternary system

4.1.4 Effect of Slag Content on the Performance of Ternary Blends

Figure 4.5 contains the expansion of ternary blends with 20% fly ash content plus various slag contents in order to observe the effect of slag content on expansion. The binary blends of slag are also included in Figure 4.5 for comparison. The ternary blends reduce the expansion as the slag content increases in the mix. For instance, 20%FA1+30%Slag mix resulted in less expansion than 20/20. Similarly, 20%FA+40%Slag resulted in less expansion than 20%FA+30% Slag. However, 20/20 mix did not excel 20% Slag binary

mix. Similar trend is observed with 20%FA+30% Slag and 20%FA+40%Slag if comparison to be made with 30% Slag and 40% Slag binary mixes, respectively.

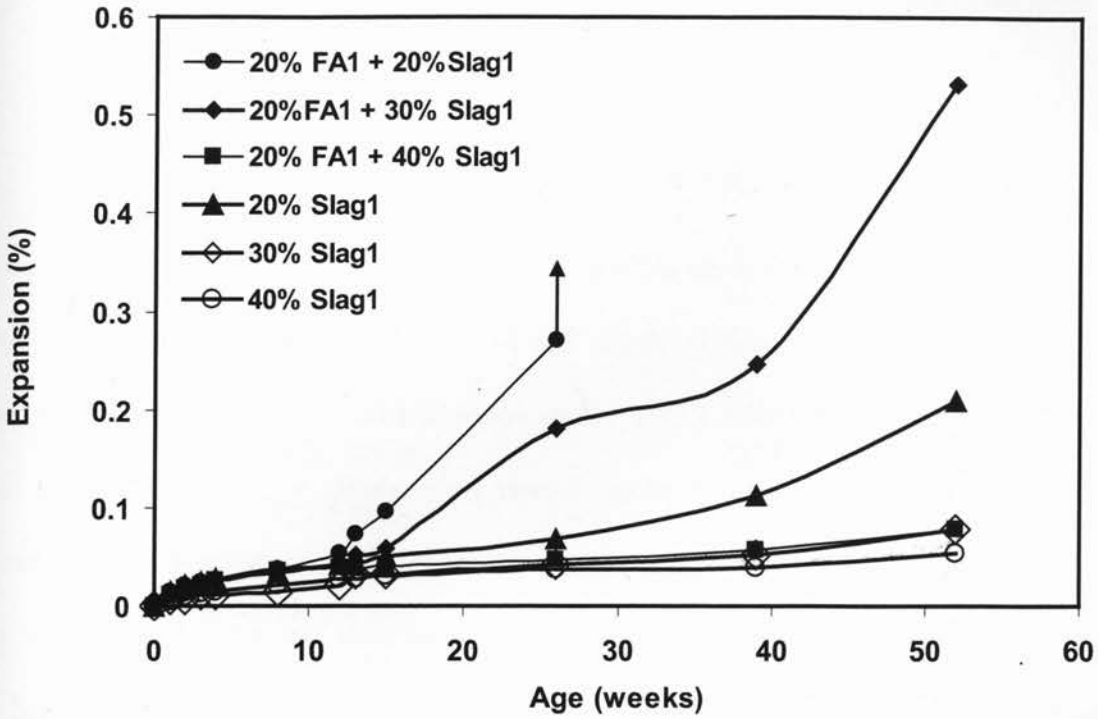

Figure 4.5: Effect of slag content on expansion of ternary blends

Contribution by slag to the performance of ternary blends could be due to several beneficial actions of slag. As a result of pozzolanic reaction, consumption of $Ca(OH)_2$ might have made Ca^{2+} unavailable for ettringite formation. Secondary gel produced due to slag's pozzolanic reaction might have reduced the permeability of the mortar bars. This is evident from the 56th day RCPT values of the mortar mixes. Increasing slag content resulted in less coulombs passing through the specimens. 20%FA+40%Slag is less permeable (2722 Coulombs) than 20%FA+30%Slag (3258 C) and 20%FA+30%Slag is more permeable than 20/20 (4017 C). Accordingly, 20%FA+40%Slag is more resistant than 20%FA+30%Slag and 20%FA+30%Slag is more resistant than 20/20. In

addition, slag results in lower Ca/Si ratio of C-S-H which could make more Al^{3+} to be incorporated into C-S-H, thus making Al^{3+} not available for delayed ettringite formation (Gollop and Taylor, 1996b).

4.1.5 Ion Migration – RCPT on Mortar Specimens

RCTP values of mortar specimens at 56 days are given in Table 4.2. The values on Table 4.2 are average of at least two specimens. The RCPT value of each specimen is presented in Appendix D. The measured RCPT values could be used as a measure of two factors: ion migration and degree of hydration. Lower permeability will limit the sulfate ions migration into the concrete/mortar hence improve the resistance while increased hydration product might incorporate more reactive alumina into C-S-H (Shehata et al., 2008). The blends with slag reduce permeability and this could be explained based on increased level of hydration due to slag. Incorporating fly ash resulted in increased permeability due to slower reaction rate of fly ash. Similar observation could be made with the ternary blends. Ternary blends with higher fly ash portion have shown increased permeability while the ones with higher slag decreased permeability. For example, 20%FA+30%slag is less permeable than 20+20 because the both have same fly ash content but former has more slag. The ternary blend 20%FA+40%Slag is less permeable than 40%FA+20%slag because former has more slag and latter has more fly ash.

Table 4.2: RCPT test results of the blends tested for sulfate attack

Mix ID	**Total Charges Passed during RCPT at 56th day (Coulombs)** * indicates OVF states before RCPT finished; predicted value at the time of OVF is given
Control (100% PC1)	6627
20% FA1	6988
40 FA1	9360*
20 Slag1	5209
30 Slag1	3874
40 Slag1	2689
20%FA2 +20%Slag1	4017
20 FA2+30 Slag1	3258
15 FA2+15 Slag1	4966
40 FA1+20 Slag2	7958
20 FA2+40 Slag1	2722
30 FA2+30 Slag1	5073

The RCPT values at 56 days are plotted against the mortar bar expansion at 9 months and shown in Figure 4.6. Two different trends were observed between mortar bar expansion and 56-day RCPT. One trend resulted in very good correlation (Correlation-1, R^2 = 0.9621) while another trend resulted in poor correlation (Correlation-2, R^2 = 0.1907). The blends composes Correlation-1 are control, 15/15, 20/20, 20%FA+30Slag, 20%FA+40%Slag, and 40% Slag. The blends on the Correlation-2 are 20%FA+40%Slag, 40% Slag, 30% Slag, 30/30, 20% Slag, and 40%FA+20%Slag. The 20%FA+40%Slag, and 40% slag blends are included in both correlations since they are located in the path of the two correlations.

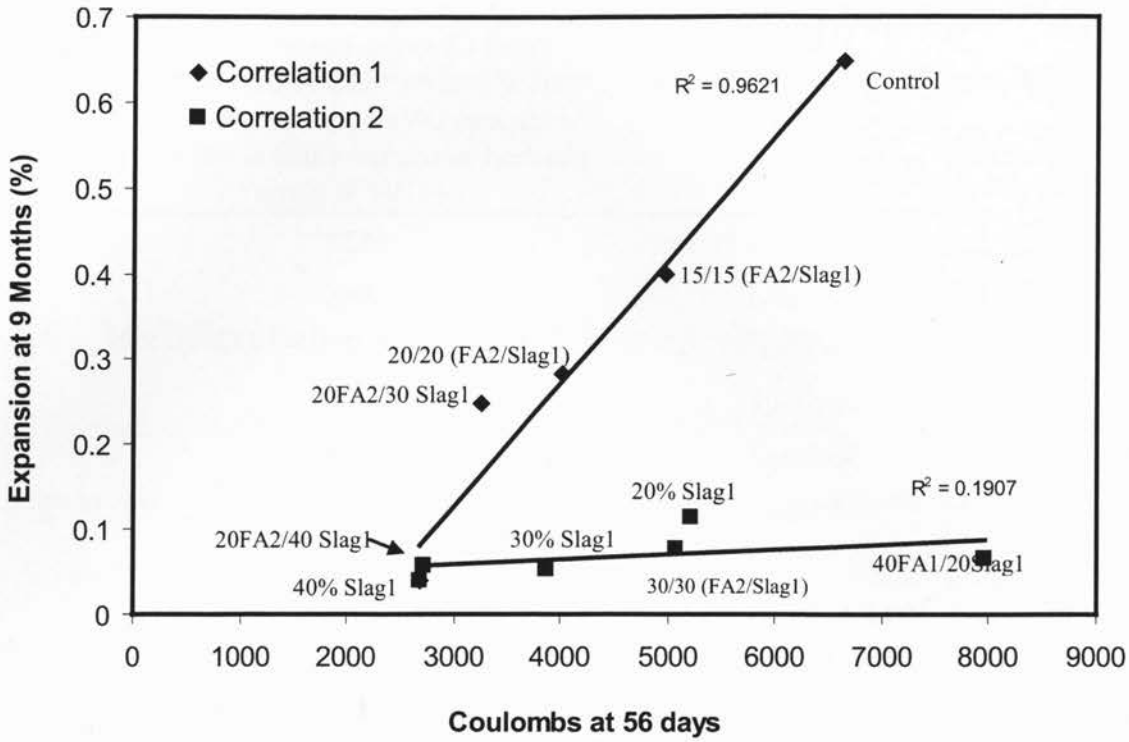

Figure 4.6: Correlation between mortar bar expansion and RCPT at 56th day

The expansion of blends located in Correlation-1 is influenced by permeability to a considerable degree. In this sense, the reduction of 15/15 and 20/20, and 20%FA+30%Slag is partly attributable to their permeability. The blends of Correlation-2 cannot be explained based on permeability criteria. For instance, 20%FA+40%Slag and 40%FA+20%Slag have a huge difference in their permeability but the expansion values are very close to each other.

This pattern reveals that the blends in Correlation-2 are mainly affected by alumina binding and $Ca(OH)_2$ consumption. Ability of slag to lower Ca/Si of C-S-H, hence to incorporate Al^{3+} into C-S-H is a prominent beneficial action of slag and is discussed elsewhere (Gollop and Taylor, 1996b; Wee et al., 2000). Thus, expansion of the binary slag blends in Correlation-2 could be due to their effectiveness in binding Al^{3+}.

The ternary blends on Correlation-2 draw special attention. Addition of slag in ternary blends might have helped to incorporate the reactive alumina from Class CH fly ash. If that is the case, 30/30 and 20%FA+30%Slag have the same slag content but the former has more fly ash content, thus, it is expectable that the former would not perform well compared to the later. However, the expansion results show that 30/30 ended up with lower 9-month expansion. Same comparison could be made with 20/20 and 40%FA+20%Slag. Hence, it is evident that in ternary blends not only slag but also the Class CH fly ash has a positive role in enhancing the resistance. The permeability trend in Figure 4.6 does not provide a ground to explain the lower 9-month expansion of 30/30 and 40%FA+20%Slag. Beside the permeability (i.e. migration of SO_4^{-2}), $Ca(OH)_2$ content plays significant role in controlling the sulfate resistance. Next section deals with the $Ca(OH)_2$ content and the expansion of mortar bars.

4.1.6 Calcium Hydroxide Contents

Table 4.3 lists the $Ca(OH)_2$ contents of the paste samples obtained from thermal gravimetric analysis conducted after 28 days of curing. The 28 days curing consisted of first 24 hours at 35°C and 100% RH and the remaining 27 days at 23°C under limewater. The details of the experimental results can be found in Appendix G. The data of ternary blends and slag from Table 4.3 are plotted in Figure 4.7 to show the relationship between the mortar bar expansion and the $Ca(OH)_2$ content of paste samples. The fly ash points are not included as the fly ash binary blends disintegrated before 6 months.

Table 4.3: $Ca(OH)_2$ contents of the paste samples

Mix	$Ca(OH)_2$ of paste samples at 28 days, %
Control (100% PC1)	19.20
20% FA2	12.52
20% Slag1	11.50
40%Slag1	9.43
15+15 (FA2+Slag1)	11.71
20+20 (FA2+Slag1)	9.51
20%FA2+30%Slag1	8.73
20%FA2+40%Slag1	7.83
40%FA2+20%Slag1	6.57
30+30 (FA2+Slag1)	7.03

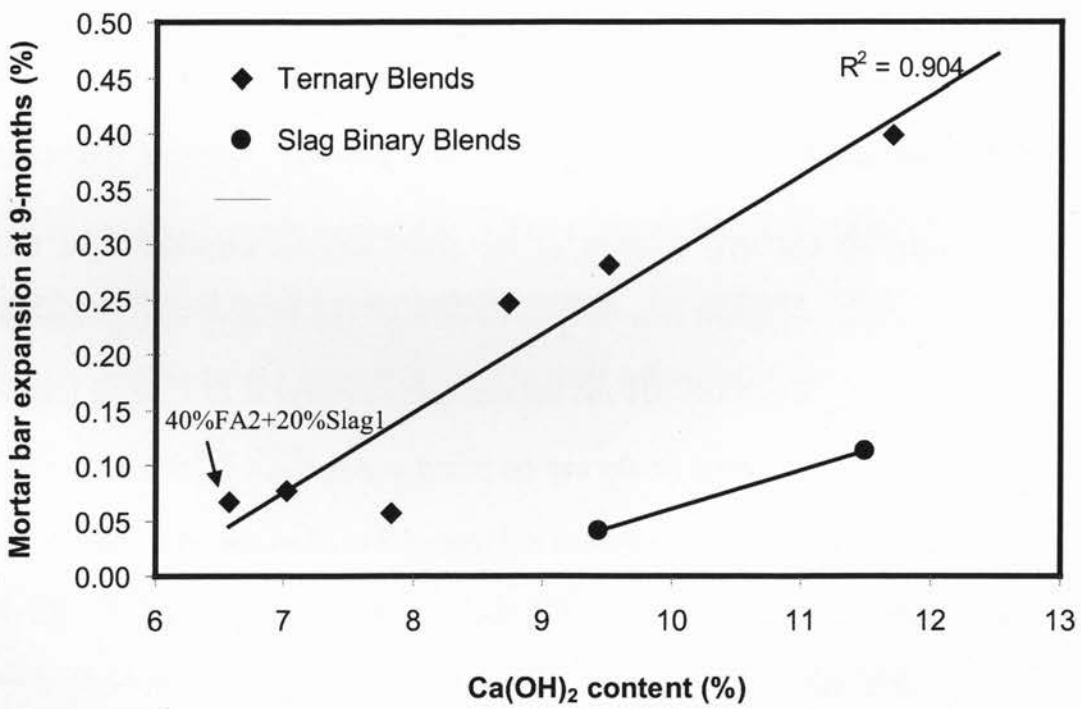

Figure 4.7: Relationship between mortar bar expansion of $Ca(OH)_2$ content of the paste

The calcium hydroxide contents of the blends with SCM is lower than the the control. Control blend contained 19.2% $Ca(OH)_2$ where adding 20% FA have reduced the $Ca(OH)_2$ to 11.5%. In addition, Figure 4.7 shows the linearity between the $Ca(OH)_2$ and the mortar bar expansion of ternary blends with R^2 of 0.904. The obtained correlation confirms that $Ca(OH)_2$ consumption is a contributing factor for the performance of ternary blends. Out of all the ternary blends tested, 40%FA+20% Slag blend resulted in lowest $Ca(OH)_2$ content. This confirms that increased $Ca(OH)_2$ consumption of 40%FA+20Slag is at least partially responsible for the excellent performance of this blend. Further, the blends 30+30, and 20%FA+40%Slag also obtained lower $Ca(OH)_2$ contents, confirming that increased $Ca(OH)_2$ consumption is a contributing factor for the reduced expansion of the mortar bars of these blends.

4.2 Alkali-silica Reaction

Appendix A contains the expansion values of concrete prisms up to 2 years age. Some of the concrete prisms were made during summer 2008 and hence they are only 1-year old by the time this document is being prepared. CSA and ASTM standards require 2 year expansion of concrete prism to determine satisfactory performance of the blend(s). However, for the purpose of evaluating the relative performance between mixes, expansion up to 1 year is considered to be sufficient.

4.2.1 Concrete Prism Expansion for Binary Blends

Figure 4.8 shows the expansion of 20%, 30% and 50% fly ash concrete prisms. It is evident from Figure 4.8, increasing the fly ash content has reduced the expansion. The

50% fly ash blend reduced the expansion significantly where 20% and 30% Class CH fly ash blends had slightly lower reduction effect than 50%FA. Note that 20% fly ash and 30% fly ash exceeded the 2-year limit of 0.04% before 26 and 39 weeks, respectively. This suggests that in order to suppress ASR expansion Class CH fly ash replacement as high as 50% is required. In the case of Class F fly ash, 25% replacement is sufficient to suppress the expansion (Thomas et al., 1999; Rogers et al., 2000). Lower efficiency of Class CH fly ashes is well known and is attributable to the higher calcium and alkali contents and lower ability to bind alkalis into hydrates (Thomas et al., 1999).

In the case of slag, the literature reports higher slag content (above 40%) is required to suppress ASR expansion below the limit. Figure 4.9 contains the concrete prism expansion of 40% and 50% slag mortar bars. Incorporating slag has significantly reduced the expansion but it is now too early to predict whether 40% slag replacement is sufficient to suppress the expansion below 0.04% at 2-years. Exact mechanism for the action of slag on ASR is not yet understood (Thomas and Innis, 1998). Yet, slag's beneficial actions are attributable to its ability to dilute the alkali content of cementing materials and reduce the pore solution alkalinity (Duchesne and Bérubé, 1994b).

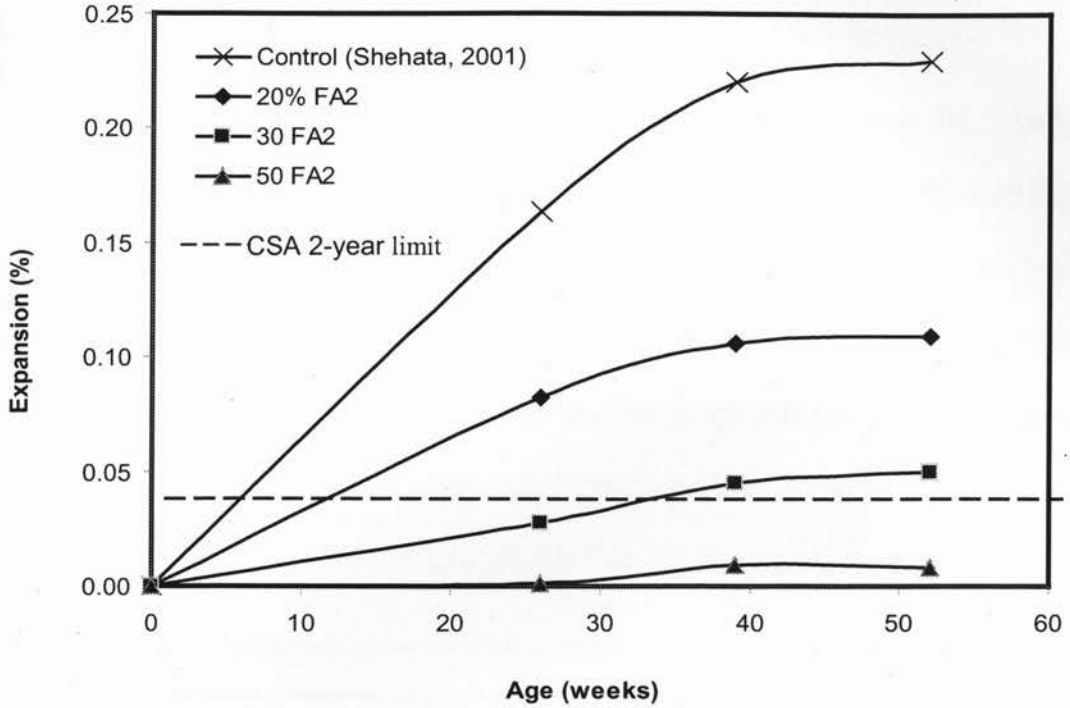

Figure 4.8: Concrete Prism expansion of fly ash binary blends

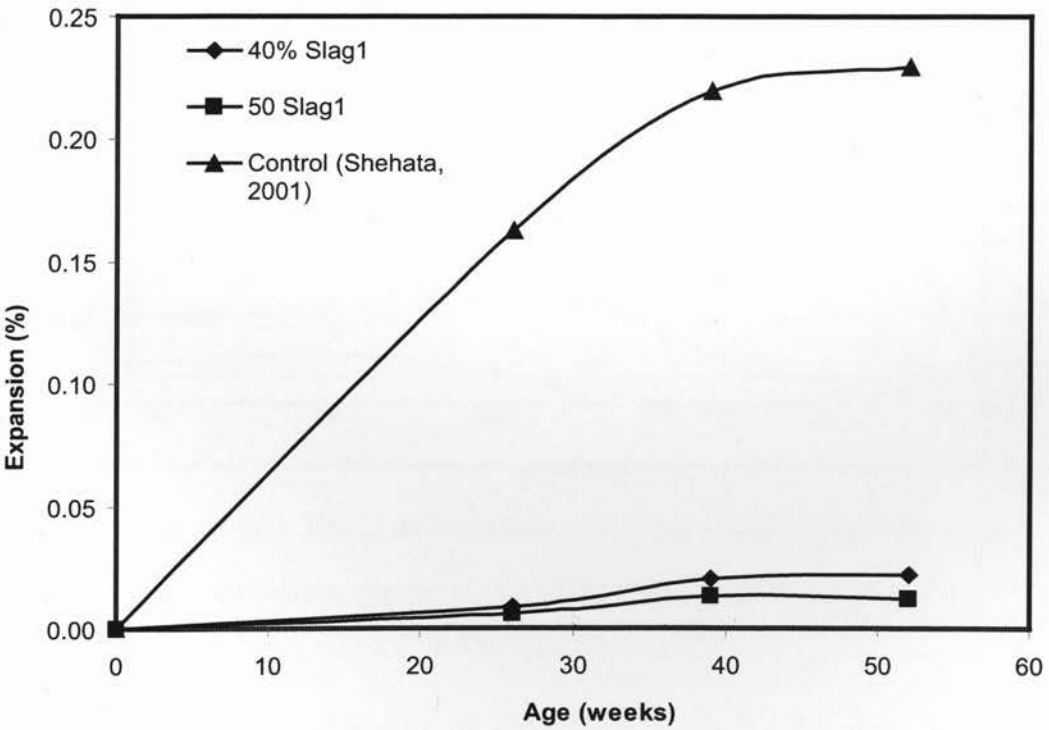

Figure 4.9: Concrete Prism Expansion of slag concrete

4.2.2 Concrete Prism Expansion of Ternary Blends: Effect of Fly Ash Content on Ternary Blends

Figure 4.10 contains the concrete prism expansion of 20% FA, 20/20 and 40% FA/20%Slag. According to Figure 4.10, at 12-months the 20% fly ash binary blends ended up with expansion of 0.109%. At 12-months, the ternary blend 20/20 has reduced the expansion to 0.02%, almost 82% reduction with respect to 20% fly ash binary blend. Further increasing the slag/fly ash content to 40FA/20Slag resulted in more reductions in expansion. It is also notable that 20/20 falls right at the CSA 2-year limit with the expansion of 0.041% at 2-year.

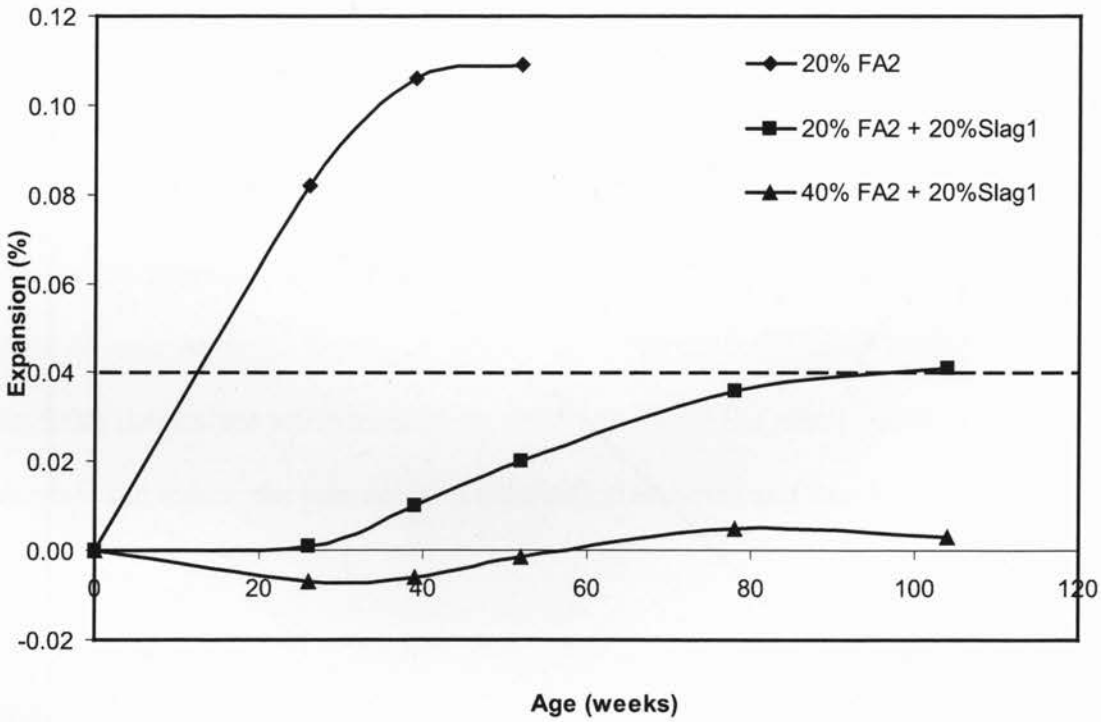

Figure 4.10: Effect of fly ash in ternary concrete prisms

4.2.3 Effect of Slag Content on Concrete Prism Expansion of Ternary Blends

Figure 4.11 contains the expansion of 20/20, 20%FA/30% Slag, and 20%FA/40%Slag. As in Figure 4.11, increasing slag content in ternary blends reduces the expansion. With respect to 20/20, 20%FA/30%Slag has reduced the expansion by 39% at 2-year. In terms of CSA acceptable criteria, 20%FA/30% Slag blend well meets the limit of 0.04 at 2-year. In addition, the 20%FA/40% Slag blend is only at the age of 1 year but from the current trend it is expectable that 20/40 will expand less than 20/30.

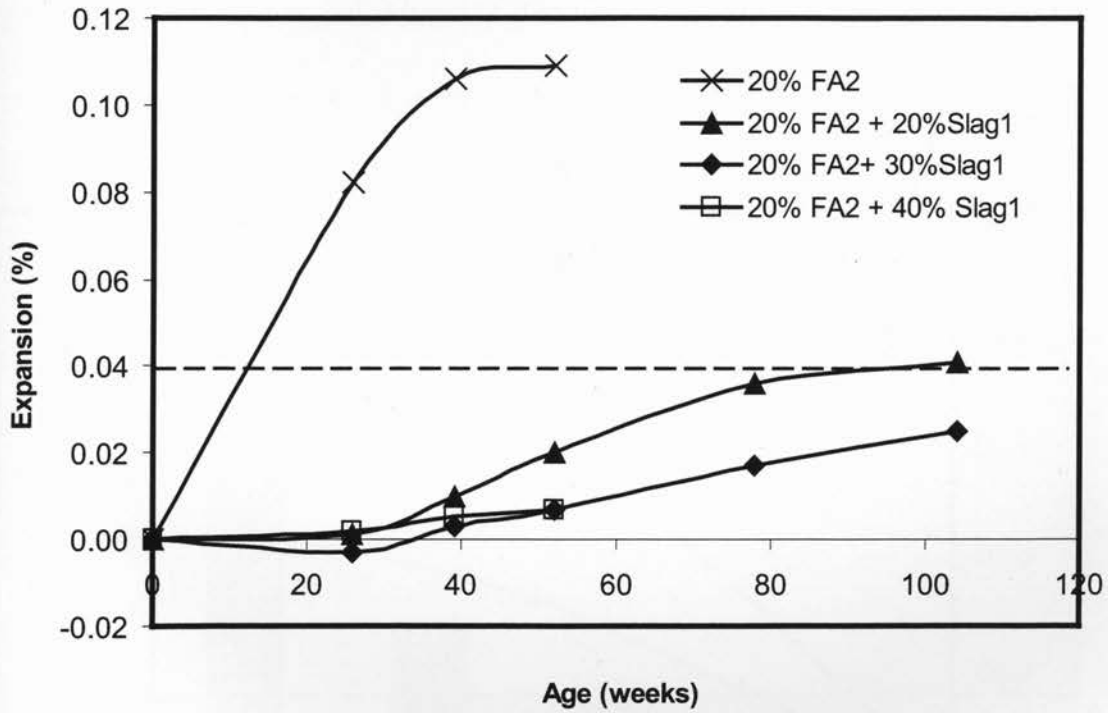

Figure 4.11: Effect of slag content in ternary concrete prisms

4.2.4 Synergy of Ternary Blends against ASR

Figure 4.12 shows that expansion of 20%FA/40%Slag is less than the individual expansion of 20%FA and 40%Slag. Synergy could be illustrated by showing that

reduction in expansion of 20%FA/40% Slag blend is less than the summation of individual reduction in expansion of 20% FA and 40% Slag binary blends where the reduction in expansion is determined with respect to the control (100% PC) blend. Using the 1-year expansion data the synergy calculation performed is shown below (Table 4.4).

Table 4.4: Synergy calculation for ASR using prism expansions

Mix	1-year expansion	Reduction
Control (Shehata, 2001)	0.23	-
20% FA2	0.109	0.121
40% Slag1	0.022	0.208
20% FA2 + 40% Slag1	0.007	0.223

Since, 0.223 is not greater than summation of 0.121 and 0.208, the reduction in expansion is not synergetic at this stage.

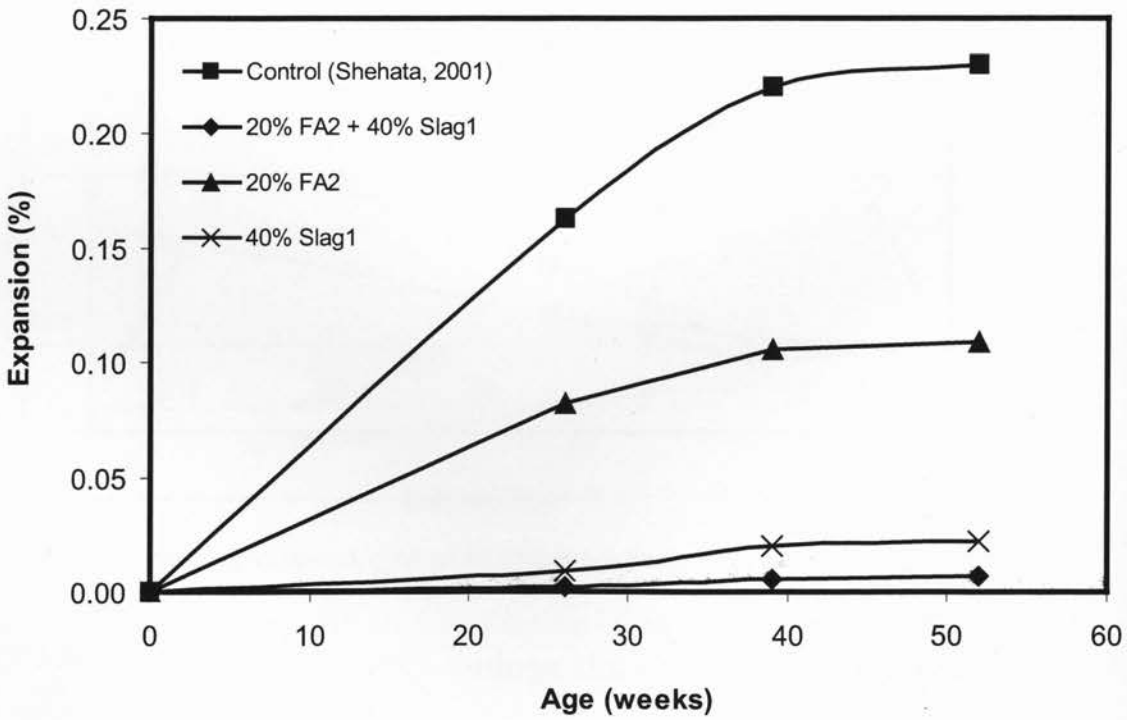

Figure 4.12: Synergetic action of fly ash-slag ternary blends

Figure 4.13 gives the expansion at 2 year for the prisms reached that age. Only two mixes (20%FA/30%Slag, and 20%FA/40%Slag) well meet the CSA 0.04% limit after two years while 20/20 falls right at the limit with 0.041% expansion. It appears that the required level of replacement of Class CH fly ash and slag in ternary blends is above 40% in order to suppress the expansion. It is worth noting that 15/15 have reduced the 2-year expansion by 63% from the control mix where 20/20, 20%FA/30% Slag, and 40%FA/20%Slag have reduced (with respect to control) by 84, 90, and 98.8%, respectively. The effect of increase in ternary fly ash/slag content from 20/20 to 20%FA/30%Slag is less pronounced on the expansion compared to that of from 15/15 to 20/20. This suggests that the rate of reduction in expansion after certain amount of ternary replacement is small. It is also evident that in order suppress the expansion to the CSA limit, the ternary replacement greater than 20/20 is required.

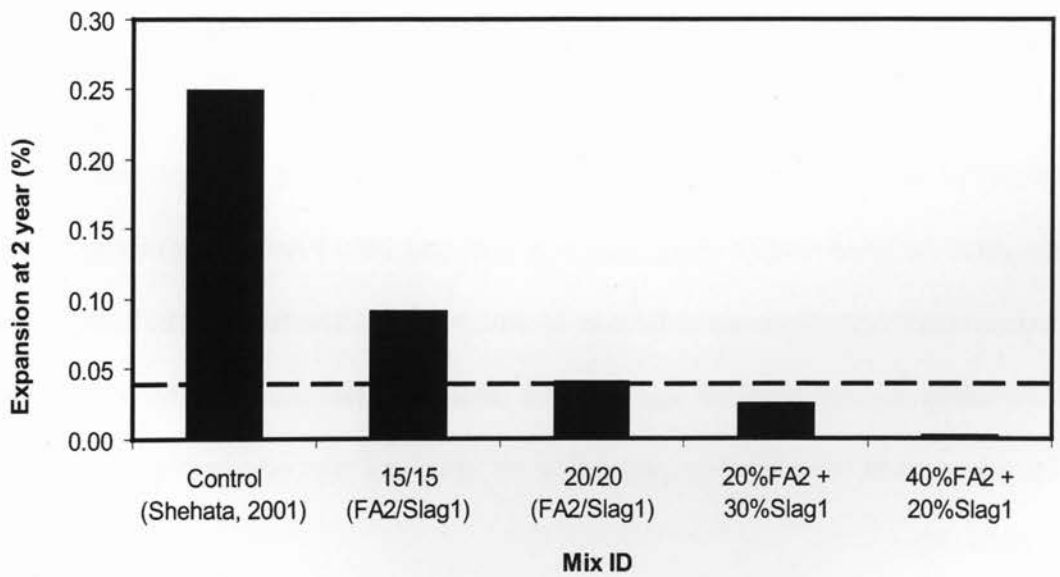

Figure 4.13: Two year concrete prism expansion of ternary blends

4.2.5 Accelerated Mortar Bar Test Results

Appendix A contains the expansion values of the accelerated mortar bar (AMBT) specimens and their average for each mix tested. Figure 4.14 contains the summary of all the blends tested using AMBT. AMBT is a quick test that could be used to screen the potential reactive aggregates. CSA adopted 0.10% expansion at 14-day as the acceptable benchmark for limestone aggregates and 0.15% for other aggregate types (Fournier and Berube, 2000). Out of the blends tested only the following blends; 50% FA, 20%FA/30%Slag, 20%FA/40%Slag and 40%FA/20%Slag meet the CSA 14-day limit of 0.10%. 50% slag binary mix fails the CSA acceptable criteria with 0.16% expansion. One could argue that in the case of binary blends, you need as high as 50% replacement level with Class CH fly ash or slag. Better performance could be achieved with 20% Class CH fly ash and 40% slag in ternary blends to meet the 0.10% limit. These ternary blends incorporate less amount of fly ash and slag than that is required if they were to be used individually in binary blends. With reference to Figure 4.14, it appears that the required replacement of Class CH fly ash and slag in ternary blends is greater than 50% as 20%FA+30%Slag mix marginally fails the CSA 14 day limit. The next level investigated is 20%FA+40% Slag and 40% Slag and 20% FA. These two mixes ended up with similar expansion values both at 14 and 28 days. The fact that 20%FA+40%Slag and 40%Slag +20%FA ended up with the similar expansion indicates that at higher replacement level, the relative proportion of slag and fly ash in ternary blends has negligible effect.

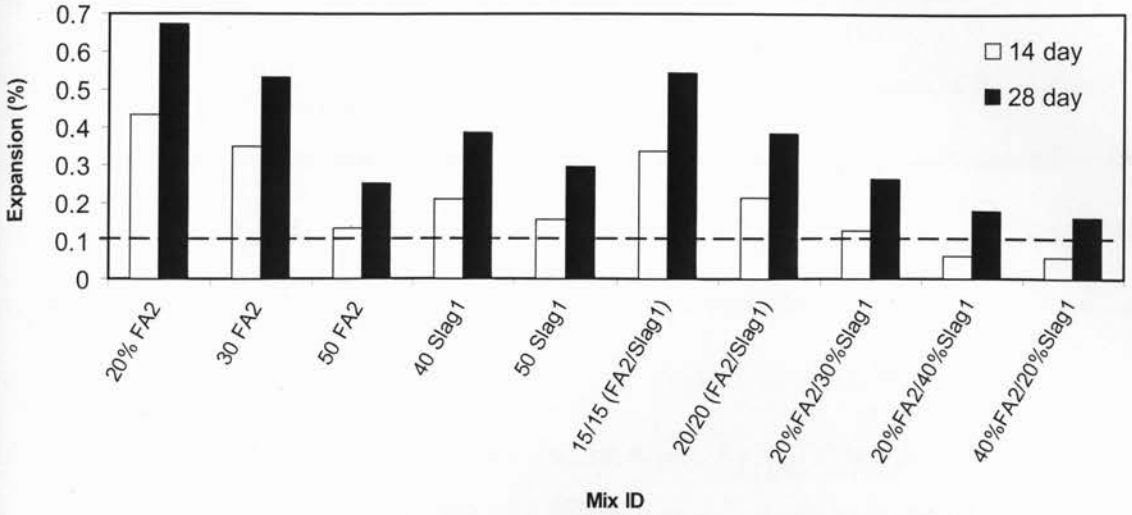

Figure 4.14: 14-day and 28-day expansion of mortar bars

4.2.6 Correlation between Accelerated Mortar Bar and Concrete Prism Tests

The advantage of AMBT is that it is a quick test that could be used to predict the poor performance of a blend. Yet, criticism has been made on AMBT due to it less reliability compared to the concrete prism test. Hence it is essential to draw the relationship between 14-day AMBT values and 2-year concrete prism expansion. Table 4.5 presents the expansion values of AMBT and concrete prism at 14-days and 1- year respectively. As few concrete prisms have not reached 2-year age, the correlation is made with 1-year prism expansion and 14-day AMBT expansion and is shown in Figure 4.15. Based on Figure 4.15, a correlation with R^2 of 0.8802 was obtained between the 14-day AMBT and 1-year concrete prism expansions.

Table 4.5: AMBT and concrete prism expansion at 14-day and 1-year, respectively

Mix	1-year Expansion of Concrete Prism Test (%)	14-day Expansion of Accelerated-Mortar Bar Test (%)
20% FA2	0.109	0.432
30 FA2	0.050	0.350
50 FA2	0.008	0.135
40 Slag1	0.022	0.211
50 Slag1	0.012	0.157
15/15 (FA2/Slag1)	0.060	0.336
20/20 (FA2/Slag1)	0.020	0.214
20 FA2/30 Slag1	0.007	0.127
20 FA2/40 Slag1	0.007	0.061
40 FA2/20 Slag1	-0.001	0.057

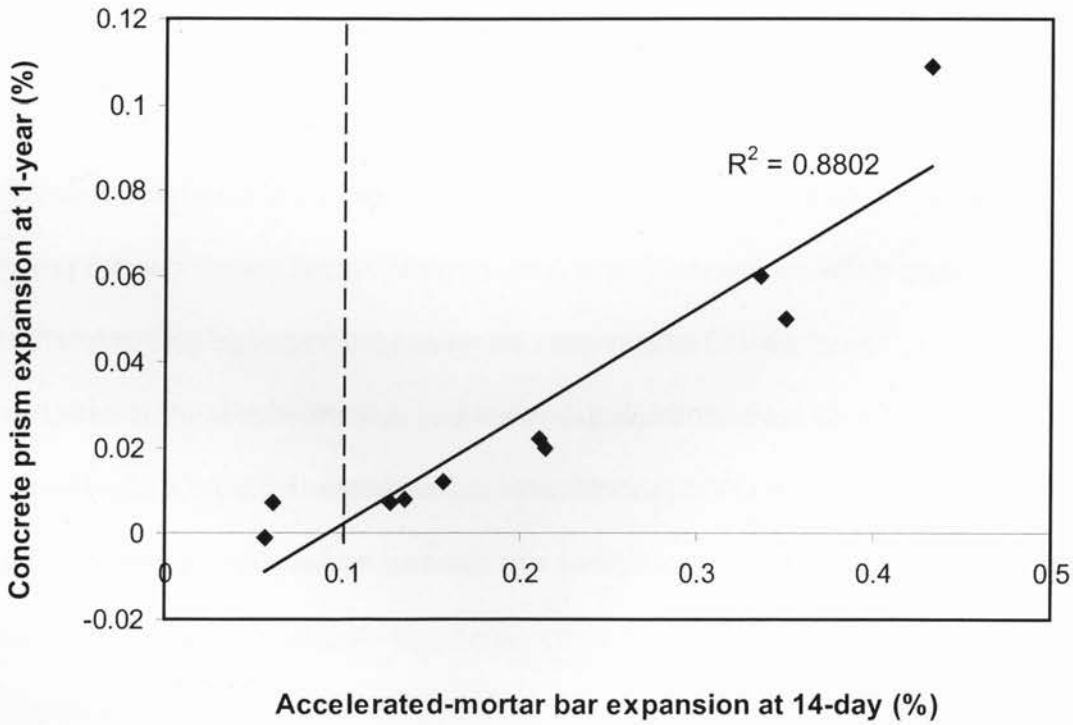

Figure 4.15: Correlation between 14-day AMBT and 1-year concrete prism

4.2.7 Alkali Binding Ability of Fly ash and/or Slag Blends

The raw data and calculations of leaching test are provided in Appendix F. Table 4.6 contains the results from the leaching test on control, binary and ternary blends. Six blends were tested include control, 15/15, 20/20, 30/30, 20% FA and 40% Slag. The change in alkali concentration on the host solution is considered to be a result of alkali release from the stored paste fragments. Increase in alkali concentration of host solution is taken as the indication of available alkalis for ASR. As in Table 4.6, control and 20% fly ash are the one released most of the alkalis in both host solutions. The ternary blends were effective in controlling the alkali release. In ternary blends, the effectiveness increases as the replacement level increases. The 40% Slag performed well in terms of reducing the alkali release however, in both solutions, 40% slag released slightly higher than 30/30.

Table 4.6: Results from leaching test

Mix	Host Solution 0 M		Host Solution 0.25 M	
	% of binder	% of alkali content of cementing materials	% of binder	% of alkali content of cementing materials
Control (100%PC)	0.911	95.53	0.883	92.61
15/15 (FA2/Slag1)	0.910	87.68	0.530	51.00
20/20 (FA2/Slag1)	0.812	68.03	0.359	30.10
30/30 (FA2/Slag1)	0.688	52.39	0.242	18.44
20 FA2	1.096	91.79	0.745	62.38
40 Slag1	0.721	75.71	0.368	35.80

Shehata and Thomas (2006) showed that alkali binding ability of hydrates affects the ASR resistance to a certain degree. Figure 4.16 shows the correlation of alkali released into 0.25 mol/L solution bottles and the 1-year concrete prism expansion. As in Figure 4.16, an exponential function fit into the points resulted in the R^2=0.9809. This excellent correlation suggests that alkali binding ability of an SCM plays a significant role in ASR expansion.

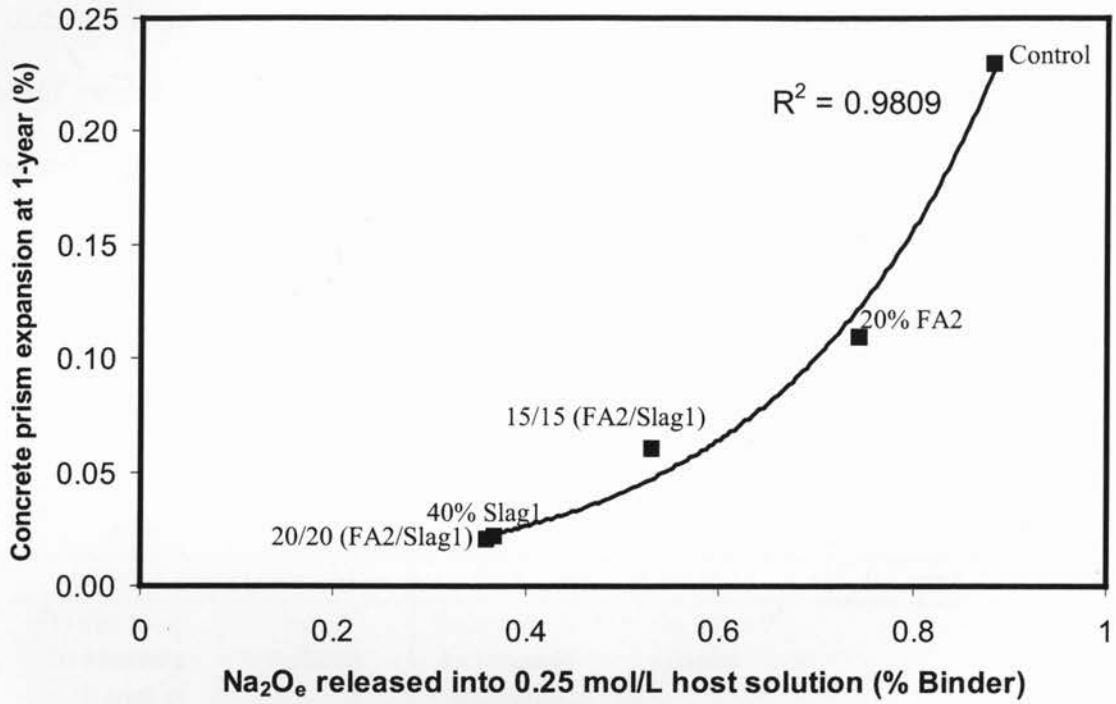

Figure 4.16: Relationship between concrete prism expansion and alkali release

The relationship shown in Figure 4.16 could be used to explain the better performance of ternary blends. Particularly, 20/20 have bound the alkalis to the similar level as of 40% Slag. This reveals that ternary blends increase the efficacy of binding alkalis despite the presence of Class CH fly ash. Shehata and Thomas (2006) stated that the efficacy of binding alkalies decreases with increasing calcium content of fly ashes. But the ternary

blends show that the 20% Class CH fly ash could be incorporated with another 20% slag to result in highly efficient alkali binding capacity. A 20% binary slag blend is not included in this study, however, from the published literature, it is evident that neither 20% slag nor 20% Class CH fly ash binary blend would expand to meet the 0.04% 2-year limit (Rogers et al., 2000). However, the two year expansion of 20/20 is 0.041%; such a reduction might have occurred mainly due to its alkali binding capacity.

In order to see the trend of correlation between released alkali and the concrete prism expansion, a few more points (Table 4.7) corresponding to the concrete prisms contained 5.25 kg/m^3 Na_2O_{eq} were taken from Shehata (2001) and added to Figure 4.16, and is shown in Figure 4.17. Figure 4.17 reveals that the current study and the points from Shehata (2001) follow similar trend; however, the points are slightly scattered in Figure 4.17, so a correlation similar to the one obtained in Figure 4.16 is not possible.

Table 4.7: Obtained values from Shehata (2001) for leaching-prism expansion correlation

Mix SF = Silica fume FM= Class F Fly ash OK = Class CH Fly ash	**Released alkalis into 0.25 M sol'n (% Binder)**	**1-year prism expansion (%)**
Control	0.803	0.230
5% SF	0.707	0.166
SF/FM 5/10	0.397	0.033
SF/OK 5/20	0.331	0.048
SF/OK 5/30	0.246	0.035

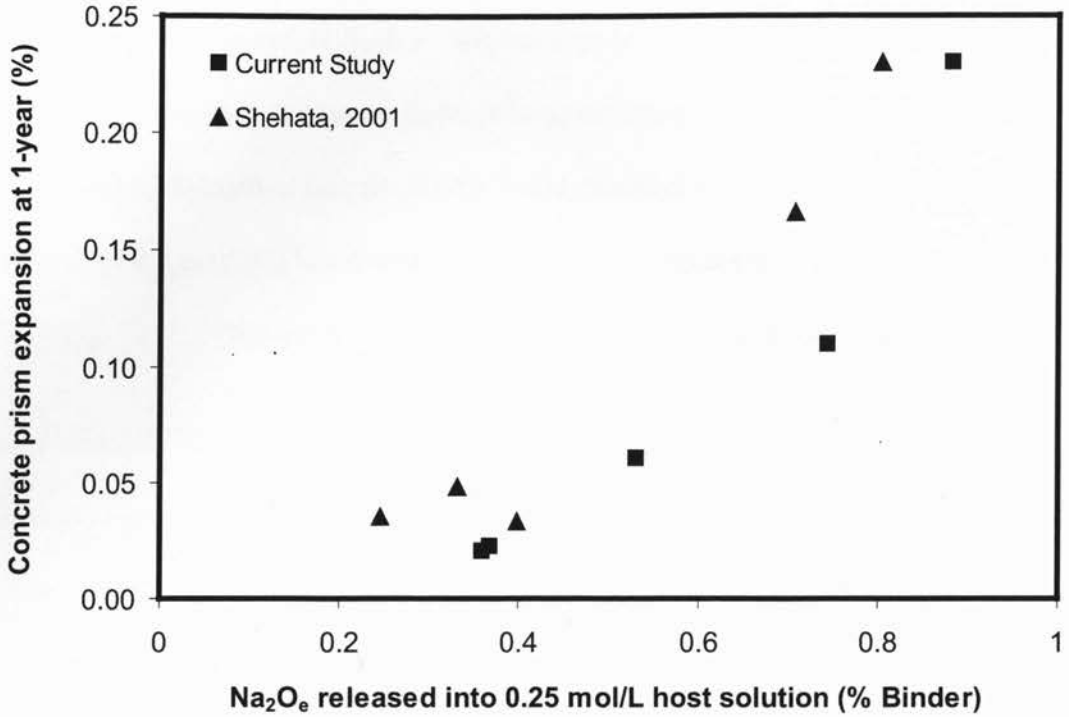

Figure 4.17: Correlation between alkali released and concrete prism expansion; points corresponding to the prism with 1.25% Na_2O_{eq} from Shehata (2001) included

4.3 Salt Scaling

Figure 4.18 summarizes the scaling results of the mixes tested. All the slabs were cured as in MTO LS412; that is 14 days in moist room followed by another 14 drying period. Collected scaling residue is reported as mass per area of the slab exposed to the salt solution. The points on Figure 4.18 are the average of three slabs except for the control where only two slabs were tested. The scaling residue of each specimen, average of at least two specimens and their standard deviations can be found in Appendix B. The mixes with slag have experienced severe scaling damage than the control where control has no significant scaling. Ternary blends have performed better than the slag concrete

but still performed poorly than the control mix. None of the mixes with SCMs have met the MTO limit of 0.8 kg/m^2 after 50 cycles.

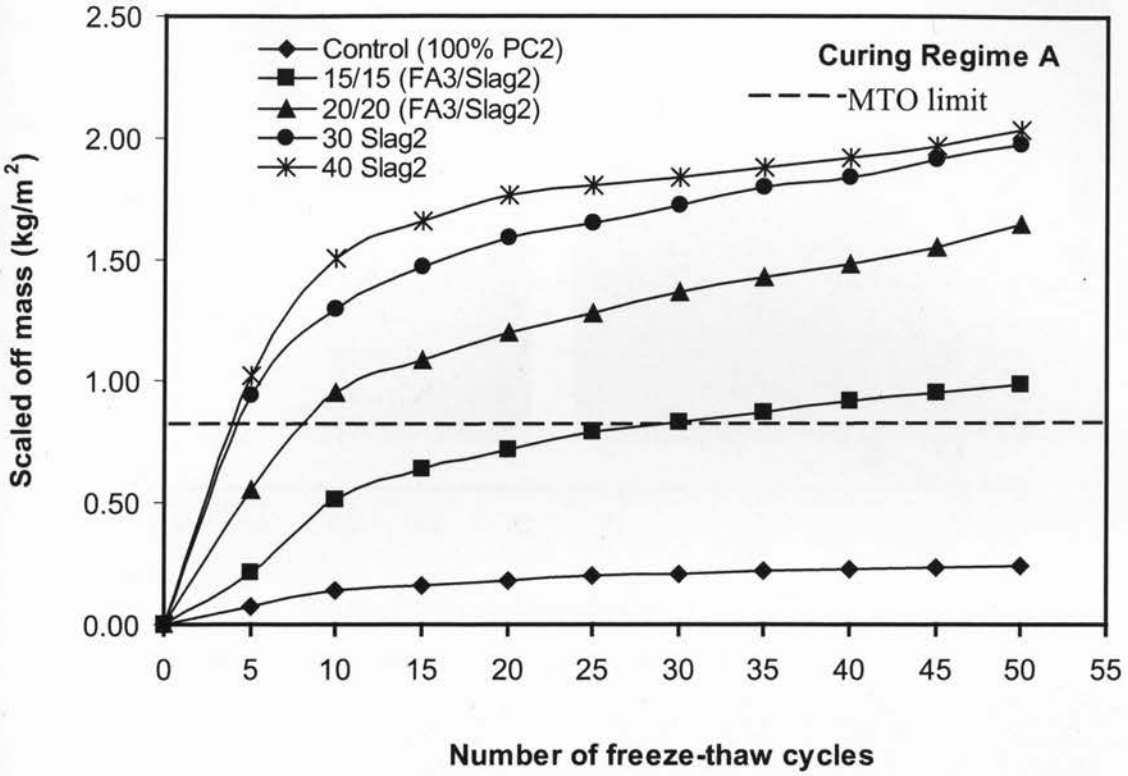

Figure 4.18 Scaling residue (conducted as per the standard MTO LS-412)

Figure 4.19 shows the scaling results of the mixes that were stored outside the moist curing room where the slabs were left tightly wrapped with polyethylene and left in the laboratory room (Curing B). The scaling of the corresponding mixes tested according to MTO LS-412 standard are also included in Figure 4.19 for comparative purposes.

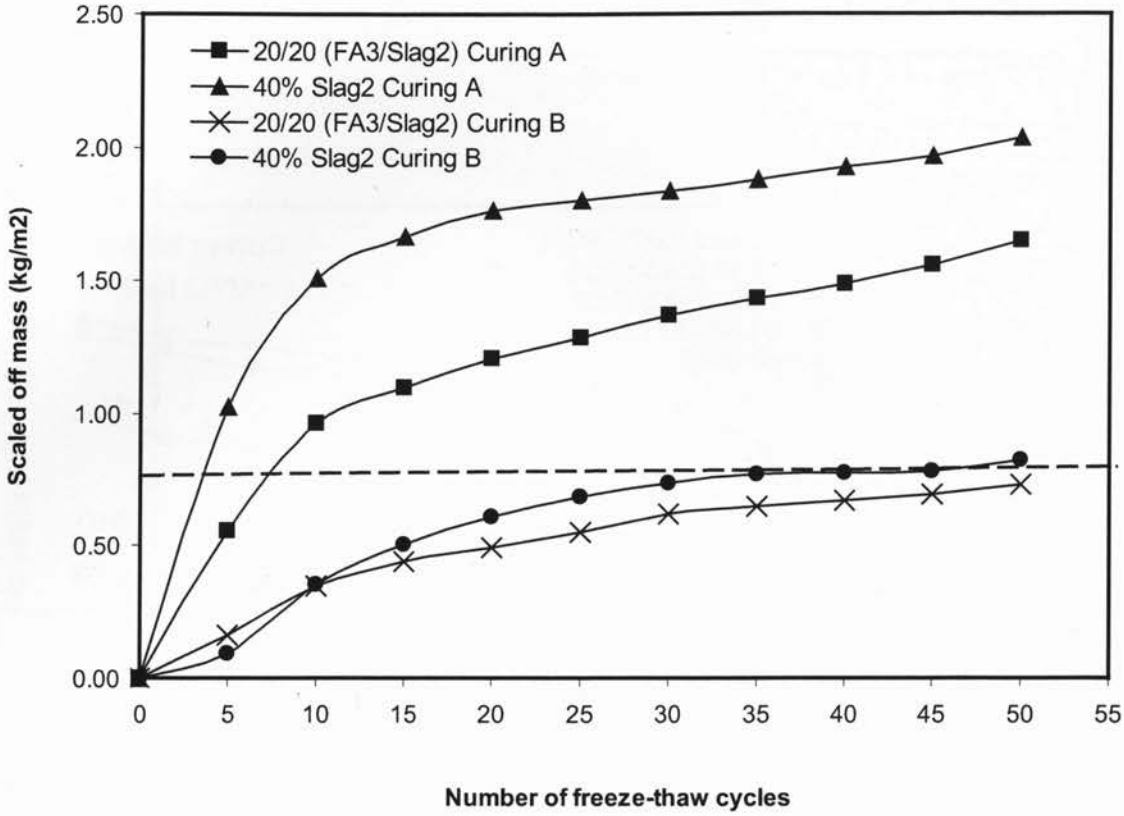

Figure 4.19: Effect of curing on scaling resistance

It is well clear that curing B have significantly improved the scaling resistance. Curing B has reduced approximately 60% and 55% scaling loss for 40% Slag and 20/20 mixes, respectively. In addition, 20/20-Curing B meets the the MTO limit of 0.8 kg/m^2 and 40% Slag mix lies at the limit with 0.82 kg/m^2 scaling residue. Pictures taken after 50 cycles are included in Figure 4.20.

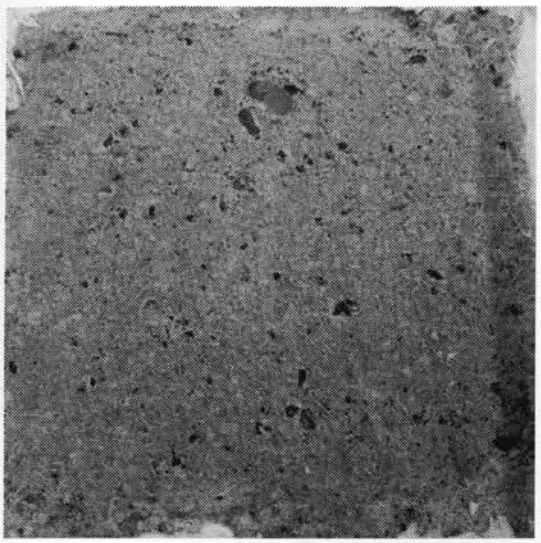

a) Control Curing A

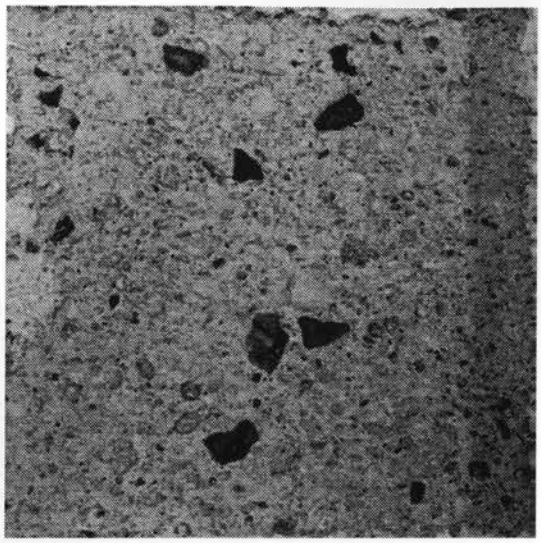

b) 30% Slag Curing A

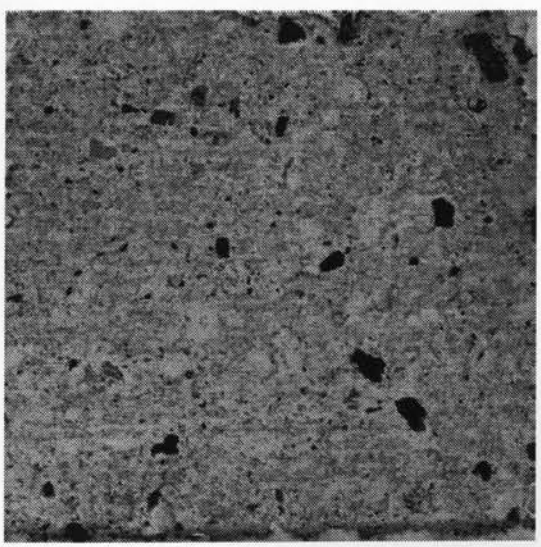

c) 15/15 Curing A

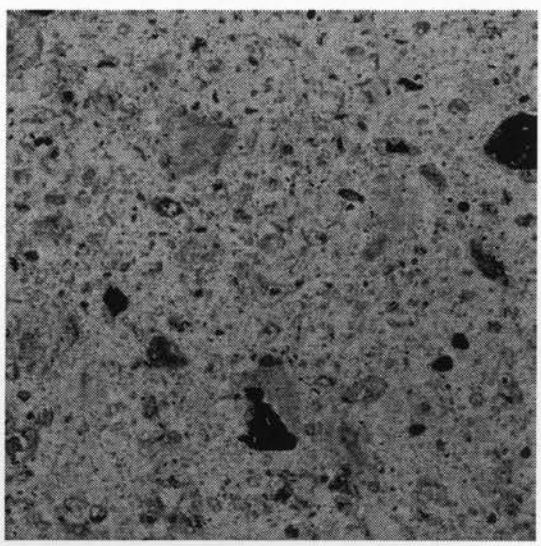

d) 40% Slag Curing A

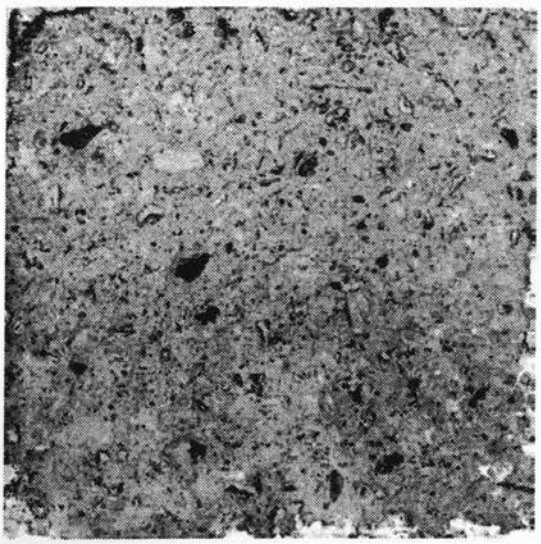

d) 40% Slag Curing B

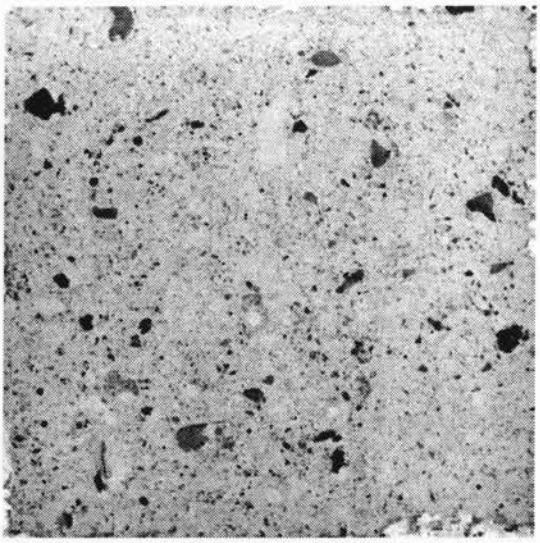

e) 20/20 Curing A

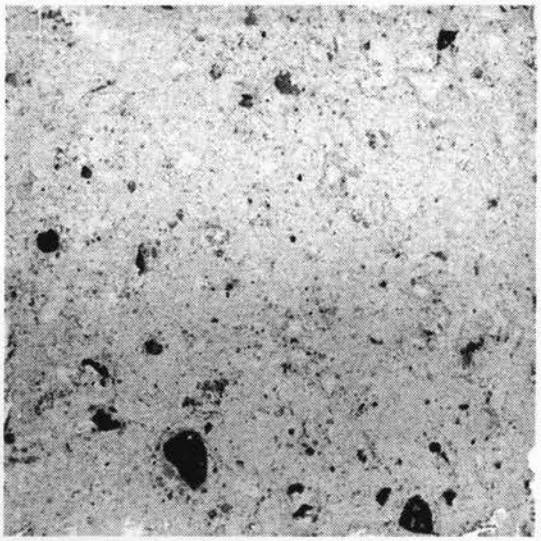

f) 20/20 Curing B

Figure 4.20: Scaling slabs after 50 cycles

4.3.1 Effect of Slag on Salt Scaling

Increased scaling of concrete containing 30% and 40% slag is in agreement with the well reported results (Valenza and Scherer, 2007; Bouzoubaa et al., 2008; Stark and Ludwig, 1997). The 40 % and 30% slag mixes produced the highest compressive strength at 28 day compared to other mixes evaluated. Poor performance of slag binary mixes gives the indication that strength is not a governing factor for scaling resistance of these two mixes.

Care was taken to eliminate the bleeding water before finishing with wood trowel. After the two strokes of finish, a 75 mm brush was used to eliminate the sheen of water from the surface. Hence, it could be expected that accumulation of bleed water might not have played a significant role in accelerated scaling. Another factor believed to influence the scaling of slag concrete is carbonation (Stark and Ludwig, 1997). As shown by Stark and Ludwig (1997), carbonation might be a dominant factor responsible for the severe scaling of slag concretes. Rate of scaling in slag concrete is very high for the first 10 cycles, marked by a steep slope in Figure 4.18. After 10 cycles, the rate of scaling stated to reduce. This pattern is most probably due to the fact that after 10 cycles the scaling depth reached non-carbonated surface.

Increasing slag content from 30% to 40% has resulted in almost same amount of scaling after 50 cycles. Both 30% and 40% followed the same trend; first 10 cycles severe scaling occurred thereafter the rate of scaling is reduced. These may be due to the fact that carbonated layer in both concrete existed approximately for the same depth; perhaps, the depth of carbonated layer for 40% slag concrete is little higher than that of 30% slag.

However, when both concrete reached the non-carbonated layer both has scaled virtually at the same rate.

4.3.2 Effect of Ternary Blend on Salt Scaling

If total SCM content is considered, ternary blends have performed relatively well. That is if 15/15 is to be evaluated against 30% slag (both have the same SCM content), then 15/15 have performed well than 30% slag. Similarly, 20/20 performed better than 40% slag. The available literature gives contradictory results regarding the performance of slag and fly ash in binary and ternary blends. For example, Bouzoubaa et al. (2008) published results showing that 35% Type F fly ash concrete scaled 2.82 kg/m^2 where 35% slag scaled 0.95 kg/m^2 after 50 freeze and thaw cycles when tested according to ASTM C672. Afrani and Rogers (1994) also showed concrete with 18% Type F fly ash scaled 1.31 kg/m^2 and concrete with 25% slag scaled 0.42 kg/m^2 after 50 freeze and thaw cycles when tested according to MTO LS412. Hooton and Boyd (1997) showed 35% slag concrete scaled 0.50 kg/m^2 after 50 cycles when tested according to MTO LS412. Bouzoubaa et al (2008), Afrani and Rogers (1994), and Hooton and Boyd (1997) give the impression that fly ash is worse than slag, and slag scaled either within the MTO limit of 0.8 kg/m^2 or marginally exceeding that limit. However, it has been shown well that slag worsen the scaling resistance mainly due to carbonation, excessive bleeding, and finishing practices (Valenza and Scherer, 2007; Stark and Ludwig, 1997). In addition, the current study has also exhibited increased scaling of 30% slag and 40% slag concretes as discussed earlier (Figure 4.18).

Scaling resistance of high calcium fly ash is not widely available as of low calcium fly ash. However, available literature suggests that ASTM Class C/CSA Class CH fly ash does not reduce the salt scaling resistance compared to Class F fly ash. Naik et al. (1998) have showed that concrete with 35% ASTM Class CH fly ash performed even better than the plain concrete. At the end of 50 cycles, Naik et al. (1998) have given ASTM Rating 0 to 35% Class CH concrete and ASTM Rating 1 to the control concrete. This indicates that Class CH fly ash enhances the resistance. On the other hand, Hooton and Boyd (1997) showed that 15% Class CH fly ash scaled 0.36% kg/m^2 where the control concrete scaled 0.14 kg/m^2.

According to the current study, 15/15 (cumulative scaling of 0.99 kg/m^2) performed better than 30% slag (1.97 kg/m^2) and 20/20 (1.65 kg/m^2) performed better than 40% slag (2.03 kg/m^2). Enhanced performance of ternary blends might be due to the enhanced performance of Class CH fly ash itself. Naik et al. (1998) results shows that Class CH fly ash performed well against salt scaling. In addition, incorporation of Class CH fly ash in ternary blends might have improved the resistance due to reduced bleeding and, thus, ended up with less porous surface layer than binary slag concrete. The bleeding results (Table 4.12) indicate that both 15/15 and 20/20 have ended up with reduced bleeding than the control. The bleeding for 15/15, 20/20, Control, 30% slag and 40% slag mixes are 0.16, 0.30, 1.34, 2.56, 2.93%, respectively (see Section 4.6).

4.3.3 Effect of Curing on Salt Scaling Resistance

Figure 4.19 shows the scaling results of the two mixes (i.e. 20/20 and 40% Slag) that went through the modified curing method (Curing B). The intention of curing outside the

curing room is to prevent the moisture dripping on the slabs. Moisture dripping will leach alkalis and calcium hydroxide which would otherwise be used for pozzolanic reaction of SCMs. The slabs were tightly wrapped as to prevent the moisture loss so that the slabs will be cured with the internal moisture. The aim is to sacrifice the moist room curing in order to prevent the leaching of alkalis from the surface. If internal curing is adequate and alkalis are prevented from leaching, then it is expected that the resistance of the slabs when exposed salt will be enhanced. On the other hand, if the internal curing is not adequate, then the surface microstructure will be coarser.

As stated above about 55 – 60% reduction in scaling loss occurred as a result of curing by plastic wrapping, which is a significant reduction. The improvement shows that internal curing was effective and adequate, and alkali leaching could have an impact on reduced scaling resistance of SCM concretes tested in the laboratories. The curing method prescribed in MTO and ASTM standards could be partially responsible for the discouraging results from accelerated laboratory testing. For example, Hooton and Boyd (1997) have observed discrepancy between the performance of lab specimens and the field concrete where the lab specimens showed severe scaling than the cores from the field. Similarly, Thomas (1997) reported several cases where concrete containing fly ash performed well in the field which is not consistent with the poor laboratory performance in the accelerated conditions such as ASTM C 671.

In order to confirm the differences in alkali retention at the concrete surface, the Leaching Test was conducted on chips from the top of concrete specimens from Curing A

and Curing B. Two cylinders (200 mm height; 100 mm diameter) from 40% slag concrete mix were made and each cured according to the respective curing regimes. Experimental details of this test are described in Chapter 3. Table 4.8 contains the alkalis released by each sample in one month into distilled water. The results indicate that the sample of Curing B leached approximately 130% of K^+ and Na^+ with respect to the sample of Curing A. The difference in alkalis leached indicates that concrete surface cured by wrapping retained more alkalis than the concrete cured in the moist room. This suggests that higher alkalis retained on the surface of 20/20 curing B and 40% curing B is a dominant factor responsible for enhanced performance of these salt scaling slabs.

Table 4.8: Leaching results of samples from two salt scaling curing regimes

Curing Regime	**K^+ (ppm)**	**Na^+ (ppm)**
A (moist room)	28.6	26.6
B (polyethylene wrapping)	66.0	62.0

4.4 Freeze-thaw Damage

Freeze-thaw damage was evaluated by performing ASTM 666, Procedure A. The damage is calculated by reduction in weight and dynamic modulus of elasticity. Dynamic modulus of elasticity is calculated using the correlated relationship between pulse velocity and dynamic modulus of elasticity. Durability Factor is then determined from the pulse velocity using Equation 10 presented in Chapter 3. Table 4.9 contains the weight loss and the Durability Factors for the concrete tested. Appendix C contains the raw data and details of calculation of durability factor. Figure 4.21 shows the photographs of the prisms after 300 freeze-thaw cycles. The results showed that no

significant amount of internal damage have occurred to the concrete as the Durability Factors are very high. However, surface scaling was observed toward the end of the test period and is evident from the pictures of Figure 4.21. Especially few specimens from 20/20 and 40% slag have scaled more than any other mixes. The scaled surfaces have also made the pulse velocity measurements difficult and variable by the end of the test period (after ~200 cycles). The surface scaling might have occurred as a result of presence of bleed water and destruction of air void at the surfaces. Still, higher Durability Factors indicate that when ternary and binary, and control mixes are adequately air entrained (~4-6%), the internal damage will be controlled to a greater extend.

Table 4.9: Freeze-thaw Resistance of Concrete Mixtures

MIX ID	Air Content %	Weight Change %	Durability Factor
Control (100% PC2)	7.2	-0.13	98.5
15/15 (FA3/Slag2)	6.2	-0.31	98.8
20/20 (FA3/Slag2)	5.0	-0.88	98.1
30% Slag2	5.8	-0.25	98.1
40% Slag2	5.8	-1.31	97.4

Figure 4.21 a) Control (100%PC2)

b) 15/15 (FA3/Slag2)

c) 20/20 (FA3/Slag2)

d) 30 Slag2

Initially at day 1, control gained the highest strength than the other mixes that contained SCMs. 15/15 and 30% Slag mixes gained second highest values followed by 20/20 and 40% slag. 15/15 and 30% slag concretes gained almost the same compressive strength, 11.5 and 11.7 MPa respectively. Similarly, 20/20 and 40% slag concretes gained very close to each other, 10.0 and 9.7 MPa respectively. This indicates that at the very early stage replacing the Portland cement with SCM lowers the strength to the same level regardless of ternary or binary mix. The total SCM content in 15/15 and 30% slag mix being equal, they both ended up with the similar strength at day 1. Same observation could be made with 20/20 and 40% slag.

At later ages, the concrete with slag content reached higher strength of all the mixes tested. Strengths of 40% slag and 30% slag at 28 and 56 days are similar but at 7 day 40% slag concrete achieved slightly lower strength than that of 30% slag. The slightly lower strength of 40% slag compared to 30% slag at 7 days could be attributed to the fact that not all the slag grains are activated before 7 days. Highest strength of slag mixes resulted due to its latently hydraulic nature (Mindess et al., 2003).

Ternary blends were superior to the control at and after day 7 but obtained lower strength than slag mixes. Having 15/15 achieved lower strength compared to 30% slag and 20/20 obtained lower than 40% slag indicates that Class CH fly ash did not enhance the strength development to the level of slag. The higher strength of 20/20 than 15/15 at later ages might be due to the higher slag content in the former mix. Further, no evidence was observed for synergetic action in ternary blends, rather it seems that slag content is the

Table 4.10: Compressive Strength

	Compressive Strength (MPa)				
Age (days)	**Control (100%PC2)**	**15/15 (FA3/Slag2)**	**20/20 (FA3/Slag2)**	**30% Slag2**	**40% Slag2**
1	13.9	11.5	10.0	11.7	9.7
7	25.6	23.5	24.3	28.2	25.5
28	29.6	33.9	33.9	36.8	38.1
56	30.8	35.0	38.6	39.5	40.9

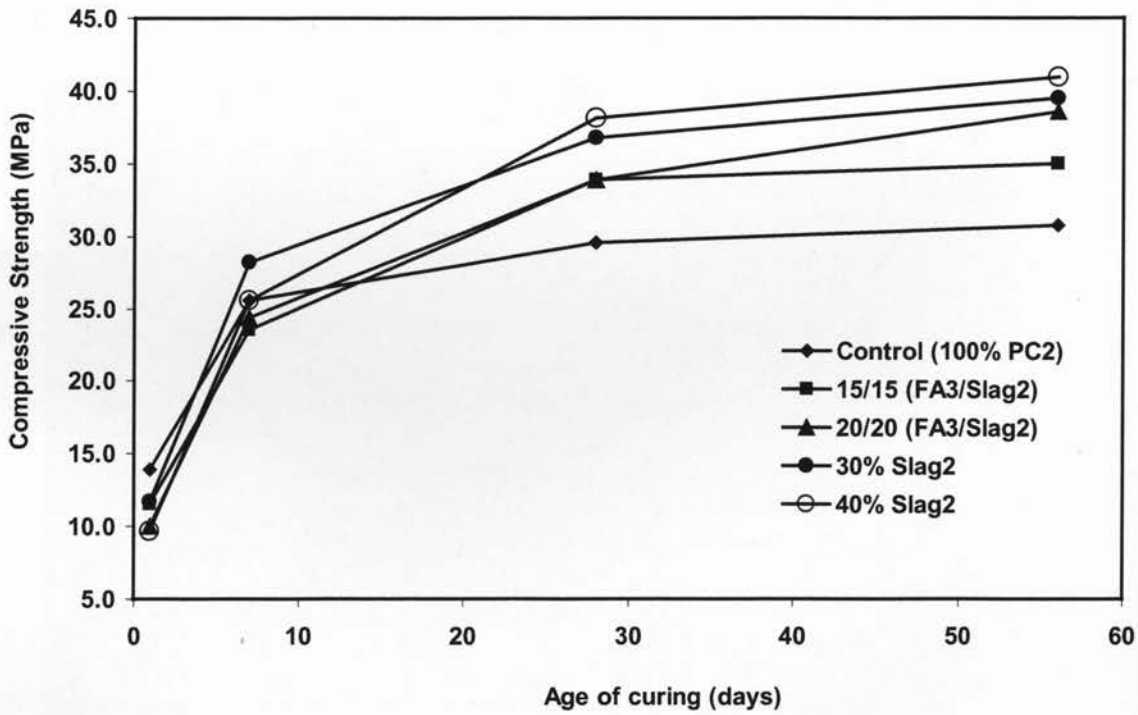

Figure 4.22: Compressive strength of cylinders

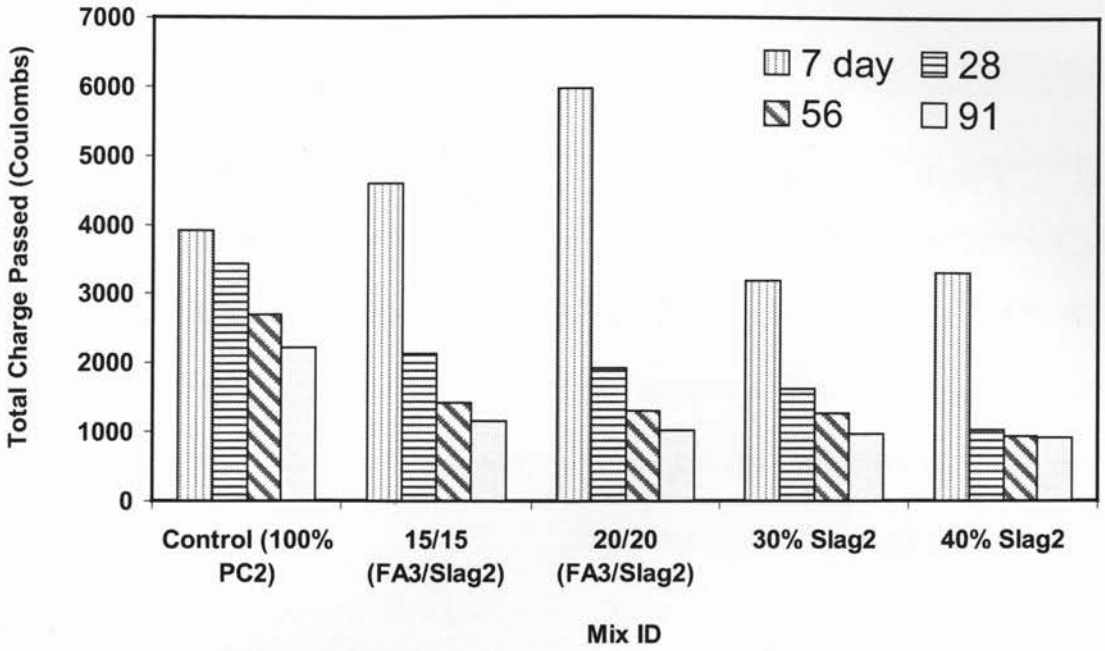

Figure 4.23: Total charges passed during the Rapid Chloride Permeability Test

At 7 day of age, the ternary blends are the least effective in terms of permeability. That is, 20/20 and 15/15 have the highest charge passed through when tested at 7 day. The slag concretes have the lowest permeability values. At 7 day, permeability of 15/15 and 20/20 are in high range (>4000 coulombs); where control and slag blends are in the moderate range (2000 – 4000 coulombs). From Figure 4.23, the dramatic decrease in permeability of ternary and binary blends from 7 day to 28 day can be observed. Blends 15/15, 20/20, 30% Slag, and 40% Slag have reduced coulombs by 54, 68, 49 and 69%, respectively; but the corresponding reduction for the control concrete is only 12%. However, such a sudden reduction for mixes with SCM is absent at 56 or 91 days. This sudden reduction after 7 day could be attributed to the pore filling effect due to increased level of hydration from SCM mixes. After 3 months, the binary slag blends permeability

dominant factor for the superior strength development. Yet, ternary blended did not worsen the case as they both (15/15 and 20/20) are higher than the control mix.

4.5.2 Ion Migration – Rapid Chloride Permeability Test

Table 4.11 summarizes the total charges passed in 6 hours when RCPT (ASTM C1202) test was conducted. The same five concrete mixes made for compressive strength test were tested for ion migration as well. The values given in Table 4.11 and Figure 4.23 are average of three specimens obtained from the same concrete cylinder.

Table 4.11: Total Charges Passed during RCPT

Age (days)	Total Charge Passed (Coulombs)				
	Control (100% PC2)	15/15 (FA3/Slag2)	20/20 (FA3/Slag2)	30% Slag2	40% Slag2
7	3915	4584	5963	3181	3284
28	3436	2125	1910	1619	1020
56	2699	1416	1298	1259	921
91	2201	1153	1015	961	904

(ASTM C1202 classification:
Total charge passed >4000 High Permeability,
2000 – 4000 Moderate Permeability,
1000 – 2000 Low Permeability,
100 – 1000 Very Low Permeability)

4.6.2 Slump

Slump was measured using the slump cone described in ASTM C143. The result shown in Table 4.12 indicates that the all the concretes tested exhibited excellent workability. It should be emphasised here that all the mixes had normal subsidence of concrete without any breaking up when the slump cone was lifted to measure the slump. Further, the all the mixes were highly cohesive and no segregation was occurred.

4.6.3 Bleeding

Concrete with slag increased the bleeding significantly compared to the control mixture where the ternary blends ended up with reduced rate of bleeding. The increased bleeding in 30% Slag and 40% Slag mixes is due to their higher slag replacement level. It is stated elsewhere that slag of fineness equal to that of Portland cement tend to increase the bleeding (Kosmatka et al., 2002). The fineness of Portland cement and slag used in this study was measured by materials passing 45μm method. Portland cement retained 4.6% while slag retained 3.9% of the initial mass on 45μm sieve. Increased bleeding in slag concrete is, hence attributable to the similar fineness of Portland cement and slag. Kosmatka et al. (2002) contains results showing that concrete containing 25% Class CH fly ash have resulted in around 0.34% bleeding where control mixture resulted in higher bleeding around 1.75%. Further, it has been widely observed that fly ash concrete reduces the bleeding (Berry and Malhotra, 1980). Most likely the incorporation of Class CH fly ash is responsible for the reduced bleeding in ternary blends. 15 and 20% fly ash in 15/15 and 20/20 have reduced the bleeding significantly.

4.6.4 Setting Time

The control concrete is the one with shortest initial set of all the mixes tested. The ones with slag took little longer than the control for initial setting time. Ternary blends are the ones with the most delayed initial setting time, exceeding the control and slag mixes. Similar observation was made for the final setting time; control reached the final setting time first, followed by slag and ternary blends. This clearly reveals that adding slag or fly ash reduces the rate of reaction and hence delays the setting. However, slag binary blends set faster than ternary blends due to the incorporation of fly ash into the ternary blends. Early setting of slag concrete than ternary blends is due to the enhanced reactivity of slag than the fly ash. Incorporation of fly ash into ternary blends have delayed the initial and final setting times and hence, made the interval between them longer. Comparing the setting times of ternary blends 15/15 and 20/20, there is around 1 hour difference between their corresponding setting times. That is 20/20 took 1 hour longer than 15/15 to reach the initial setting time and 1 hour delayed to reach the final setting. However, 30% slag and 40% took approximately same time to reach the initial and final setting.

Chapter 5. Conclusions and Recommendations

5.1 Conclusions

Based on the materials used and experimental works conducted in this study, the following conclusions were made:

1. The binary blends with Class CH fly ash had low sodium sulfate resistance than the control mix.

2. The binary blends with slag significantly improved the resistance to sodium sulfate attack and resulted in much less expansion even at 20% replacement level. At 30% and 40% slag replacement levels, the expansion met the ASTM limits of 0.05% at 6 month and 0.1% at 1 year. It could be stated that 30 – 40% low alumina slag is sufficient to suppress the expansion to the acceptable level.

3. All the ternary blends reduced the expansion due to sulfate with respect to the control blend where the binary blends with Class CH fly ash resulted in expansion higher than control. The incorporation of slag as little as 20% into the blend made possible to incorporate Class CH fly ash with increased resistance. The ternary blend with 40% Class CH fly ash + 20% slag resulted in superior performance and this is viewed as a significant finding since 40% Class CH fly ash binary blend dramatically reduced the resistance.

4. Some correlation was obtained between the $Ca(OH)_2$ content in the paste samples of ternary blends at 28 days and the expansion of sulfate attack mortar bar at 9 months. This shows $Ca(OH)_2$ consumption is a contributing factor in resisting sulphate attack. Further, the blend 40%FA+20%Slag resulted in the lowest $Ca(OH)_2$ content of all the samples tested confirms that $Ca(OH)_2$ consumption of this blend is a contributing factor for reduced expansion of its mortar bar under sulfate solution.

5. Based on accelerated mortar bar (AMBT) and concrete prisms expansion, binary Class CH fly ash blends reduces the expansion due to ASR but not significantly effective. Higher replacement (>50%) levels might work to satisfy the expansion requirements.

6. Incorporation of slag in the levels of 40% and 50% also reduces the ASR expansion. However, both 40% and 50% did not meet the CSA AMBT limit of 0.1 at 14-day.

7. Expansions of ternary concrete prisms of Class CH fly ash and slag are smaller than the individual expansions of corresponding binary blends.

8. An excellent correlation existed between the alkali binding capacity and the ASR concrete prism expansion; and this suggests that alkali binding ability of the binary and ternary blends is a contributing factor in controlling ASR expansion.

9. A very good correlation was found between 14-day expansion of AMBT and 1-year expansion of concrete prisms; this suggest AMBT could be used as a quick screening tool to detect potential ASR aggregates.

10. Salt scaling resistance of concrete containing slag is significantly reduced despite the highest strength development.

11. The ternary concretes, in comparison to concrete of same level of slag replacement, (ie. 15/15 vs 30% slag), have improved the scaling resistance. The exact reasons for this improvement are unknown. But the potential reasons could be partially attributable to the lower bleeding of ternary blends.

12. Storing outside the curing room with the slab tightly wrapped using polyethylene enhanced the salt scaling resistance significantly. The possible reasons for such a beneficial action are attributable to prevention of alkali leaching from the concrete surface. The alkalis are necessary for slag to activate and for the pozzolanic reaction of SCMs.

13. The tested control, slag and ternary blends resulted satisfactory performance against freeze-thaw cycles. The durability factors at the end of 300 cycles are very high, indicating that adequate air entrainment provide sufficient protection.

14. Generally, the strength development rate is higher for the concretes with slag replacement. The ternary blends scored the next highest development rate followed by the control concrete.

15. At later age, the concrete with slag replacement is less permeable followed by the ternary blends. Less permeability of binary and ternary blends is due to the formation of secondary C-S-H and pore refinement. The control concrete resulted in higher permeability than the ones with SCM replacement.

16. Air content and slump increase with the increased Class CH fly ash and/or slag content in the mix. The bleeding for the ternary blends are significantly lower than that of the control and slag mixes where slag mixes have excessive bleeding. The reduced bleeding for the ternary blends might be due to the presence of Class CH fly ash in them.

17. Ternary blends resulted in delayed initial and final setting times followed by the slag concretes. The control reached the initial and final setting times faster than other concretes. Delayed setting of ternary concretes might be due to lower reactivity of fly ash than slag. The binary blends with slag are relatively faster than the ternary blends and this indicates that slag has higher reactivity than Class CH fly ash in fresh concrete.

5.2 Recommendations

Class CH fly ash lacks the consumer confidence in using as supplementary cementing material as a result of reported poor performance against sulfate attack and alkali-silica reaction. Ternary blends tested in the current study are promising as a remedy to incorporate Class CH fly ash in concrete. The results showed that in ternary blends of

fly ash and slag, more Class CH fly ash could be incorporated with increased resistance to sulfate attack. Ternary blends performed satisfactorily in the case of ASR as well. Hence, the results of this study provide the basis to draw the attention towards ternary blends of Class CH fly ash and slag as a mean for safe incorporation of Class CH fly ash. It is recommended to further investigate the mechanism of slag/Class CH fly ash ternary blends and its applicability in real cases.

The ternary blends produced higher salt scaling residue than the MTO limit of 0.80 kg/m^2. In order to overcome such a shortfall, it has been shown to enhance to salt scaling resistance by preventing alkali leaching. This study adopted the polyethylene wrapping as a way to cure using the internal moisture and to prevent any water dripping. If plastic wrapping is not a applicable method to the field practices, it is recommended to consider curing compounds or any other suitable methods rather than applying moist stream or any other ways by which alkalis might be washed away.

References

Afrani, I. and Rogers, C. 1994. "The effects of different cementing materials and curing on concrete scaling". Cement, Concrtete and Aggregates, 16(2), 132 – 139.

Arano, N. and Kawamura, M. 2000. "Comparative consideration on the mechanisms of ASR suppression due to different mineral admixtures". Bérubé, M.A., Fournier, B., Durand B., editors. Proceedings of the 11th International Conference on Alkali-Aggregate Reaction in Concrete, Quebec City, 11 – 16 June, 553–562.

Bellmann, F. and Stark, J. 2007. "Prevention of thaumasite formation in concrete exposed to sulfate attack". Cement and Concrete Research, 37(8), 1215 – 1222.

Berry, E. E. 1980. "Strength development of some blended-cement mortars". Cement and Concrete Research, 10(1), 1 – 11.

Berry, E. E. and Malhotra, V. M. 1980. "Fly ash for use in concrete: A critical review". ACI Journal, 77(2), 59 – 73.

Bleszynski, R.F. and Thomas, M.D.A. 1998. "Microstructural studies of alkali–silica reaction in fly ash concrete immersed in alkaline solutions". Advanced Cement Based Materials 7(2), 66–78.

Bilodeau, A., Carette, G. G., Malhotra, V. M., and Langley, W. S. 1991. "Influence of curing and drying on salt scaling resistance of fly ash concrete". Malhotra, V. M., editor. Proceeding of 2nd CANMET/ACI International Conference on Durability of Concrete, August. ACI Special Publication-126, American Concrete Institute, Detroit, Michigan, 201 – 228.

Bilodeau, A., Sivasundaram, V., Painter, K. E., and Malhotra, V. M. 1994. "Durability of concrete incorporating high volumes of fly ash from sources in the U.S.". ACI Materials Journal, 91(1), 3 – 12.

Boyd, A. J. and Hooton, R. D. 2007. "Long-term scaling performance of concretes containing supplementary cementing materials". Journal of Materials in Civil Engineering, 19(10), 820 – 825.

Bouzoubaa, N., Bilodeau, A., Fournier, B., Hooton, R. D., Gagne, R., and Jolin, M. 2008. "Deicing salt scaling resistance of concrete incorporating supplementary cementing materials: Laboratory and field test data". Canadian Journal of Civil Engineering, 35(11), 1261 – 1275.

Brown, P. W. 2002. "Thaumasite formation and other forms of sulfate attack". Cement and Concrete Composites, 24(3-4), 301 – 303.

Carrasquillo, R. L. and Snow, P. G. 1987. "Effect of fly ash on alkali-aggregate reaction in concrete." ACI Materials Journal, 84(4), 299 – 305.

Chatterji, S. and Thaulow, N. 2000. "Some fundamental aspects of alkali silica reaction". Bérubé, M.A., Fournier, B. and Durand, B., editors. Proceedings of the 11th International Conference on Alkali–Aggregate Reaction in Concrete, Quebec City, 11 – 16 June, 21–29.

Cohen, M. D. 1983. "Theories of expansion in sulfoaluminate type expansive cements: Schools of thought". Cement and Concrete Research, 13(6), 809 – 818.

Collepardi, M. 2003. "A state-of-the-art review on delayed ettringite attack on concrete". Cement and Concrete Composites, 25(4-5), 401 – 407.

Copuroglu, O. and Schlangen, E. 2008. "Modeling of frost salt scaling". Cement and Concrete Research 38 (1), 27–39.

Dehuai, W. and Zhaoyuan, C. 1997. "On predicting compressive strengths of mortars with ternary blends of cement, GGBFS and fly ash". Cement and Concrete Research, 27(4), 487 – 493.

Diamod, S. and Thaulow, N. 1974. "A study of expansion due to alkali–silica reaction as conditioned by the grain size of the reactive aggregate". Cement and Concrete Research, 4(4), 591–607.

Douglas, E. and Pouskouleli, G. 1991. "Prediction of compressive strength of mortars made with Portland cement-blast furnace slag-fly ash blends". Cement and Concrete Research, 21(4), 523 – 534.

Duchesne, J. and Bérubé, M. A. 1994a. "The effectiveness of supplementary cementing materials in suppressing expansion due to ASR: Another look at the reaction mechanisms. Part 1: Concrete expansion and portlandite depletion". Cement and Concrete Research, 24(1), 73 – 82.

Duchesne, J. and Bérubé, M. A. 1994b. "The effectiveness of supplementary cementing materials in suppressing expansion due to ASR: Another look at the reaction mechanisms. Part 2: Pore solution chemistry". Cement and Concrete Research, 24(2), 221 – 230.

Dunstan Jr., E. R. 1980. "A possible method for identifying fly ashes that will improve the sulfate resistance of concretes". Cement, Concrete, and Aggregates, 2(1), 20 – 30.

Escadeillas, G., Aubert, J., Segerer, M., and Prince, W. 2007. "Some factors affecting delayed ettringite formation in heat-cured mortars". Cement and Concrete Research, 37(10), 1445 – 1452.

Fournier, B. and Bérubé, M. A. 2000. "Alkali–aggregate reaction in concrete: A review of basic concepts and engineering implications". Canadian Journal of Civil Engineerig. 27 (2), 167–191.

Freeman, R. B. and Carrasquillo, R. L. 1995. "Adjustments in gypsum content for production of sulfate-resistant blended cements containing high-calcium fly ash". ACI Materials Journal, 92(4), 411 – 418.

Gollop, R. S. and Taylor, H. F. W. 1996a. "Microstructual and microanalytical studies of sulfate attack: IV. Reactions of a slag cement paste with sodium and magnesium sulfate solutions". Cement and Concrete Research, 26(7), 1013 – 1028.

Gollop, R. S. and Taylor, H. F. W. 1996b. "Microstructural and microanalytical studies of sulfate attack: V. Comparison of different slag blends". Cement and Concrete Research, 26(7), 1029 – 1044.

Hime, W. G. and Mahter, B. 1999. ""Sulfate attack," or is it?" Cement and Concrete Research, 29(5), 789 – 791.

Hooton, R. D. and Boyd, A. 1997. "Effect of finishing, forming and curing on de-icer salt scaling resistance of concretes". Setzer, M. J. and Auberg, R., editors. Proceeding of the Internatinal RILEM workshop on Resistance of Concrete to Freezing and Thawing with or without de-icing chemicals, Essen, Germany, 9 June. University of Essen, Germany and E&F Spon., London, 174 – 183.

Hooton, D. H. 2000. "Canadian use of ground granulated blast-furnace slag as a supplementary cementing material for enhanced performance of concrete". Canadian Journal of Civil Engineering, 27(4), 754 – 760.

Kosmatka, S. H., Kerkhoff, B., Panarese, W. C., MacLeod, N. F., McGrath, R. J. 2002. "Design and Control of Concrete Mixtures, 7th Canadian Edition". Cement Association of Canada: Ottawa.

Malhotra, V. M. 1990. "Durability of concrete incorporating high-volume of low-calcium (ASTM Class F) fly ash". Cement and Concrete Composites, 12(4), 271 – 277.

Malvar L. J., Cline. G. D., Burke, D. F., Rollings, R., Sherman, T. W., and Greene, J. L. 2002. "Alkali-silica reaction mitigation: State of the art and recommendations." ACI Materials Journal, 99(5), 480 – 489.

Malvar, L. J. and Lenke, L. R. 2006. "Efficiency of fly ash in mitigating alkali-silica reaction based on chemical composition." ACI Materials Journal, 103(5), 319 – 326.

Mangat, P. S. and Khatib, J. M. 1995. "Influence of fly ash, silica fume, and slag on sulfate resistance of concrete". ACI Materials Journal, 95(5), 542 – 552.

Marchand, J., Maltais, Y., Machabee, Y., Talbot, C., and Pigeon, M. 1997. "Effects of fly ash on microstructure and deicer salt scaling resistance of concrete". Frost Resistance of Concrete, Setzer, M. J and Auberg, R., editors. Proceeding of the International RILEM workshop on Resistance of Concrete to Freezing and Thawing with or without de-icing chemicals, Essen, Germany, 9 June, 11 –20.

Mehta, P. K. 1986. "Effect of fly ash composition on sulfate resistance of cement". ACI Journal, 83(6), 994 – 1000.

Mindess, S., Young, J. F., and Darwin, D. 2003. "Concrete (2nd edition)". Prentice Hall: New Jersey.

Monteiro, P. J. M., Wang, K., Sposito, G., Dos Santos, M. C. and De Andradef, W. P. 1997. "Influence of mineral admixtures on the alkali-aggregate reaction". Cement and Concrete Research, 27(12), 1899 – 1909.

Mulenga, D. M., Stark, J. and Nobst, J. S. 2003. "Thaumasite formation in concrete and mortars containing fly ash". Cement and Concrete Composites, 25(8), 907 – 912.

Multon, S., Cyr, M., Sellier, A., Leklou, N., and Petit, L. 2008. "Coupled effects of aggregate size and alkali content on ASR expansion". Cement and Concrete Research, 38 (3), 350–359.

Naik, T. R., Singh, S., Ramme, B. 1998. "Mechanical properties and durability of concrete made with blended fly ash". ACI Materials Journal, 95(4), 454 – 462.

Nehdi, M. and Hayek, M. 2005. "Behavior of blended cement mortars exposed to sulfate solutions cycling in relative humidity". Cement and Concrete Research, 35(4), 731 – 742.

Nehdi, M., Pardhan, M., and S. Koshowski. 2004. "Durability of self-consolidating concrete incorporating high-volume replacement composite cements". Cement and Concrete Research, 34(11), 2103 – 2112.

Neville, A. 2004. "The confused world of sulfate attack on concrete". Cement and Concrete Research, 34(8), 1225 – 1296.

Panesar, D. K. and Chidiac, S. E. 2007. "Multi-variable statistical analysis for scaling resistance of concrete containing GGBFS". Cement and Concrete Composites, 29(1), 39 – 48.

Pigeon, M., Marchand, J., and Pleau, R. 1996. "Frost resistant concrete". Construction and Building Materials, 10(5), 339 – 348.

Prezzi, M., Monteiro, P.J.M. and Sposito, G. 1997. "The alkali–silica reaction, Part I: Use of double-layer theory to explain the behavior of reaction product gels". ACI Materials Journal, 94(1), 10–17.

Ramlochan, T., Zacarias, P., Thomas, M. D. A., and Hooton, R.D. 2003. "The effect of pozzolans and slag on the expansion of mortars cured at elevated temperature: Part I. Expansive behaviour". Cement and Concrete Research, 33(6), 807–814.

Ramyar, K. and Inan, G. 2007. "Sodium sulfate attack on plain and blended cements". Building and Environment, 42(3), 1368 – 1372.

Rasheeduzzafar and Hussain, S. E. 1991. "Effect of microsilica and blast furnace slag on pore solution composition and alkali-silica reaction". Cement and Concrete Composites, 13(3), 219 – 225.

Rogers, C., Grattan-Bellew, P.E., Hooton, R.D., Ryell, J., and Thomas, M.D.A. 2000. "Alkali-aggregate reactions in Ontario". Canadian Journal of Civil Engineering, 27(2), 246 – 260.

Roy, D. M., and Idorn, G. M., 1982. "Hydration, structure, and properties of blast furnace slag cements, mortars and concrete". Journal of the American Concrete Institute, 79(6), 444 – 457.

Santhanam, M., Cohen, M. D., and Olek, J. 2003. "Mechanism of sulfate attack: A fresh look: Part 2, Proposed Mechanisms". Cement and Concrete Research, 33(3), 341 – 346.

Santhanam, M., Cohen, M. D., and Olek, J. 2001. "Sulfate attack research – whither now?" Cement and Concrete Research, 31(6), 845 – 851.

Saouma, V. and Perotti, L. 2006. "Constitutive Model for alkali-aggregate reactions." ACI Materials Journal, 103(3), 194 – 202.

Shashiprakash, S. G. and Thomas, M. D. A. 2001. "Sulfate resistance of mortars containing high calcium fly ashes and combinations of highly reactive pozzolans and fly ash". Malhotra, V. M., editor. Proceeding of the 7th CANMET/ACI International Conference on Fly Ash, Silica Fume, Slag, and Natural Pozzolan in Concrete, Chennai, India, 22–27 July. ACI Special Publication-199, American Concrete Institute, Farmington Hills, Michigan, 221–237.

Shehata, M. H. 2001. "Effect of fly ash and silica fume on alkali-silica reaction in concrete". Ph.D. Thesis, University of Toronto.

Shehata, M. H. and Thomas, M. D. A. 2000. "The effect of fly ash composition on the expansion of concrete due to alkali-silica reaction". Cement and Concrete Research, 30(7), 1063 – 1072.

Shehata, M. H. and Thomas, M. D. A. 2006. "Alkali release characteristics of blended cements". Cement and Concrete Research, 36(6), 1166 – 1175.

Shehata, M. H., Adhikari, G., and Radomski, S. 2008. "Long-term durability of blended cement against sulfate attack". ACI Materials Journal, 105(6), 594 – 602.

Shon, C. -S., Zollinger, D. G., and Sarkar, S. L., 2004. "Evaluation of ASR Resistance of fly ash-slag combinations using the modified ASTM C 1260 test method". Malhotra, V. M., editor. Proceeding of the Eighth CANMET/ACI International Conference on Fly Ash, Silica Fume, Slag, and Natural Pozzolans in Concrete, ACI Special Publication-221, American Concrete Institute, Farmington Hills, Michigan, 249-264.

Stark, J. and Ludwig, H. 1997. "Freeze-thaw and freeze-deicing salt resistance of concretes containing cement rich in granulated blast furnace slag". ACI Materials Journal, 94(1), 47 – 55.

Swamy, N. and Al-Asali, M. M. 1988. "Expansion of concrete due to alkali-silica reaction." ACI Materials Journal, 85(1), 33 – 40.

Talbot, C., Pigeon, M., and Marchand, J. 2000. "Influence of fly ash and slag on deicer salt scaling resistance of concrete". Proceeding of 5th international conference on durability of concrete, Spain, June. ACI Special Publication-192, American Concrete Institute, Farmington Hills, Michigan, 645 – 657.

Taylor, H. F. W., Famy, C., and Scrivener, K. L. 2001. "Delayed ettringite formation". Cement and Concrete Research, 31(5), 683 – 693.

Thomas, M.D.A. 1997. "Laboratory and field studies of salt scaling in fly ash concrete". Frost Resistance of Concrete, Setzer, M. J. and Auberg, R., editors. Proceeding of the Internatinal RILEM workshop on Resistance of Concrete to Freezing and Thawing with or without de-icing chemicals, Essen, Germany, 9 June. University of Essen, Germany and E&F Spon., London, 21 – 30.

Thomas, M.D.A. and Innis, F.A. 1998. "Effect of slag on expansion due to alkali–aggregate reaction in concrete". ACI Materials Journal, 95 (6), 716–724.

Thomas, M. D. A., Fournier, Folliard, K. J., Shehata, M. H., Ideker, J. H., and Rogers, C. 2007. "Performance limits for evaluating supplementary cementing materials using accelerated mortar bar test". ACI Materials Journal, 104(2), 115 – 122.

Thomas, M. D. A., Shehata, M. H., Shashiprakash, S. G., Hopkins, D. S., and Cail, K. 1999. "Use of ternary cementitious systems containing silica fume and fly ash in concrete". Cement and Concrete Research, 29(8), 1207 – 1214.

Tian, B. and Cohen, M. D. 2000. "Does gypsum formation during sulfate attack on concrete lead to expansion?". Cement and Concrete Research, 30(1), 117 – 123.

Tikalsky, P. J., Carrasquillo, R. L., and Snow, P. G. 1990. "Sulfate resistance of concrete containing fly ash". Proceeding of the G.M. Idorn international symposium on durability of concrete, Toronto, Ontario, March. ACI Special Publication-131, American Concrete Institute, Detroit, Michigan, 255 – 265.

Tikalsky, P. J. and Carrasquillo, R. L. 1992. "Influence of fly ash on the sulfate resistance of concrete". ACI Structural Journal, 89(1), 69 – 75.

Tikalsky, P. J. and Carrasquillo, R. L. 1993. "Fly Ash evaluation and selection for use in sulfate-resistant concrete". ACI Materials Journal, 90(6), 545 – 551.

Valenza, J. J. and Scherer, G. W. 2007a. "A review of salt scaling: I. Phenomenology". Cement and Concrete Research, 37(7), 1007 – 1021.

Valenza, J. J. and Scherer, G. W. 2007b. "A review of salt scaling: II. Mechanism". Cement and Concrete Research, 37(7), 1022 – 1034.

Valenza, J. J. II and Scherer, G. W. 2007c. "Mechanism for salt scaling of a cementitious surface". Materials and Structures 40(3), 259–268.

Wee, T. H., Suryavanshi, A. K., Wong, S. F., and Anisur Rahman, A. K. M. 2000. "Sulfate resistance of concrete containing mineral admixtures". ACI Materials Journal, 97(5), 536 – 549.

Appendices

Appendix A

Expansion of Sulfate Attack Bars, ASR Prisms, and AMBT

1. Sulfate Attack Mortar Bars Expansion in % (Average of 3 specimens)

* not due yet

Mix ID	Expansion (%) with weeks													
	0	1 week	2	3	4	8	12	13	15	26	39	52	78	104
Control (100% PC1)	0	0.013%	0.018	0.026	0.029	0.045	0.073	0.084	0.115	0.306	0.647	1.568	**Broke**	
20% FA1	0	0.020	0.028	0.034	0.039	0.093	0.132	**Broke**						
40% FA1	0	0.016	0.025	0.032	0.045	0.100	0.219	0.289	**Broke**					
30% Slag1	0	0.007	0.007	0.012	0.011	0.015	0.022	0.032	0.033	0.043	0.053	0.079	0.216	0.647
40% Slag1	0	0.006	0.010	0.013	0.015	0.021	0.028	0.027	0.031	0.037	0.040	0.054	0.072	0.140
20% FA2/ 20%Slag1	0	0.017	0.024	0.026	0.032	0.041	0.049	0.052	0.059	0.160	0.281	**Broke**		
20% FA1/ 30%Slag1	0	0.011	0.017	0.021	0.026	0.037	0.041	0.053	0.059	0.181	0.247	0.531	**Broke**	
15% FA2/ 15%Slag1	0	0.008	0.017	0.023	0.026	0.038	0.053	0.060	0.071	0.159	0.398	**Broke**		
40%FA1/ 20%Slag1	0	0.019	0.025	0.028	0.031	0.041	0.047	0.049	0.051	0.059	0.066	0.077	0.110	0.195
20%FA1/ 40%Slag 1	0	0.012	0.018	0.022	0.026	0.036	0.039	0.040	0.041	0.047	0.057	0.078	0.182	0.355
30% FA2/ 30% Slag 1	0	0.018	0.026	0.027	0.029	0.042	0.045	0.046	0.049	0.061	0.077	*	*	*

2. ASR Prism Expansion (Average of 3 specimens)

Mix ID	Expansion (%) with weeks										
	1 week	2	4	8	13	18	26	39	52	78	104
30% FA2/ 30% Slag1	0.009%	-0.008	-0.007	-0.005	-0.004	-0.004	-0.003	0.003	0.007	0.017	0.025
15% FA2/ 15%Slag1	-0.006	-0.003	-0.002	0.002	0.008	0.020	0.035	0.052	0.060	0.080	0.092
20% FA2/ 20%Slag1	-0.013	-0.014	-0.012	-0.014	-0.006	-0.006	0.001	0.010	0.020	0.036	0.041
40% FA2/ 20% Slag1	-0.012	-0.013	-0.012	-0.013	-0.009	-0.009	-0.007	-0.006	-0.001	0.005	0.003
20%FA2/ 40% Slag1	-0.008	-0.009	-0.009	-0.001	0.000	0.000	0.002	0.005	0.007	*	*
20% FA2	-0.006	-0.006	0.000	0.018	0.039	0.056	0.082	0.106	0.109	*	*
30% FA2	-0.007	-0.006	-0.003	0.000	0.006	0.010	0.028	0.045	0.050	*	*
50% FA 2	-0.006	-0.005	-0.003	-0.003	-0.006	-0.007	0.001	0.009	0.008	*	*
40% Slag1	-0.004	-0.002	-0.002	-0.001	-0.001	-0.002	0.009	0.020	0.022	*	*
50% Slag1	-0.002	0.000	0.000	0.002	0.000	-0.001	0.006	0.013	0.012	*	*

* not due yet

3. Accelerated Mortar Bar Expansion (%) (Average of 3 specimens)

Time (days)	20%FA2/ 40%Slag1	20%FA2/ 20%Slag1	40%FA2/ 20%Slag1	20%FA2/ 30%Slag1		Time (days)	15%FA2/ 15%Slag1	20% FA2	30% FA2	50% FA2	40% Slag1	50% Slag1
0	0.0000	0.0000	0.0000	0.0000		0	0.0000	0.0000	0.0000	0.0000	0.0000	0.0000
2	0.0095	0.0315	0.0059	0.0168		3	0.0957	0.1293	0.1121	0.0400	0.0517	0.0365
5	0.0221	0.1069	0.0229	0.0441		7	0.2176	0.2963	0.2507	0.0856	0.1363	0.0904
7	0.0285	0.1411	0.0267	0.0589		10	0.2747	-	-	-	0.1667	0.1215
9	0.0349	0.1649	0.0336	0.0819		14	0.3357	0.4317	0.3501	0.1349	0.2112	0.1573
14	0.0607	0.2141	0.0568	0.1269		21	-	0.5400	0.4339	0.1840	0.2960	0.2267
21	0.1224	0.2952	0.1064	0.1899		28	0.5424	0.6736	0.5331	0.2533	0.3861	0.2969
28	0.1784	0.3829	0.1629	0.2629		-						

Appendix B

Salt Scaling Residue

The exposed area for each of the specimens tested is taken as 576 mm^2

x indicates that the dyke failed

Control
(100% PC2)

	Collected Residue (g)			Residue expressed as mass per area (kg/m^2)					
Cycles	A	B	C	A	B		Standard Deivation	Average	Cumulative Average
0	0	0	-						0
5	3.09	5.14		0.054	0.089		0.025	0.071	0.071
10	3.64	4.34		0.063	0.075		0.009	0.069	0.141
15	1.04	1.29		0.018	0.022		0.003	0.020	0.161
20	1.2	1.37		0.021	0.024		0.002	0.022	0.183
25	1.09	0.79		0.019	0.014		0.004	0.016	0.200
30	0.59	0.52		0.010	0.009		0.001	0.010	0.209
35	0.53	0.41		0.009	0.007		0.001	0.008	0.217
40	0.44	0.32		0.008	0.006		0.001	0.007	0.224
45	0.86	0.63		0.015	0.011		0.003	0.013	0.237
50	0.51	0.26		0.009	0.005		0.003	0.007	0.244

30% Slag2

	Collected Residue (g)			Residue expressed as mass per area (kg/m^2)					
Cycles	A	B	C	A	B	C	Standard Deviation	Average	Cum. Ave.
0	0	0	0						0
5	41.09	63.26	58.29	0.71	1.10	1.01	0.20	0.94	0.94
10	15.19	26.32	19.52	0.26	0.46	0.34	0.10	0.35	1.294
15	7.22	16.07	7.49	0.13	0.28	0.13	0.09	0.18	1.473
20	5.57	8.12	6.29	0.10	0.14	0.11	0.02	0.12	1.588
25	2.01	6.35	2.91	0.03	0.11	0.05	0.04	0.07	1.653
30	2.36	6.8	3.26	0.04	0.12	0.06	0.04	0.07	1.725
35	3.69	6.18	3.16	0.06	0.11	0.05	0.03	0.08	1.801
40	1.26	3.96	1.85	0.02	0.07	0.03	0.02	0.04	1.842
45	x	3.41	4.99		0.06	0.09	0.02	0.07	1.914
50		3.35	3		0.06	0.05	0.00	0.06	1.970

Salt Scaling (Continued)

15/15 (FA3/Slag2)

	Collected Residue (g)			Residue expressed as mass per area (kg/m^2)					
Cycles	A	B	C	A	B	C	Standard Deviation	Ave.	Cum. Ave.
0	0	0	0						0
5	14.55	10.83	11.3	0.25	0.19	0.20	0.04	0.21	0.212
10	12.35	16.77	22.85	0.21	0.29	0.40	0.09	0.30	0.513
15	6.6	7.2	8.72	0.11	0.13	0.15	0.02	0.13	0.643
20	3.31	6.64	3.57	0.06	0.12	0.06	0.03	0.08	0.722
25	4.05	6.56	1.86	0.07	0.11	0.03	0.04	0.07	0.794
30	2.93	2.34	1.68	0.05	0.04	0.03	0.01	0.04	0.834
35	2.7	0.74	3.56	0.05	0.01	0.06	0.03	0.04	0.874
40	2.76	3.69	1.6	0.03	0.06	0.05	0.02	0.05	0.921
45	2.52	1.96	0.99	0.02	0.03	0.04	0.01	0.03	0.953
50	3.25	1.95	0.83	0.01	0.03	0.06	0.02	0.03	0.988

20/20 (FA3/Slag2)

Curing Regime A (A=Moist room curing)

	Collected Residue (g)			Residue expressed as mass per area (kg/m^2)					
Cycles	A	B	C	A	B	C	Standard Deviation	Average	Cum. Ave.
0	0	0	0						0
5	33.59	30.71	31.97	0.58	0.53	0.56	0.03	0.54	0.544
10	29.57	22.87	23.44	0.51	0.40	0.41	0.06	0.40	0.946
15	11.67	7.73	7.21	0.20	0.13	0.13	0.04	0.13	1.076
20	11.79	7.3	5.93	0.20	0.13	0.10	0.05	0.11	1.191
25	6.55	4.78	2.45	0.11	0.08	0.04	0.04	0.06	1.253
30	6.13	5.97	2.49	0.11	0.10	0.04	0.04	0.07	1.327
35	4.4	4.2	2.02	0.08	0.07	0.04	0.02	0.05	1.381
40	2.93	4.5	2.23	0.05	0.08	0.04	0.02	0.06	1.439
45	4.18	3.25	4.28	0.07	0.06	0.07	0.01	0.07	1.505
50	6.27	5.2	4.8	0.11	0.09	0.08	0.01	0.09	1.591

Salt Scaling (Cont'd)

20/20 (FA3/Slag2)

Curing Regime B (B=wrapped and kept in the laboratory)

	Collected Residue (g)			Residue expressed as mass per area (kg/m^2)					
Cycles	A	B	C	A	B	C	Standard Deviation	Average	Cum Ave.
0	0	0	0						0
5	15.03	6.6	6.47	0.26	0.11	0.11	0.09	0.16	0.163
10	11.38	11.08	9.26	0.20	0.19	0.16	0.02	0.18	0.346
15	6.48	4.99	4.05	0.11	0.09	0.07	0.02	0.09	0.436
20	4.96	2.02	2.25	0.09	0.04	0.04	0.03	0.05	0.489
25	4.54	2.92	2.85	0.08	0.05	0.05	0.02	0.06	0.549
30	5.62	2.44	4.12	0.10	0.04	0.07	0.03	0.07	0.620
35	1.25	1.01	2.37	0.02	0.02	0.04	0.01	0.03	0.646
40	1.3	1	1.5	0.02	0.02	0.03	0.00	0.02	0.668
45	1.44	1.2	*	0.03	0.02		0.00	0.02	0.691
50	2.32	2.05	*	0.04	0.04		0.00	0.04	0.729

40% Slag2

Curing Regime A (A=Moist room curing)

	Collected Residue (g)			Residue expressed as mass per area (kg/m^2)					
Cycles	A	B	C	A	B	C	Standard Deviation	Average	Cum Ave.
0	0	0	0						0
5	57.63	59.02	60.01	1.00	1.02	1.04	0.02	1.02	1.022
10	28.94	27.99	26.48	0.50	0.49	0.46	0.02	0.48	1.505
15	9.84	9	8.04	0.17	0.16	0.14	0.02	0.16	1.661
20	6.61	5.52	5.58	0.11	0.10	0.10	0.01	0.10	1.763
25	3.21	3.68	x	0.06	0.06	x	0.03	0.04	1.803
30	2.87	2.86		0.05	0.05		0.03	0.03	1.836
35	2.64	2.16		0.05	0.04		0.01	0.04	1.878
40	2.33	2.56		0.04	0.04		0.00	0.04	1.920
45	2.8	2.45		0.05	0.04		0.00	0.05	1.966
50	4.23	3.29		0.07	0.06		0.01	0.07	2.031

Salt Scaling (Cont'd)

40% Slag2

Curing Regime B (B=wrapped and kept in the laboratory)

	Collected Residue (g)			Residue expressed as mass per area (kg/m^2)					
Cycles	A	B	C	A	B	C	Standard Deviation	Average	Cum Ave.
0									0
5	4.71	4.81	6.39	0.08	0.08	0.11	0.02	0.09	0.092
10	15.75	15.74	13.15	0.27	0.27	0.23	0.03	0.26	0.350
15	6.76	7.72	11.92	0.12	0.13	0.21	0.05	0.15	0.503
20	4.508	5.14	7.96	0.08	0.09	0.14	0.03	0.10	0.605
25	6.99	1.539	x	0.12	0.03	x	0.07	0.07	0.679
30	5.32	1.2		0.09	0.02		0.05	0.06	0.736
35	3.038	0.684		0.05	0.01		0.03	0.03	0.768
40	0.3	0.55		0.01	0.01		0.00	0.01	0.775
45	0.27	0.42		0.00	0.01		0.00	0.01	0.781
50	2.91	1.37		0.05	0.02		0.02	0.04	0.819

Appendix C

Freeze-thaw Test Results and Calculations

1) Durability Factors for Freeze-thaw Specimens

Column #	Description
1	Mix ID
2	Initial mass of the prisms before F/T commenced
3	Volume of the specimen is computed by taking the dimensions 75x75x285 mm
4	Density is computed by dividing mass/volume
5	Poisson ratio is taken as 0.15
6	Measured time that pulse takes to travel between the transducers at the beginning of the F/T test.
7	Measured time that pulse took to travel between the transducers at the end of the F/T test
8	Initial pulse velocity is calculated by dividing Column 6 by the distance between the two transducers. The distance between the two transducers is 75 mm.
9	Final pulse velocity is calculated by dividing Column 7 by the distance between the two transducers. The distance between the two transducers is 75 mm.

10	Initial dynamic modulus of elasticity, E_d, calculated the relationship with pulse velocity as given in ASTM C597. The equation is $$V = \sqrt{\frac{E_d(1 - v_d)}{\rho(1 + v_d)(1 - 2v_d)}}$$ The parameters of this equation are stated in Chapter 3 of this thesis
11	The equation in Column 10 is used to calculate the modulus of elasticity at the end of the test (300 cycles). The pulse velocity at 300 cycles is substituted into the equations.
12	Percentage of initial dynamic modulus after 300 F/T cycles is calculated by diving Column 10 by Column 11.
13	Durability Factor After 300 cycles is taken as percentage of initial dynamic modulus. Column 13 is average of durability factor for 3 specimens.

Continued on next page

Column 1	2	3	4	5	6	7	8	9	10	11
Mix ID	Mass (kg)	Vol (m^3)	Density (kg/m^3)	Piosson	t_i (μs)	t_f (μs)	v_i (m/s)	v_f (m/s)	E_{di} (N/m^2)	E_{df} (N/m^2)
Control a	3.851	0.001603	2402.183	0.15	18.3	18.5	4098.4	4054.1	38212322448	37390576084
Control b	3.849	0.001603	2400.936	0.15	18.4	18.5	4076.1	4054.1	37778469511	37371157451
Control c	3.856	0.001603	2405.302	0.15	17.6	17.7	4261.4	4237.3	41366024444	40899932113
15/15 a	4.03	0.001603	2513.84	0.15	17.2	17.4	4360.5	4310.3	45266847168	44232210550
15/15 b	4.016	0.001603	2505.107	0.15	16.7	16.8	4491.0	4464.3	47851202547	47283240782
15/15 c	4.068	0.001603	2537.544	0.15	17.1	17.1	4386.0	4386.0	46229672637	46229672637
20/20 a	4.017	0.001603	2505.731	0.15	18.2	18.4	4120.9	4076.1	40298710577	39427412842
20/20 b	4.077	0.001603	2543.158	0.15	18	18	4166.7	4166.7	41814585483	41814585483
20/20 c	3.983	0.001603	2484.522	0.15	17.3	17.6	4335.3	4261.4	44223203032	42728442780
30 Slag a	4.017	0.001603	2505.731	0.15	17.2	17.3	4360.5	4335.3	45120825080	44600704640
30 Slag b	3.97	0.001603	2476.413	0.15	17.1	17.3	4386.0	4335.3	45115978459	44078864182
30 Slag c	4.012	0.001603	2502.612	0.15	17.2	17.4	4360.5	4310.3	45064662739	44034647326
40 Slag a	4.086	0.001603	2548.772	0.15	17.2	17.5	4360.5	4285.7	45895865391	44335780628
40 Slag b	4.133	0.001603	2578.09	0.15	17.8	18	4213.5	4166.7	43346845246	42388933481
40 Slag c	4.077	0.001603	2543.158	0.15	18	18.2	4166.7	4120.9	41814585483	40900633065

Continued from previous page

	Column 12	13
	% P	Average DF
Control a	97.8	98.5
Control b	98.9	
Control c	98.8	
15/15 a	97.7	98.8
15/15 b	98.8	
15/15 c	100	
20/20 a	97.8	98.2
20/20 b	100	
20/20 c	96.6	
30 Slag a	98.8	98.1
30 Slag b	97.7	
30 Slag c	97.7	
40 Slag a	96.6	97.4
40 Slag b	97.8	
40 Slag c	97.8	

2) Freeze-thaw Specimens Weight Change Results

Control (100% PC)

Cycle	A (g)	B	C
0	3851.7	3849.2	3856.4
35	3854.7	3852	3859.3
70	3853.8	3852.9	3856.7
105	3856.9	3854.4	3860.7
140	3859.9	3855.9	3860.7
175	3859.6	3856.1	3860.7
210	3858.6	3855	3857.1
245	3853.1	3856.9	3856.4
280	3853.1	3857.4	3857.3
300	3841.3	3849	3852

30% Slag2

Cycle	A (g)	B	C
0	4017.2	3970.6	4012.6
35	4019.3	3971.9	4015
70	4019.3	3973	4013.8
105	4018.6	3973.7	4014
140	4018.5	3974.9	4013.6
175	4016.5	3974.3	4011.1
210	4011.8	3973.1	4006.7
245	4011.6	3970.7	4001.3
280	4010.5	3971.7	3999.3
300	4006.9	3969.5	3994.2

Freeze-thaw Specimen Weight Loss (Cont'd)

15/15 (FA3/Slag2)

Cycle	A (g)	B	C
0	4030.2	4016.0	4068.3
35	4024.2	4017.6	4071.8
70	4025.1	4018.0	4069.5
105	4027.7	4019.4	4070.5
140	4028.7	4019.3	4070.0
175	4028.7	4020.6	4067.0
210	4026.5	4018.3	4065.2
245	4024.5	4016.7	4064.7
280	4022.2	4012.4	4059.2
300	4013.7	4010.3	4052.7

20/20 (FA3/Slag2)

Cycle	A (g)	B	C
0	4017	4077	3983
35	4019	4080	3990
70	4021	4081	3994
105	4021	4082	3994
140	4019	4078	3995
175	4015	4077	3992
210	4010	4065	3981
245	4000	4058	3972
280	3990	4044	3965
300	3982	4039	3950

Freeze-thaw Specimen Weight Loss (Cont'd)

40% Slag2

Cycle	A (g)	B	C
0	4086.1	4133.6	4077
35	4086	4133	4075
70	4080	4122	4071
105	4072	4115	4063
140	4069	4112	4052
175	4060	4109	4040
210	4052	4105	4033
245	4048	4100	4025
280	4040	4092	4028
300	4035	4082	4019

Appendix D

Compressive Strength and Rapid Chloride Permeability Test

1) Compressive Strength of Concrete Cylinders

30% Slag2

Age	A (kN)	B	C	A (MPa)	B	C	Average MPa
1	96.4	89.2	90.2	12.3	11.4	11.5	11.7
7	220.1	228.4	216.2	28.0	29.1	27.5	28.2
28	294.6	283.4	--	37.5	36.1	--	36.8
56	300.7	323.5	306.0	38.3	41.2	39.0	39.5

Control (100% PC2)

Age	A (kN)	B	C	A (MPa)	B	C	Average MPa
1	114.8	102.4	110.1	14.6	13.0	14.0	13.9
7	191.5	211.9	199.5	24.4	27.0	25.4	25.6
28	227.7	224.1	244.6	29.0	28.5	31.1	29.6
56	236.8	239.0	249.3	30.2	30.4	31.7	30.8

Compressive Strength (Cont'd)

15/15 (FA3/Slag2)

Age	A (kN)	B	C	A (MPa)	B	C	Average MPa
1	91.5	85.7	94.2	11.6	10.9	12.0	11.5
7	174.6	195.3	--	22.2	24.9	--	23.5
28	277.0	267.3	253.9	35.3	34.0	32.3	33.9
56	271.2	283.2	270.6	34.5	36.1	34.5	35.0

20/20 (FA3/Slag2)

Age	A (kN)	B	C	A (MPa)	B	C	Average MPa
1	80.8	78.4	76.7	10.3	10.0	9.8	10.0
7	195.3	196.5	181.9	24.9	25.0	23.2	24.3
28	262.4	287.3	248.9	33.4	36.6	31.7	33.9
56	286.3	305.9	317.0	36.4	38.9	40.4	38.6

40% Slag2

Age	A (kN)	B	C	A (MPa)	B	C	Average MPa
1	70.3	93.1	64.0	9.0	11.9	8.1	9.7
7	196.7	204.3	--	25.0	26.0		25.5
28	285.2	309.7	304.0	36.3	39.4	38.7	38.1
56	328.5	304.2	330.6	41.8	38.7	42.1	40.9

2) Rapid Chloride Permeability Test on Concrete Specimens

Values represent the total charge passed (in coulombs) through the specimens (A, B, and C) over 6 hour period.

Control (100% PC2)

Age (days)	Total charge passed (Coulombs)			
	A	B	C	Average
7	3954	3786	4006	3915
28	3178	3465	3664	3436
56	2895	2677	2526	2699
91	2690	1884	2030	2201

30% Slag2

Age (days)	Total charge passed (Coulombs)			
	A	B	C	Average
7	2672	3476	3394	3181
28	1822	1383	1651	1619
56	1427	1474	877	1259
91	975	753	1155	961

Rapid Chloride Permeability Test on Concrete Specimens (Cont'd)

15/15
(FA3/Slag2)

Age (days)	Total charge passed (Coulombs)			
	A	B	C	Average
7	5060	4107	-	4584
28	2205	1818	2431	2125
56	1906	1303	1528	1416
91	1143	1277	1038	1153

20/20
(FA3/Slag2)

Age (days)	Total charge passed (Coulombs)			
	A	B	C	Average
7	6901	6139	4850	5963
28	1400	1944	2388	1910
56	1553	982	1360	1298
91	1079	818	1147	1015

Rapid Chloride Permeability Test on Concrete Specimens (Cont'd)

40% Slag2

Age (days)	Total charge passed (Coulombs)			
	A	**B**	**C**	**Average**
7	4099	3065	2687	3284
28	1114	937	1009	1020
56	870	1013	881	921
91	926	991	795	904

3) Rapid Chloride Permeability Conducted on Mortar Specimens

Mix	RCPT at 56th day (Coulombs)			
	Specimen A	Specimen B	Specimen C	Average
Control (100% PC1)	6690	6908	6283	6627
20% FA1	7415	7246	6304	6988
40% FA1	9283	9436	-	9360
20% Slag1	5518	4901	-	5209
30% Slag1	3804	3944	-	3874
40% Slag1	2618	2761	-	2689
15% FA2/15%Slag1	5676	4597	4627	4967
20%FA2/20%Slag1	4484	3897	3671	4017
20%FA2/30%Slag1	3690	2825	-	3257
20%FA2/40%Slag1	2809	2540	2817	2722
40%FA1/20%Slag1	7225	8691	-	7958
30%FA2/30%Slag2	5284	5211	4724	5073

Appendix E

Bleeding and Setting Time

1) Bleeding Data

Row #	Description	Control (100% PC2)	15/15 (FA3/Slag2)	30%Slag2	20/20 (FA3/Slag2)	40% Slag2
1	Mass of container and concrete.	13.938	12.942	13.531	8.047	12.914
2	Mass of container	3.656	3.656	3.656	2.959	3.656
3	Mass of concrete (Row 1 – Row 2)	10.282	9.286	9.875	5.087	9.258
4	Bleed water	9	1	16.5	1	18
5	Mass of effective water in the concrete batch	1.816	1.816	1.815	1.817	2.27
6	Mass of the concrete batch	27.734	27.734	27.797	27.687	34.71
7	Mass of water in the specimen (Row5/Row6)xRow3	0.673257	0.60804	0.644786	0.333855	0.605394
8	Bleeding % (Row 4/Row6)x10^{-3}	0.013368 =1.34%	0.001645 = 0.16%	0.02559 = 2.56%	0.002995 =0.30%	0.029733 = 2.97%

2) Setting Time

Control (100% PC)

Elapsed Time (hour)	Penetration Force (lb)	Needle Diameter (inch)	Area of Needle (in^2)	Penetration Force (psi)	Penetration Force (MPa)
3.0	85	1/4	0.04908	1732	11.9
3.5	175	1/4	0.04908	3566	24.6
4.0	44	1/10	0.007854	5602	38.6
4.5	130	1/10	0.007854	16552	114.1

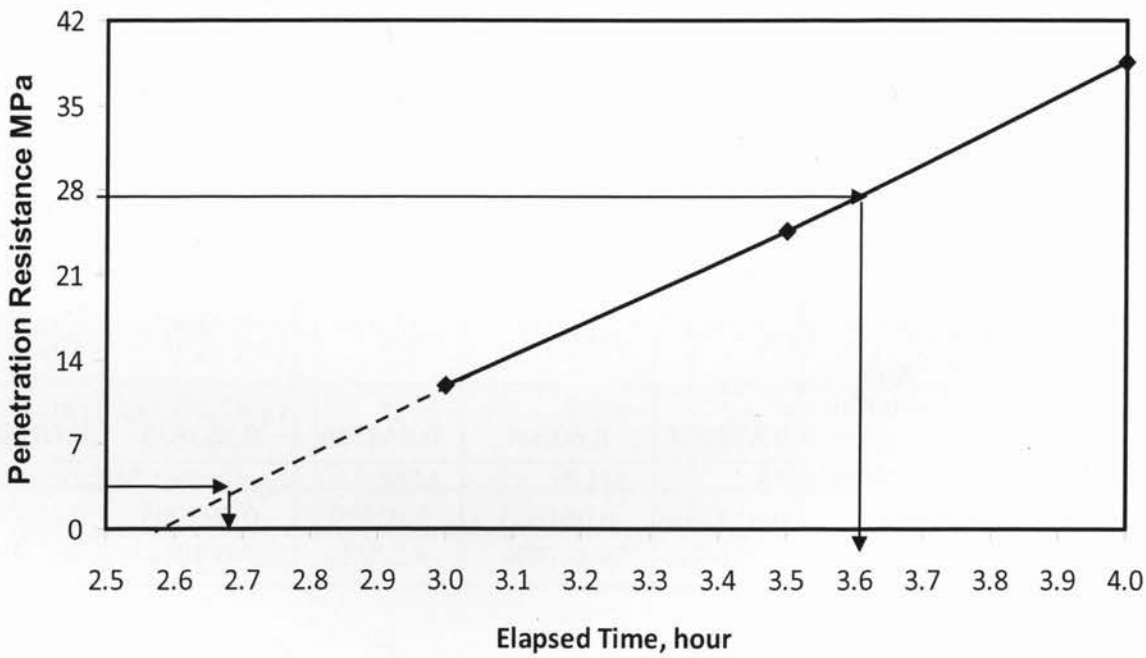

Setting Time 15%FA3/15%Slag2

Time (hr)	Force (lb)	Needle Diameter (in)	Needle Area (in^2)	Force (psi)	Force (MPa)
4.0	22	1/4	0.04908	448	3.1
4.5	30	1/4	0.04908	611	4.2
5.0	42	1/4	0.04908	856	5.9
5.5	65	1/4	0.04908	1324	9.1
6.0	100	1/4	0.04908	2037	14.0
6.5	200	1/4	0.04908	4075	28.1

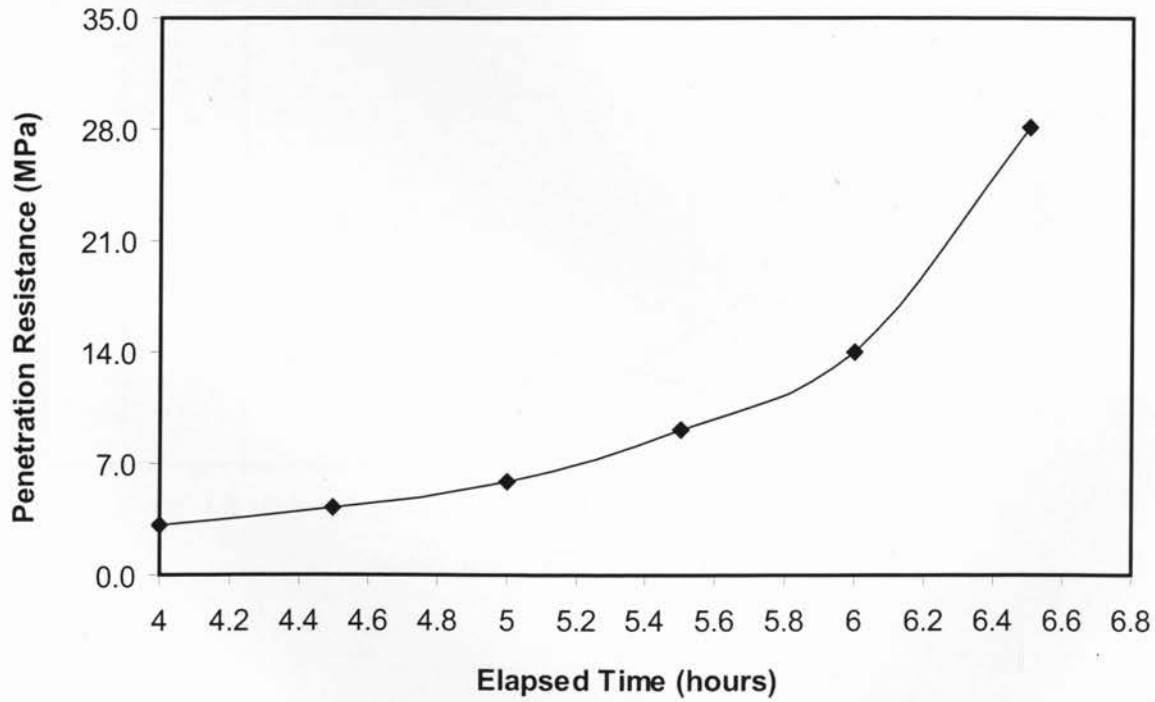

Setting Time 30% Slag2

Time (hr)	Force (lb)	Needle Size (in)	Needle Area (in^2)	Force (psi)	Force (MPa)
3.0	15	1/4	0.04908	306	2.1
4.0	50	1/4	0.04908	1019	7.0
4.5	77	1/4	0.04908	1569	10.8
5.0	130	1/4	0.04908	2649	18.3
5.5	185	1/4	0.04908	3769	26.0
5.75	36	1/10	0.007854	4584	31.6

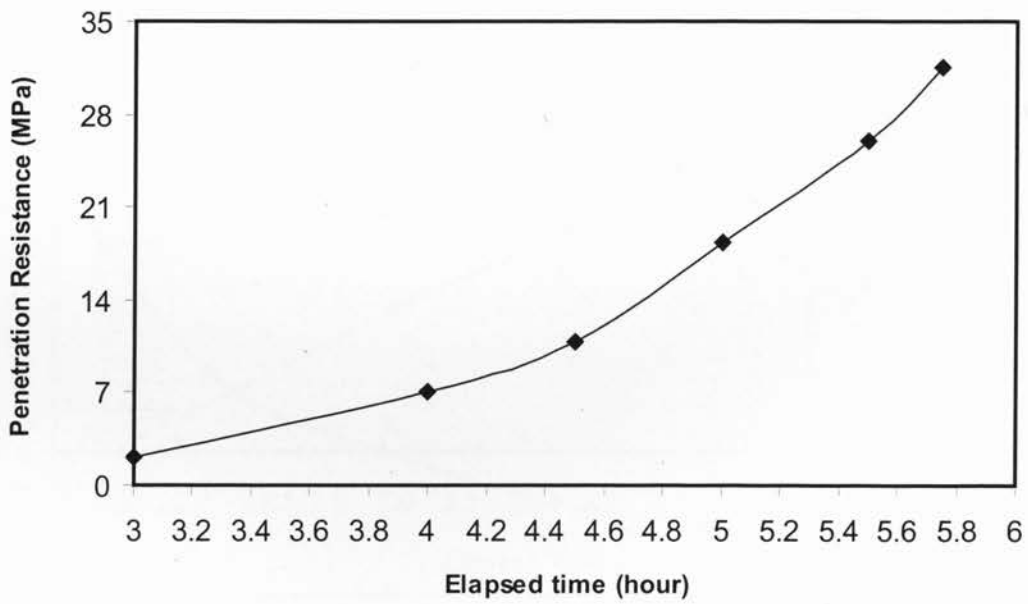

Setting Time 20% FA3/20% Slag2

Time (hr)	Force (lb)	Needle Diameter (in)	Needle Area (in^2)	Force (psi)	Force (MPa)
5.0	20	1/2	0.19635	102	0.7
5.5	20	1/4	0.04908	407	2.8
6.0	40	1/4	0.04908	815	5.6
6.5	72	1/4	0.04908	1467	10.1
7.5	180	1/4	0.04908	3667	25.3
8.0	11	1/20	0.001963	5604	38.6

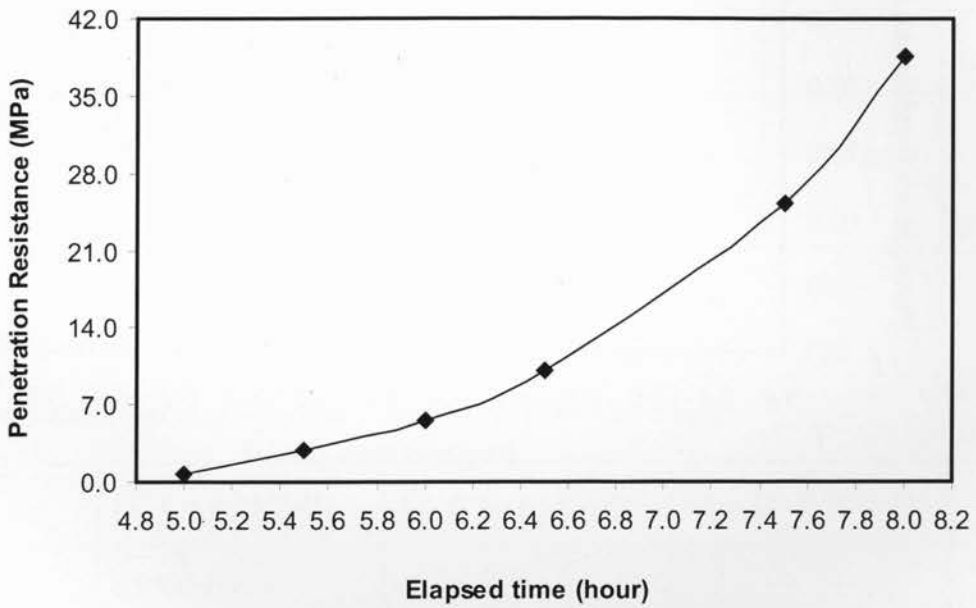

Setting Time 40% Slag2

Time (hr)	Force (lb)	Needle Diameter (in)	Needle Area (in^2)	Force (psi)	Force (MPa)
3.6	26	1/4	0.04908	530	3.7
4.0	59	1/4	0.04908	1202	8.3
4.5	114	1/4	0.04908	2323	16.0
5.0	162	1/4	0.04908	3301	22.8
5.5	205	1/4	0.04908	4177	28.8

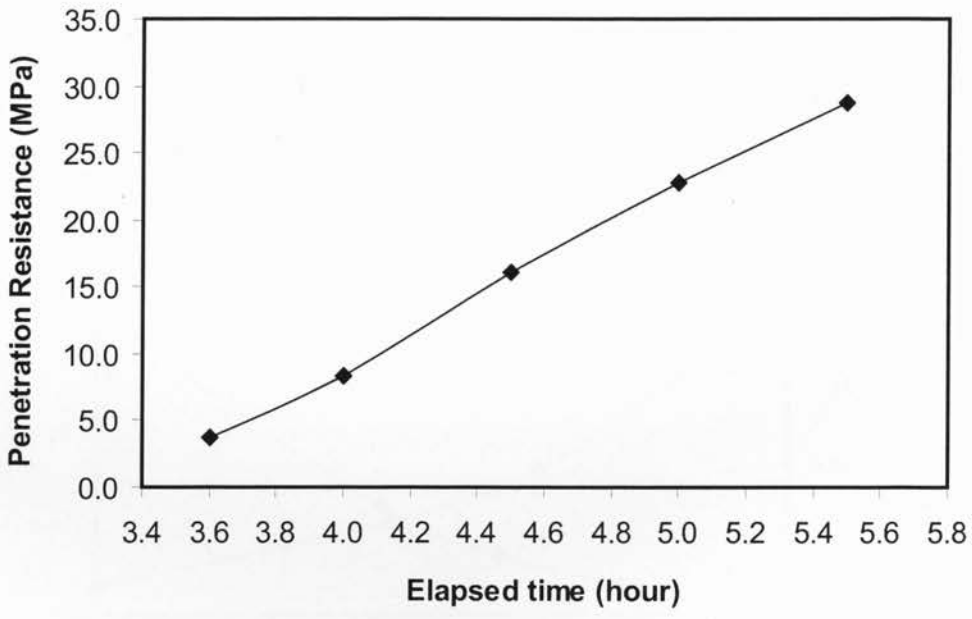

Appendix F

Leaching Test Data

1) Non-evaporable Water Content of Leaching Paste Fragments

	Control (100% PC1)	15/15 (FA2/Slag1)	20/20 (FA2/Slag1)	30/30 (FA2/Slag1)	20%FA2	40%Slag1
Mass of fragments before ignition (g)	0.9881	1.0022	1.00	1.0016	1.0065	1.0017
Mass of fragments after ignition (g)	0.8084	0.8276	0.83	0.838	0.8312	0.8398
Loss on Ignition (LOI)	18.19%	17.42%	17.00%	16.33%	17.42%	19.28%

2) Alkali Content of Cementing Materials

This table shows total alkali content of the binder in binary and ternary blends

Na_2O_e of Raw Materials	PC 1 = 0.95354%	FA 2 = 2.15714%	Slag 1 = 0.95164%	
Control	0.95354x1.0	-	-	Na_2O_e 0.95354%
15/15	0.95354x0.7	2.15714x0.15	0.95164x0.15	1.0384%
20/20	0.95354x0.60	2.15714x0.20	0.95164x0.20	1.1939%
30/30	0.95354x0.40	2.1571x0.30	0.95146x0.30	1.3141%
20% FA	0.95354x0.80	2.1571x0.20	-	1.1943%
40% Slag	0.95354x0.60	-	0.95146x0.40	0.9528%

3) Leaching Test Results and Calculation

Column #	Description
1	Mix ID
2	Concentration of K^+ ions (ppm) in the blank solution as measured by the flame photometer. This concentration is after the dilution of the original solution at the dilution ratio of 1 to 100.
3	Final K^+ is measured from the each bottle with paste fragments. The solution from the bottles is diluted at the ratio of 1 to 100 and the concentration of the diluted solution was measured for ppm of K^+ with the flame photometer
4	Concentration of Na^+ ions (ppm) in the blank solution as measured by the flame photometer. This concentration is after the dilution of the original solution at the dilution ratio of 1 to 100.
5	Final Na^+ is measured from the each bottle with paste fragments. The solution from the bottles is diluted at the ratio of 1 to 100 and the concentration of the diluted solution was measured for ppm of K^+ with the flame photometer
6	Column6=Column3 – Column2 to get the change in the concentration of K^+ with respect to the blank bottle
7	Column7 = Column5 – Column4 to get the change in the concentration of Na^+ with respect to the blank
8	Conversion of K^+ from ppm to mol/L. The following operation is carried out. Mol/L of K^+ = $(\text{Column6x } 100)\text{x}\frac{1\text{ mol/L}}{39000\text{ ppm K+}}$
9	Conversion of Na+ from ppm to mol/L Mol/L of K^+ = $(\text{Column7x } 100)\text{x}\frac{1\text{ mol/L}}{23000\text{ ppm Na+}}$
10	Covert K^+ and Na^+ into Na_2O_e $(K^+ + Na^+)/2$ = (Column 8+Column9)/2
11	Finding the number of moles (Mol/L)xVolume will give the number of moles. Each bottle was filled with 15 mL of solution. So, volume is 0.015 L Number of moles Na_2O_e = Column 10 x 0.015
12	Mass of Na_2O_e = Molecular weight of Na_2O_e x Number of moles of Na_2O_e = 62 g x Column 11

13	Weight of the solid content of the paste fragments in each bottle is calculated as the total weight of the paste fragment added to the bottle minus the evaporable and non-evaporable water content of the paste fragments. Since the added paste fragments were dried before soaking in the solution, the evaporable water content does not have to be determined. The non evaporable water content is determined using the loss on ignition furnace by heating to 1050°C. The LOI results are given in the table in a table in this appendix. Solid content = 1.5 g – (LOI%x1.5g)
14	Released alkali as % of solid content = (Column 12/Column 13)x100%
15	Average of the bottles from each samples (i.e. average of Column 14)
16	Standard deviation of the values on Column 14
17	Alkali content of the raw cementing materials
18	Available alkali as percentage of alkali content of the cementing materials
19	Average of the thee values from Column 18

Leaching Results from Distilled Bottles

Continued on next page

Column 1	2	3	4	5	6	7	8	9	10	11
Mix	Initial K^+ ppm	Final K^+ ppm	Initial Na^+ ppm	Final Na^+ ppm	Difference in K^+ concentration ppm	Difference in Na^+ concentration ppm	Difference in K^+ concentration mol/L	Difference in Na^+ concentration mol / L	Na_2O_e of K^+ and Na^+ mol/L	# of moles of Na_2O_e
control a	0.00	8.4	0.00	0.8	8.4	0.8	0.0215	0.0035	0.01251	0.00018763
control b	0.00	8.6	0.00	0.6	8.6	0.6	0.0221	0.0026	0.01233	0.00018495
control c	0.00	7.8	0.00	0.6	7.8	0.6	0.0200	0.0026	0.01130	0.00016957
15/15 a	0.00	4.8	0.00	2.6	4.8	2.6	0.0123	0.0113	0.01181	0.00017709
15/15 b	0.00	4.2	0.00	3.2	4.2	3.2	0.0108	0.0139	0.01234	0.00018512
15/15 c	0.00	4.6	0.00	3.0	4.6	3.0	0.0118	0.0130	0.01242	0.00018629
20/20 a	0.00	3.6	0.00	3.0	3.6	3.0	0.0092	0.0130	0.01114	0.00016706
20/20 b	0.00	4	0.00	2.2	4.0	2.2	0.0103	0.0096	0.00991	0.00014866
20/20 c	0.00	3.6	0.00	3.2	3.6	3.2	0.0092	0.0139	0.01157	0.00017358
30/30 a	0.00	2.6	0.00	2.6	2.6	2.6	0.0067	0.0113	0.00899	0.00013478
30/30 b	0.00	3.0	0.00	2.6	3.0	2.6	0.0077	0.0113	0.00950	0.00014247
30/30 c	0.00	3.0	0.00	2.6	3.0	2.6	0.0077	0.0113	0.00950	0.00014247
20 FA a	0.00	6.0	0.00	3.2	6.0	3.2	0.0154	0.0139	0.01465	0.00021973
20 FA b	0.00	6.2	0.00	3.0	6.2	3.0	0.0159	0.0130	0.01447	0.00021706
20 FA c	0.00	6.2	0.00	3.2	6.2	3.2	0.0159	0.0139	0.01491	0.00022358
40 Slag a	0.00	3.6	0.00	1.8	3.6	1.8	0.0092	0.0078	0.00853	0.00012793
40 Slag b	0.00	3.8	0.00	2.6	3.8	2.6	0.0097	0.0113	0.01052	0.00015786
40 Slag c	0.00	3.8	0.00	2.0	3.8	2.0	0.0097	0.0087	0.00922	0.00013829

Continued from previous page (Leaching results of distilled (0 mol/L) original solution)

1	12	13	14	15	16	17	18	19
Mix	Mass of Na_2O_e (g)	Mass of solid content of the paste fragments stored (g)	Alkali Released as % of solid content of the paste fragments stored	Average of Column 14	Standard deviation of Column 14	Alkali content of raw binder (%)	Alkali Released as % of alkali content of raw binder	Average of Column 17
control a	0.01163278	1.230	0.94575414			0.9535	99.18348	
control b	0.01146689	1.230	0.93226745			0.9535	97.7691	
control c	0.01051304	1.230	0.85471898	0.9109	0.0491	0.9535	89.63641	95.53
15/15 a	0.0109796	1.245	0.88189547			1.0384	84.92495	
15/15 b	0.01147726	1.245	0.92186807			1.0384	88.77424	
15/15 c	0.01154983	1.245	0.92769741	0.9105	0.0249	1.0384	89.33559	87.68
20/20 a	0.01035753	1.245	0.83192973			1.1939	69.68286	
20/20 b	0.00921706	1.245	0.74032585			1.1939	62.01007	
20/20 c	0.01076187	1.245	0.86440746	0.8122	0.0643	1.1939	72.40321	68.03
30/30 a	0.00835652	1.260	0.66321601			1.3141	50.47114	
30/30 b	0.00883344	1.260	0.70106705			1.3141	53.35163	
30/30 c	0.00883344	1.260	0.70106705	0.6885	0.0219	1.3141	53.35163	52.39
20 FA a	0.01362341	1.245	1.09424991			1.1943	91.62577	
20 FA b	0.01345753	1.245	1.08092571			1.1943	90.51008	
20 FA c	0.01386187	1.245	1.11340345	1.0962	0.0163	1.1943	93.22957	91.79
40 Slag a	0.00793144	1.215	0.65279326			0.9528	68.51458	
40 Slag b	0.00978729	1.215	0.80553835			0.9528	84.5461	
40 Slag c	0.00857425	1.215	0.70569938	0.7213	0.0776	0.9528	74.0674	75.71

Leaching Results from the bottles with 0.25 mol/L solution

Continued on next page

1	2	3	4	5	6	7	8	9	10	11
Mix	Initial K^+ ppm	Final K^+ ppm	Initial Na^+ ppm	Final Na^+ ppm	Difference in K^+ concentration ppm	Difference in Na^+ concentration ppm	Difference in K^+ concentration mol/L	Difference in Na^+ concentration mol / L	Na_2O_e of K^+ and Na^+ mol/L	# of moles of Na_2O_e
control a	88.0	11.6	91.8	14.8	3.8	3.2	0.0097436	0.0139130	0.0118283	0.0001774
control b	88.0	11.6	93.2	14.0	5.2	2.4	0.0133333	0.0104348	0.0118841	0.0001783
control c	88.0	11.6	96.2	12.0	8.2	0.4	0.0210256	0.0017391	0.0113824	0.0001707
15/15 a	88.0	11.6	87.6	15.0	-0.4	3.4	-0.0010256	0.0147826	0.0068785	0.0001032
15/15 b	88.0	11.6	91.4	13.0	3.4	1.4	0.0087179	0.0060870	0.0074025	0.0001110
15/15 c	88.0	11.6	92.8	12.0	4.8	0.4	0.0123077	0.0017391	0.0070234	0.0001054
20/20 a	88.0	11.6	90.8	12.0	2.8	0.4	0.0071795	0.0017391	0.0044593	0.0000669
20/20 b	88.0	11.6	91	12.0	3.0	0.4	0.0076923	0.0017391	0.0047157	0.0000707
20/20 c	88.0	11.6	91.1	12.2	3.1	0.6	0.0079487	0.0026087	0.0052787	0.0000792
30/30 a	88.0	11.6	88.8	12.8	0.8	1.2	0.0020513	0.0052174	0.0036343	0.0000545
30/30 b	88.0	11.6	88.6	12.6	0.6	1.0	0.0015385	0.0043478	0.0029431	0.0000441
20 FA a	88.0	11.6	92.6	13.8	4.6	2.2	0.0117949	0.0095652	0.0106800	0.0001602
20 FA b	88.0	11.6	92.4	13.4	4.4	1.8	0.0112821	0.0078261	0.0095541	0.0001433
20 FA c	88.0	11.6	92.2	13.6	4.2	2.0	0.0107692	0.0086957	0.0097324	0.0001460
40Slag a	88.0	11.6	92.4	11.6	4.4	0.0	0.0112821	0.0000000	0.0056410	0.0000846
40Slag b	88.0	11.6	92.8	10.6	4.8	-1.0	0.0123077	-0.0043478	0.0039799	0.0000597

Continued from previous page (Leaching results of 0.25 mol/L solution)

1	12	13	14	15	16	17	18	19
Mix	**Mass of Na_2O_e (g)**	**Mass of solid content of the paste fragments stored (g)**	**Alkali Released as % of solid content of the paste fragments stored**	**Average of Column 14**	**Standard deviation of Column 14**	**Alkali content of raw binder (%)**	**Alkali Released as % of alkali content of raw binder**	**Average of Column 18**
Control a	0.0109826	1.230	0.8928937			0.954	93.6399	
control b	0.0110343	1.230	0.8971014			0.954	94.0812	
control c	0.0105685	1.230	0.8592313	0.883	0.021	0.954	90.1096	92.61
15/15 a	0.0063867	1.245	0.5129857			1.038	49.3996	
15/15 b	0.0068732	1.245	0.5520624			1.038	53.1626	
15/15 c	0.0065212	1.245	0.5237942	0.530	0.020	1.038	50.4404	51.00
20/20 a	0.0041405	1.245	0.3325677			1.194	27.8560	
20/20 b	0.0043785	1.245	0.3516904			1.194	29.4578	
20/20 c	0.0049013	1.245	0.3936770	0.359	0.031	1.194	32.9746	30.10
30/30 a	0.0033745	1.260	0.2678160			1.314	20.3810	
30/30 b	0.0027327	1.260	0.2168817	0.242	0.036	1.314	16.5048	18.44
		1.260						
20 FA a	0.0099164	1.245	0.7964997			1.194	66.6940	
20 FA b	0.0088710	1.245	0.7125264			1.194	59.6626	
20 FA c	0.0090366	1.245	0.7258291	0.745	0.045	1.194	60.7765	62.38
40 Slag a	0.0052377	1.215	0.4310858			0.953	45.2450	
40 Slag b	0.0036954	1.215	0.3041455	0.368	0.090	0.953	31.9219	38.58

Appendix G

Thermal Gravimetric Analysis for $Ca(OH)_2$ content of paste samples

$Ca(OH)_2$ (%) = [($Ca(OH)_2$ water loss x 4.1127) / Total Mass of Sample]x100%

A. 20%FA2+40%Slag1

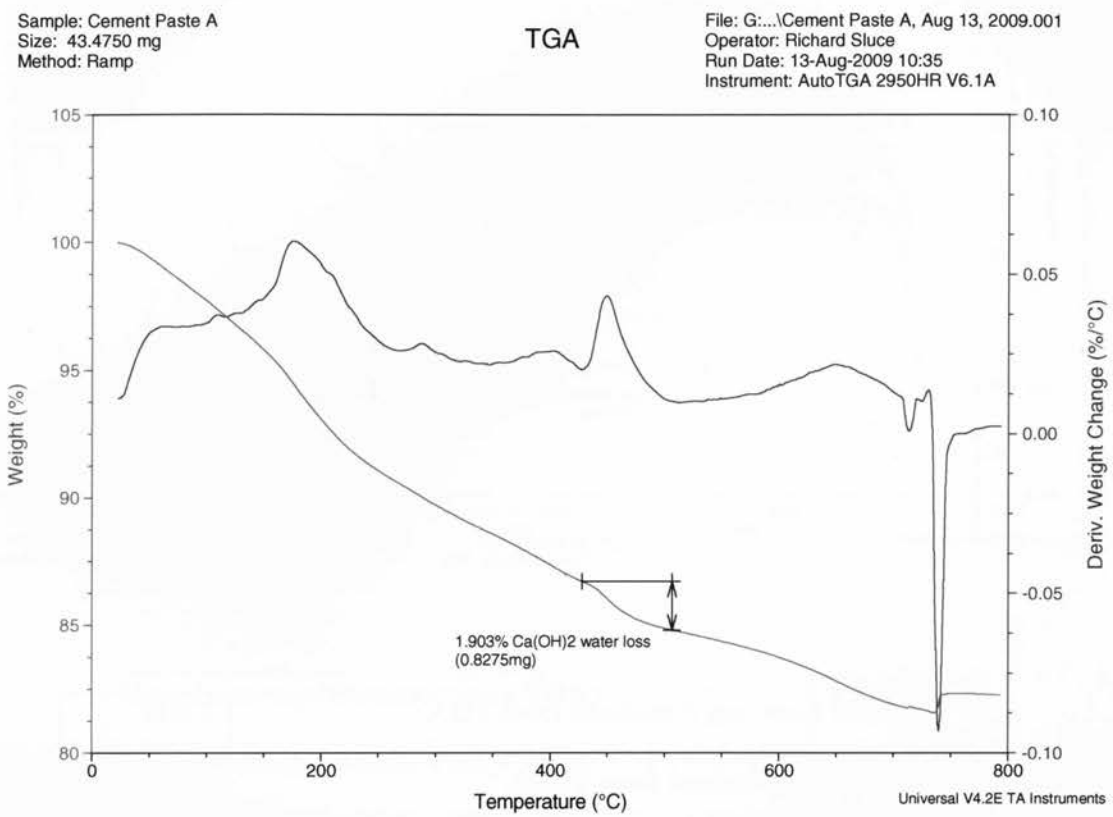

Mass Loss, mg (Obtained from TGA)	0.8275
% Loss (Obtained from TGA)	1.903
Total Sample Mass (mg)	=(0.8275)/(1.903/100)=43.484
Mass of $Ca(OH)_2$ (mg)	=0.8275x4.1127=3.403
% $Ca(OH)_2$ in Paste Sample	=(3.403/43.484)x100% =7.827

B. 20%FA2+20%Slag 1

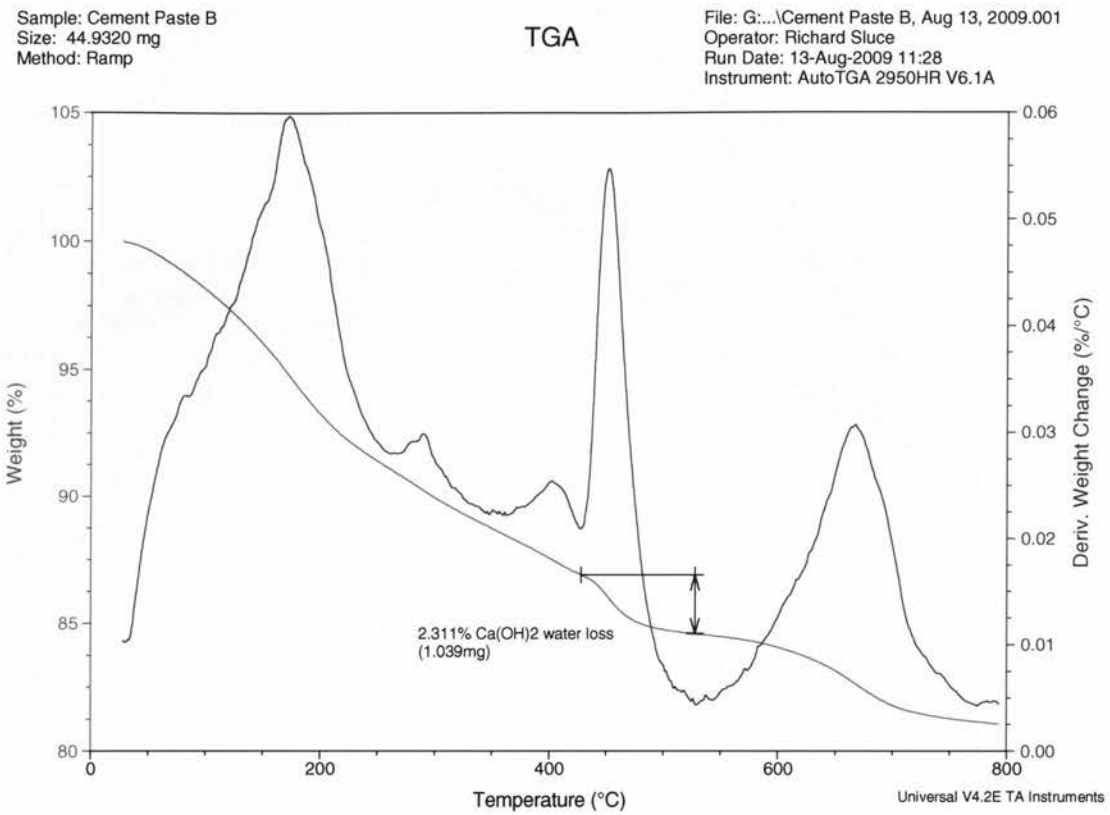

Mass Loss, mg (Obtained from TGA)	1.039
% Loss (Obtained from TGA)	2.311
Total Sample Mass (mg)	44.959
Mass of $Ca(OH)_2$ (mg)	4.273
% $Ca(OH)_2$ in Paste Sample	9.505

C. 20%FA2+30%Slag1

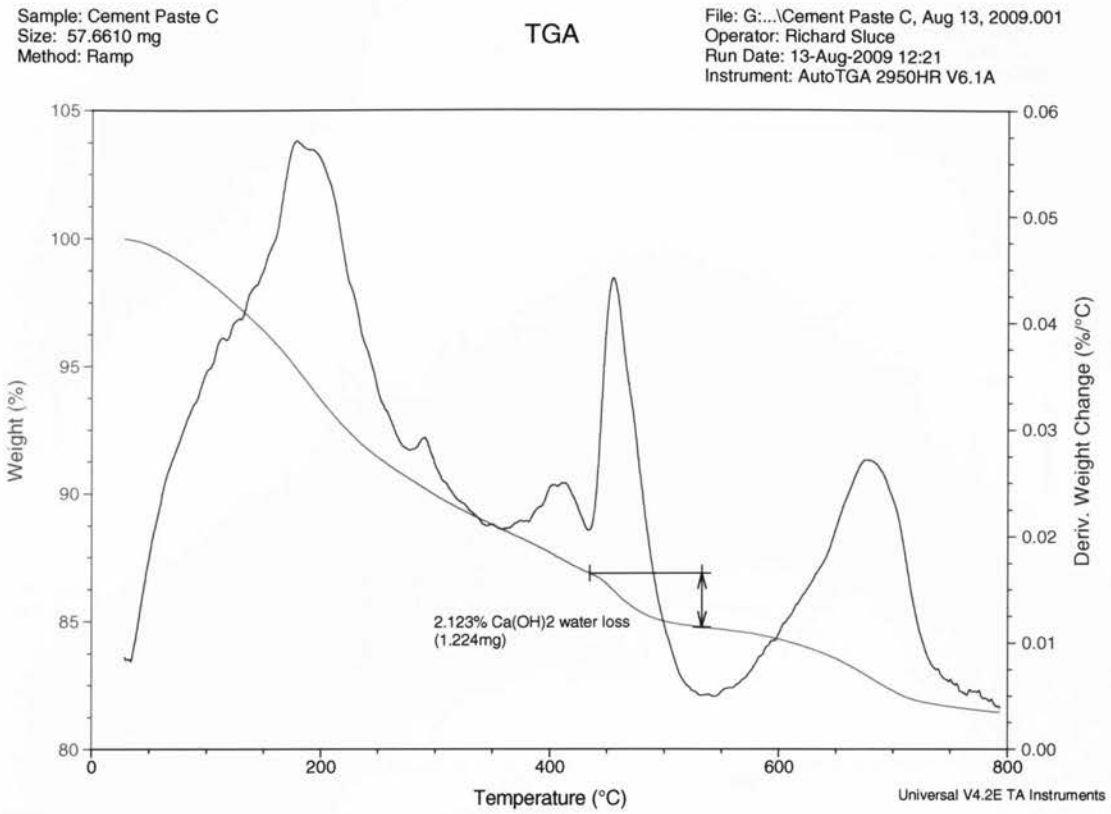

Mass Loss, mg (Obtained from TGA)	1.224
% Loss (Obtained from TGA)	2.123
Total Sample Mass (mg)	57.654
Mass of $Ca(OH)_2$ (mg)	5.034
% $Ca(OH)_2$ in Paste Sample	8.732

D. 15%FA2+15%Slag1

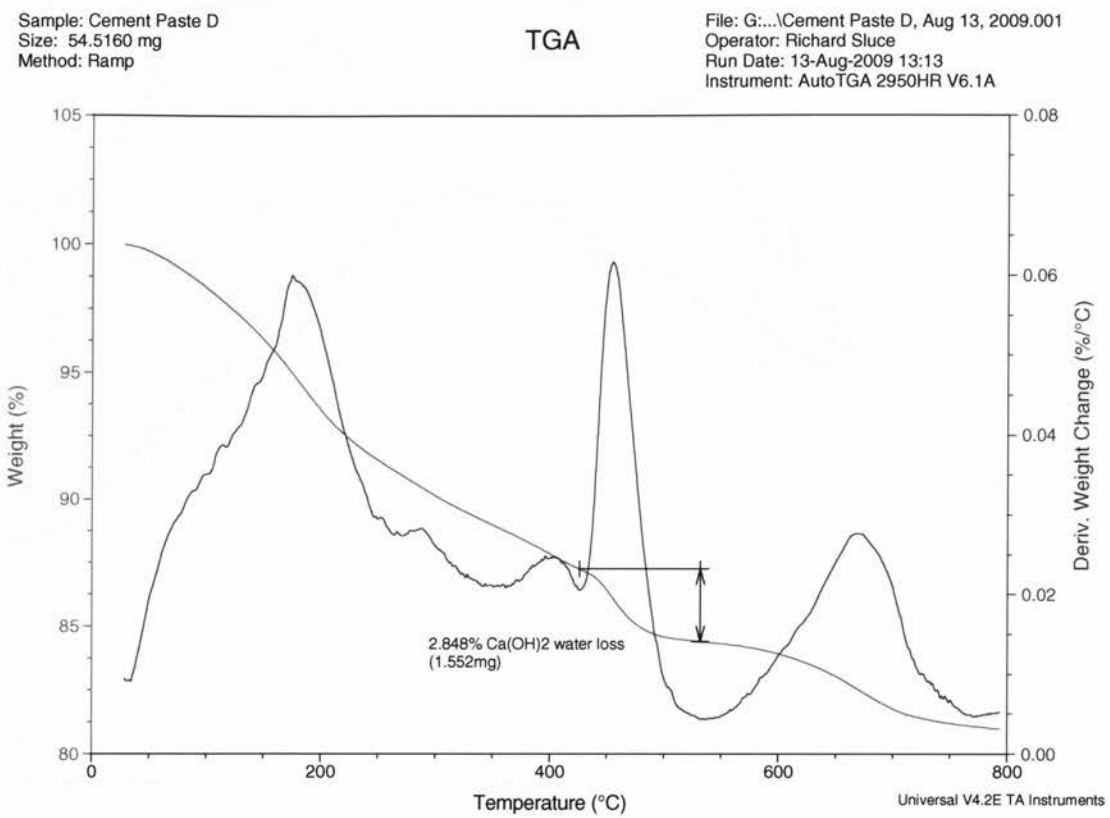

Mass Loss, mg (Obtained from TGA)	1.552
% Loss (Obtained from TGA)	2.848
Total Sample Mass (mg)	54.494
Mass of $Ca(OH)_2$ (mg)	6.383
% $Ca(OH)_2$ in Paste Sample	11.713

E: 30%FA2+30%Slag1

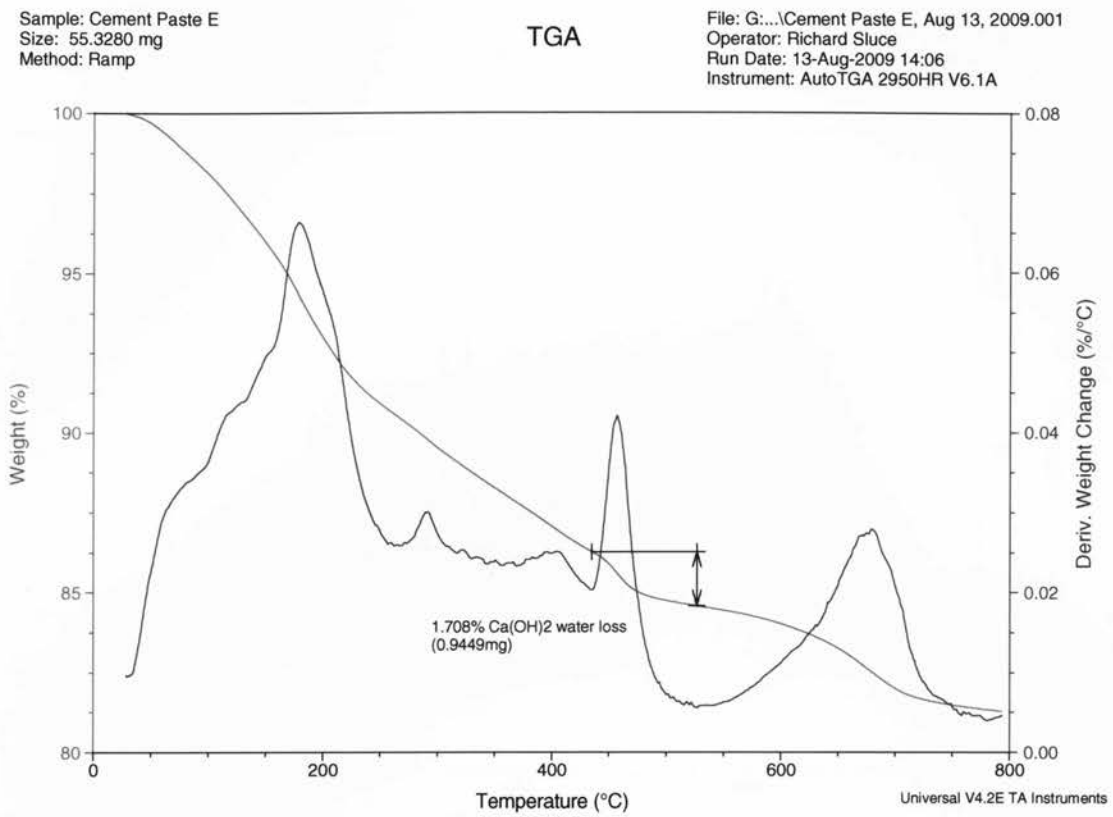

Mass Loss, mg (Obtained from TGA)	0.9449
% Loss (Obtained from TGA)	1.708
Total Sample Mass (mg)	55.322
Mass of $Ca(OH)_2$ (mg)	3.886
% $Ca(OH)_2$ in Paste Sample	7.025

F. 20%FA2

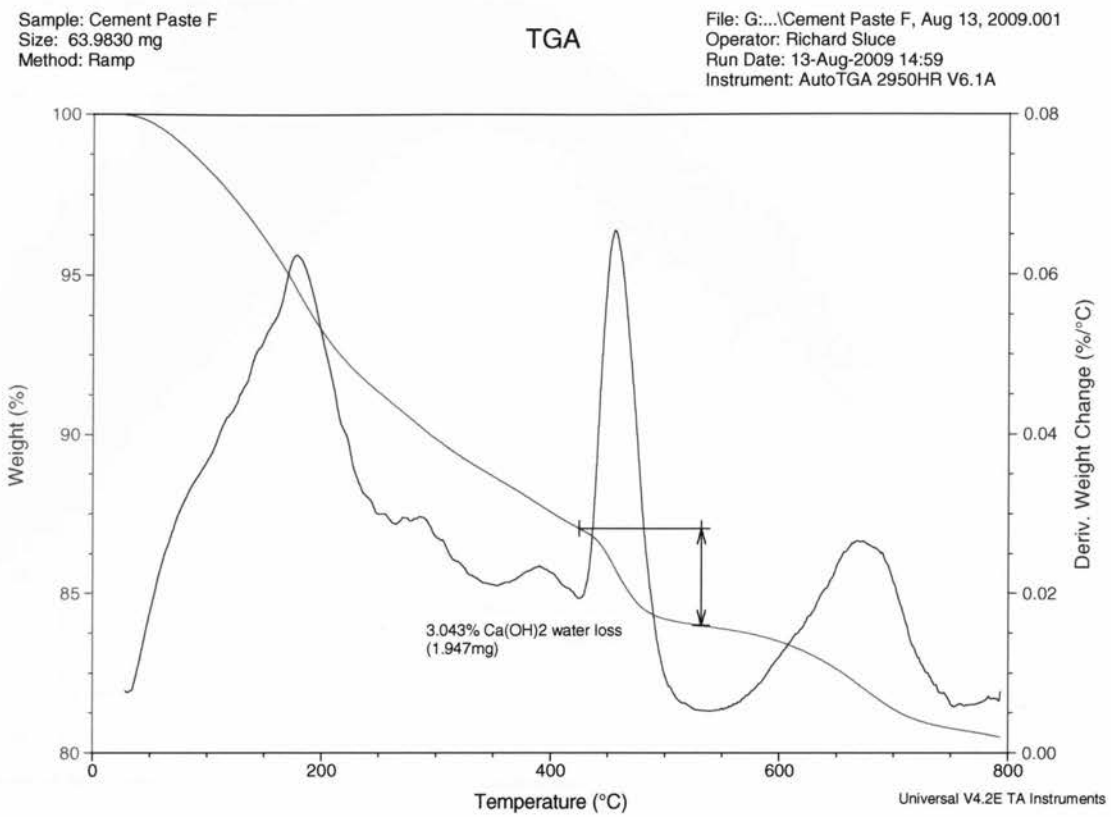

Mass Loss, mg (Obtained from TGA)	1.947
% Loss (Obtained from TGA)	3.043
Total Sample Mass (mg)	63.983
Mass of $Ca(OH)_2$ (mg)	8.008
% $Ca(OH)_2$ in Paste Sample	12.515

G. 40%FA2+20%Slag1

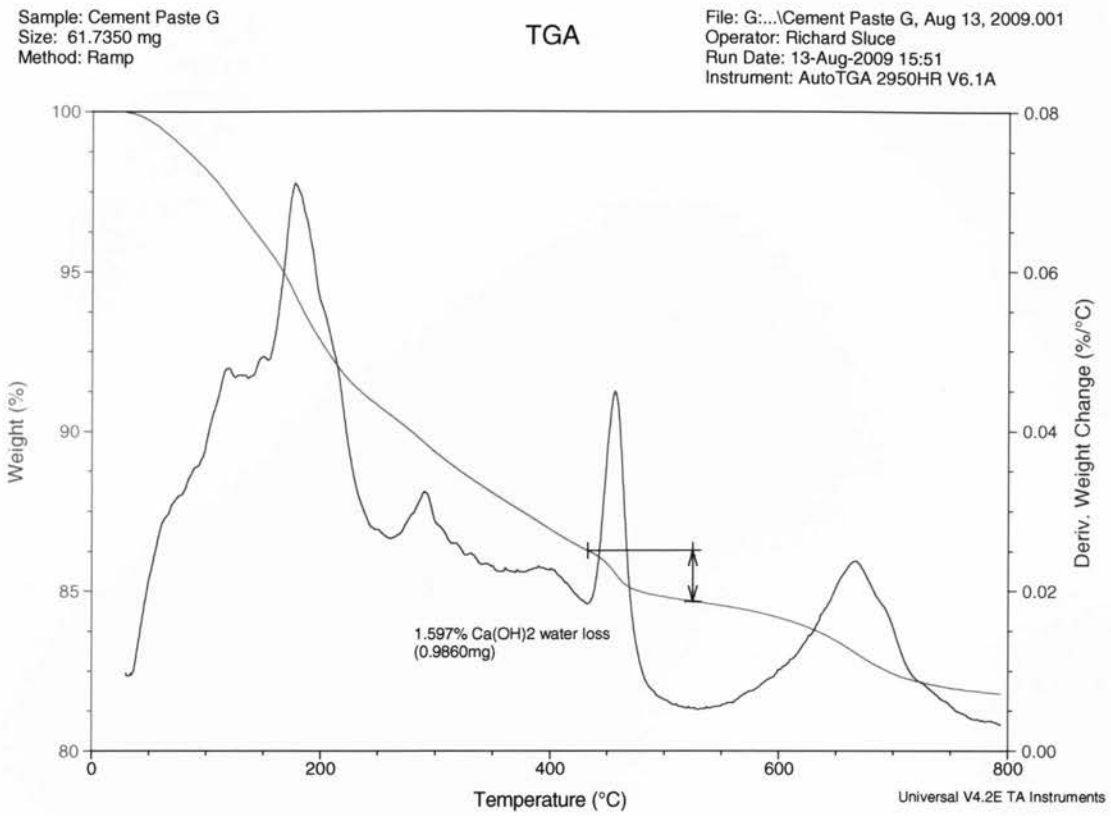

Mass Loss, mg (Obtained from TGA)	0.9860
% Loss (Obtained from TGA)	1.597
Total Sample Mass (mg)	61.741
Mass of $Ca(OH)_2$ (mg)	4.055
% $Ca(OH)_2$ in Paste Sample	6.568